B.H. LEVELTON & ASSOCIATES LIMITED

VOLUME III

DEVELOPMENT OF CEMENTITIOUS GROUTS FOR POST-TENSIONED CONCRETE MEMBERS USE IN OFFSHORE STRUCTURES AND IN THE ARCTIC ENVIRONMENT

Prepared for

Energy Mines and Resources Canada
Mineral Sciences Laboratories
555 Booth Street
Ottawa, Ontario
K1A 0G1

Attention: H.S. Wilson
Scientific Authority

And

Supply and Services Canada
Science and Professional Services Directorate
Place du Portage
Phase III, 11C1
11 Laurier Street
Hull, Quebec
K1A 0S5

Attention: E.K. Fresque, P.Eng.
Senior Science Procurement Officer

by

B.H. Levelton & Associates Ltd.
8805 Osler Street
Vancouver, B.C.
V6P 4G1

122 pp

P.T. Seabrook, P.Eng. N.A. Cumming, P.Eng.

January 15, 1988

Levelton File : 184-612
Contract No. : 23SQ-23440-4-9212
Serial No. : OSQ84-00205
FC/RN : 214-131-000000-425252-0415

MICROMEDIA

VOLUME III

EVALUATION OF PULSE-ECHO TECHNOLOGY FOR DETECTION OF VOIDS IN GROUTED DUCTS

INTRODUCTION

Phase I of this study comprised the development of an optimum grout formulation for the grouting of post-tensioning ducts for offshore structures exposed to the arctic environment. This work is reported separately in Volume I of this report.

Phase II addresses the need for more effective techniques for testing and inspection of the grouted ducts to determine whether any voids or zones of low-density grout exist within the duct. It was concluded therein that the nondestructive test technique that held the greatest potential was the pulse-echo technique, and that further work would best be directed towards evaluation of the available pulse-echo systems on a full-scale section with representative reinforcing, duct arrangement and strand. This work is reported in Volume II.

Work on the full-scale section comprised Phase III of the study and is reported herein. The general background and objectives are described in more detail in Volume I.

IX. EVALUATION OF PULSE-ECHO TECHNIQUES

A. Approach

From information developed during Phase I of the study, a test specimen was designed to represent a typical icewall of a concrete offshore drilling structure. It contained seven tendon ducts which contained intentional voids of various sizes, locations and types. The ducts were fabricated at Levelton's Vancouver laboratory and shipped to the University of Ottawa, where the full scale specimen was cast using the ducts.

Three groups who have made recent advances in pulse-echo technology were invited to survey the specimen to attempt to identify and locate the voids. They were:

1. U.S. Department of Commerce
   National Bureau of Standards
   Gaithersburg, Maryland

   Mr. N.J. Carino and Ms. M. Sansalone

2. U.S. Army Corps of Engineers
   Waterways Experiment Station
   Vicksburg, Mississippi

   Messrs. M. Alexander and H.T. Thornton, Jr.

3. Techno Scientific Inc.
   Woodbridge, Ontario

   Dr. M. Macacek

All three groups attended the University of Ottawa during the week of October 18 to 23, 1987. They were provided with the sizes and locations of the ducts and the nature of the reinforcing, but were not availed of the sizes or locations of voids in the ducts.

Each group surveyed the specimen to attempt to locate the voids and reported the results to Levelton. A Levelton representative attended during the testing to observe and assist.

After completion of the testing, two core samples were taken from the specimen to examine the nature of the concrete and grouted duct.

B. Details of Test Specimen

Plates 1 and 2 provide details of the test specimen. The overall dimensions are 1.0 m thick by 1.5 m high by 2.0 m long. There were five vertical ducts and two horizontal ducts arranged as shown. One face of the specimen contained reinforcing steel representative of that which might be found in an actual offshore structure.

Most of the voids were made by fabricating plexiglass tubes of the appropriate size and shape. The ends were capped and the tubes were filled with water in some cases. The tubes were slid into the ducts to the appropriate locations and grouting was completed.

In two cases, the above procedure was not used. At the top of duct C, the void was formed by grouting up to the bottom of the void, then packing crushed ice into the duct after the grout had set, after which the remaining grout was placed. The void in duct D is completely air-filled, with no tube used.

The sizes and locations of the voids were selected on the basis of the critical void size versus depth of cover. This is discussed in Article 7.0 of Appendix 3, in Volume I.

C. Test Methodology

1. National Bureau of Standards

The National Bureau of Standards has developed a concept to which they refer as the "impact-echo" procedure. Details of the concept and the physics involved are covered in their report which forms Appendix 10.

The procedure uses a small mechanical impact to create a stress pulse, which is received by a point-contact transducer that has been developed by NBS. The most unique feature of the NBS system is the interpretation of the data. The pulse is received by the transducer in the form of a displacement history on a time scale. This data is then mathematically transformed to a frequency spectrum for analysis. This procedure has several potential advantages:

- the point-contact transducer uses a strip of lead foil as the coupling medium and does not require the use of the usual grease or gel-based couplant;

- the frequency spectrum has been found to be much more reproducible than the amplitude waveform;

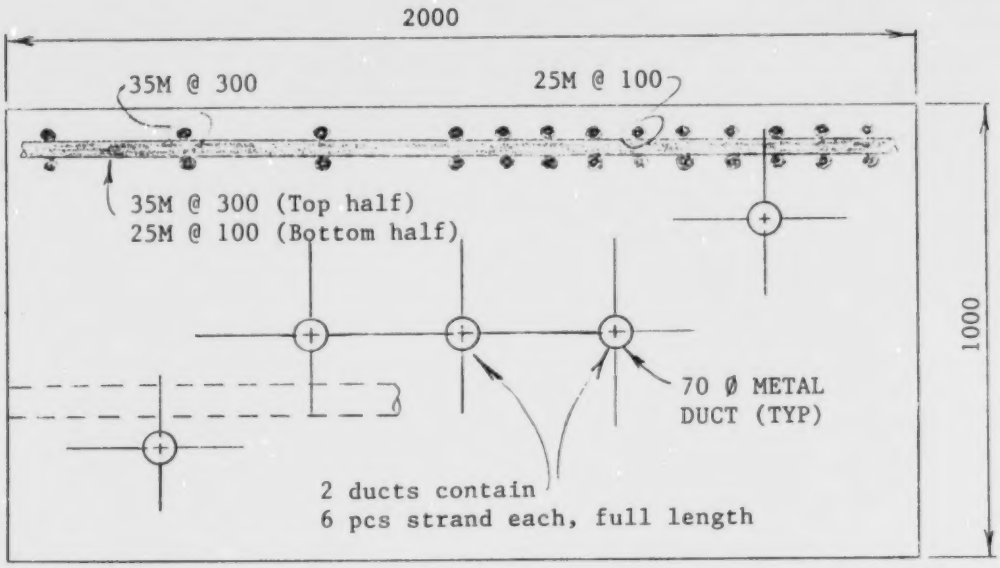

PLAN

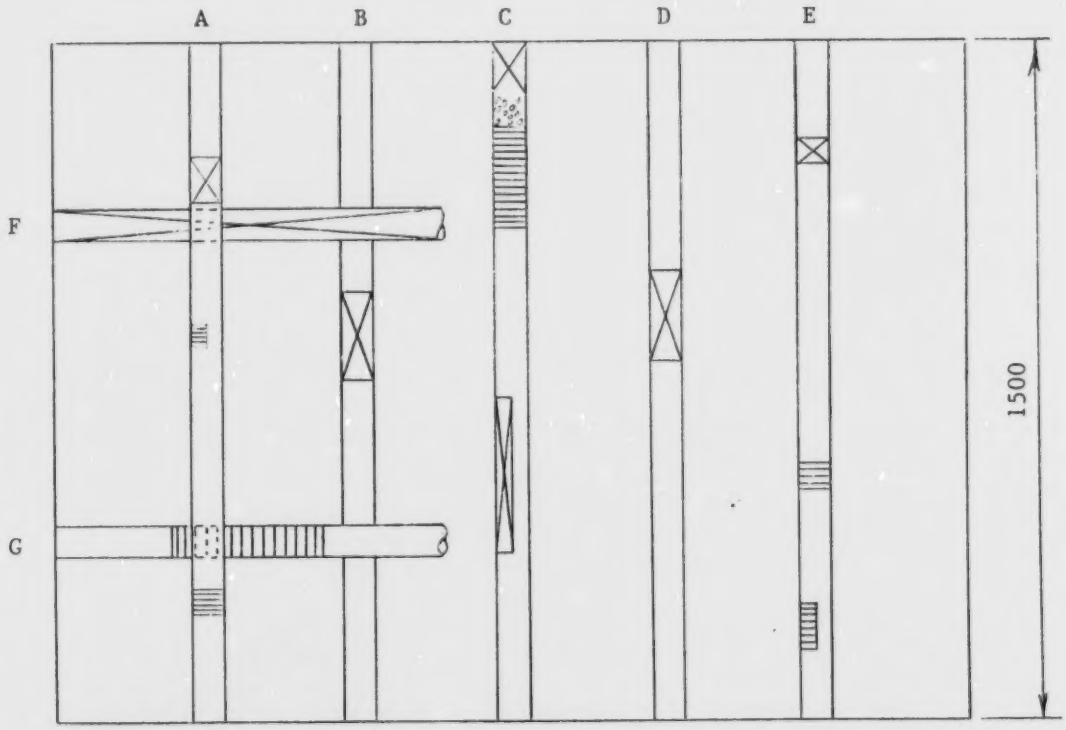

SCALE: 1:15 ELEVATION

LEGEND

Air-filled void
Water filled void
Low density grout

PLATE 1: DETAILS OF TEST SPECIMEN

PLATE 2: COMPLETED TEST SPECIMEN

- it is possible to correlate mathematically peaks in the frequency spectrum with depth below the surface to the defect.

The specimen was surveyed along the centreline of each duct. A frequency spectrum was recorded at each test location, which were spaced 100 mm apart. Both the reinforced and unreinforced faces of the specimen were surveyed.

Plates 3 to 7 show the various components of the apparatus and the survey in progress. Details of the data analysis and interpretation appear in Appendix 10.

2. U.S. Army Corps of Engineers

The U.S. Army Corps of Engineers has developed an ultrasonic pitch-catch and pulse-echo system for inspection of concrete. The term pitch-catch refers to a configuration where separate transmit and receive transducers are used. The term pulse-echo refers to a single transducer arrangement which both sends and receives the pulse. Both configurations use an ultrasonic pulse, rather than a mechanical impact as described above. The chief difference, from a practical viewpoint, is that an ultrasonic pulse can be collimated, whereas a mechanical impact sends out a spherical wavefront.

Appendix 11 is a paper which describes the system and its features. It was developed primarily for use on slabs, and operates at a pulse frequency of 200 kHz. This limits the depth of signal penetration to about 0.6 m, which imposes obvious difficulties when surveying icewalls that may be upwards of one metre thick.

The test specimen was surveyed from both sides, along the centrelines of the ducts. The system is capable of surveying the lines continuously, rather than at discrete intervals, as in the procedure used by NBS.

The signal, amplitude versus time, is displayed on an oscilloscope, which has the capability of storing the waveform on a disc. Plates 8 through 11 show the system components and the survey in progress. It can be seen that the transducers are relatively large, and that the use of a grease-based couplant is required.

3. Techno Scientific Inc.

Techno Scientific uses an ultrasonic pitch-catch configuration. The features of this system are highly sensitive, optimized transducers, and a means of digital data acquisition

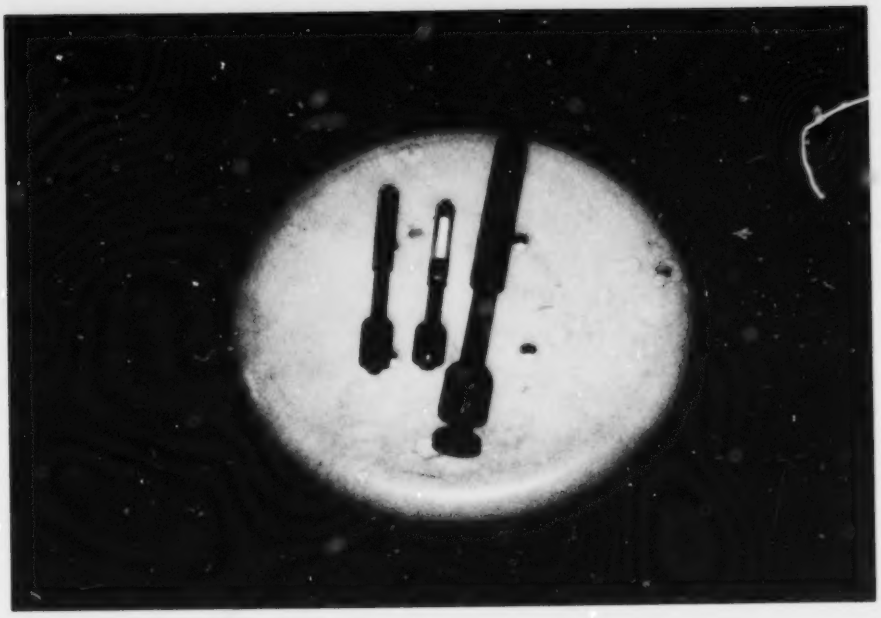

PLATE 3: Various impactors used by National Bureau of Standards.

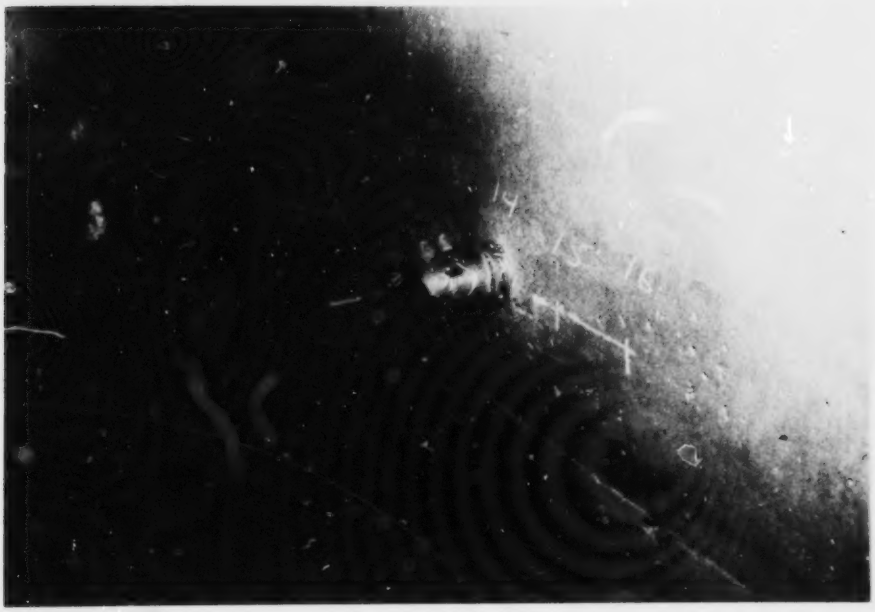

PLATE 4: Point-contact receiving transducer used by National Bureau of Standards.

PLATE 5: National Bureau of Standards data processing equipment. Waveform analyzer at bottom, disc drive at centre, plotter on top.

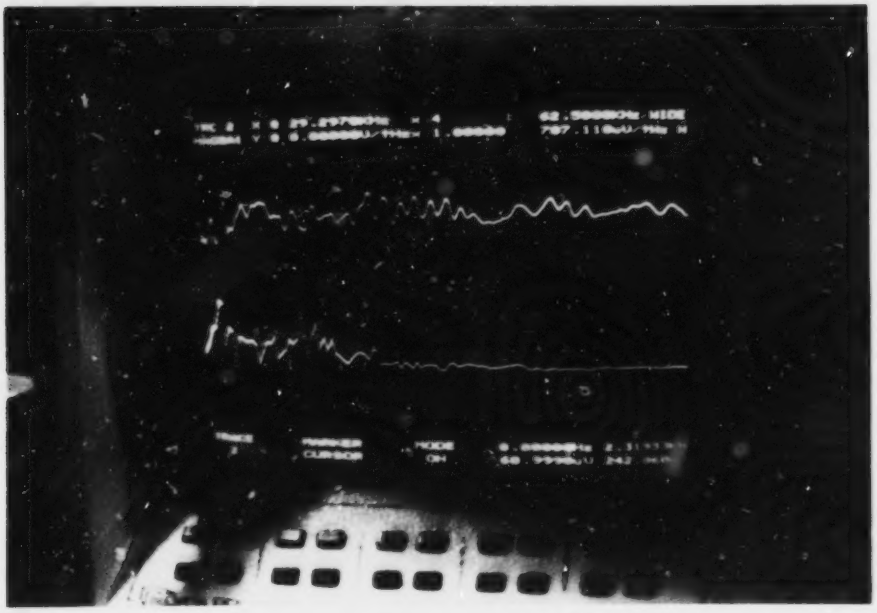

PLATE 6: Typical signal display, NBS system. Upper plot is amplitude versus time; lower plot is amplitude versus frequency.

PLATE 7: Impact-echo survey in progress. Waveforms are recorded at points spaced 100 mm apart along the centreline of the duct.

PLATE 8: USACE transducers

PLATE 9: USACE transducers

PLATE 10: Storage oscilloscope used by USACE, showing typical waveform of amplitude versus time.

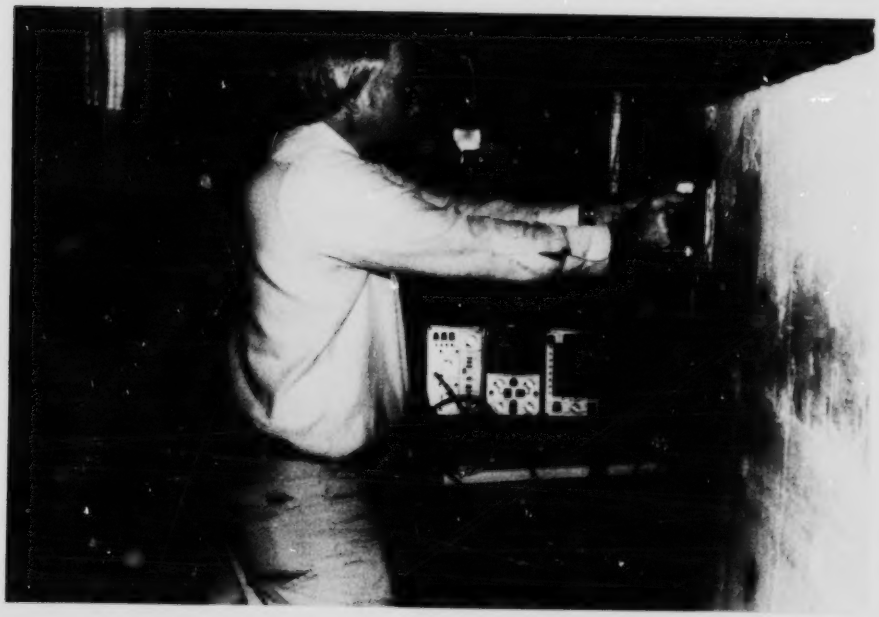

PLATE 11: USACE survey in progress.

and signal processing. Details of the development of this system are given in TSI's report to CANMET under file 23SQ.23440-4-9249.

TSI surveyed the test specimen along each duct at intervals of 100 mm. Both faces were surveyed. At each test location a waveform was recorded, which represented an averaging of a number of individual waveforms sampled. This averaging process suppresses the random noise while the signal increases, thereby enchancing the signal to noise ratio.

Plates 12 and 13 show the equipment and a typical waveform.

D. Results

1. National Bureau of Standards

The NBS report in Appendix 10 discusses the data interpretation and results in some detail. Plate 14 shows the locations of the voids as reported by NBS, with a transparent overlay showing the actual locations.

NBS reported their results as three categories of signal:

- positive indication of void (denoted "Y" in their report);
- positive indication but less certainty (denoted "Y?" in their report);
- no indication.

The results gave a Y or Y? in almost all cases where an actual void existed. In addition, there were numerous indications where no voids existed. Several explanations exist:

(a) In some cases it appeared that voids in adjacent ducts would give a Y or Y? indication.

(b) A core taken through one of the ducts revealed minute shrinkage of the grout which resulted in a very thin separation (about 0.05 mm) between the grout and the inner wall of the duct, around about 30% of the perimeter. The impact-echo procedure would see this as a duct-to-air interface and return a Y or Y? indication.

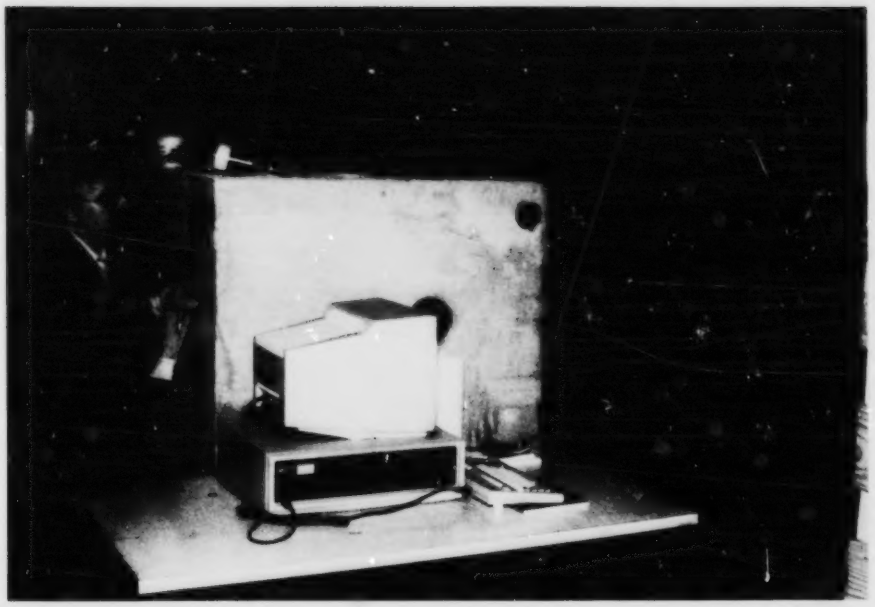

PLATE 12: TSI system: Transducer (1 of 2) on top of specimen. Oscilloscope and pulse generator on right, micro-computer for data acquisition in foreground.

PLATE 13: Typical waveform produced by TSI equipment.

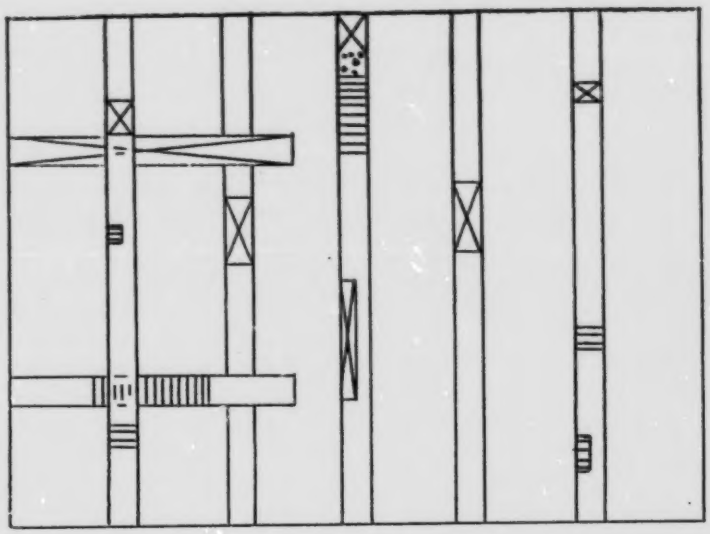

Unreinforced Face

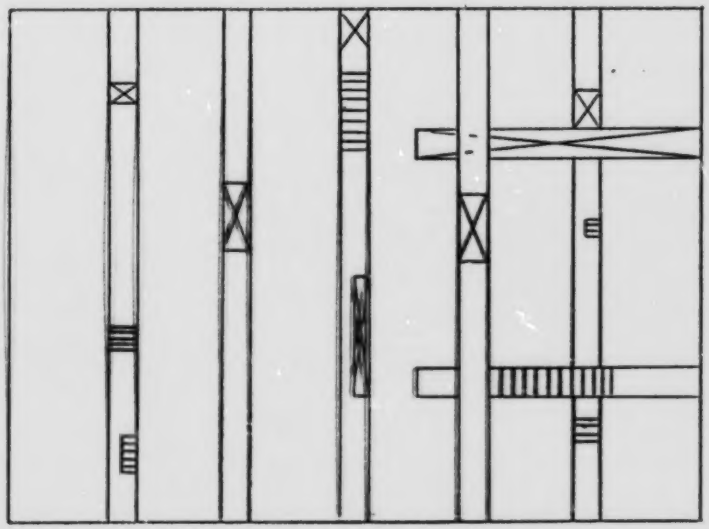

Reinforced Face

LEGEND

Air filled void

Water filled void

PLATE 14A OVERLAY SHOWING ACTUAL VOID LOCATIONS

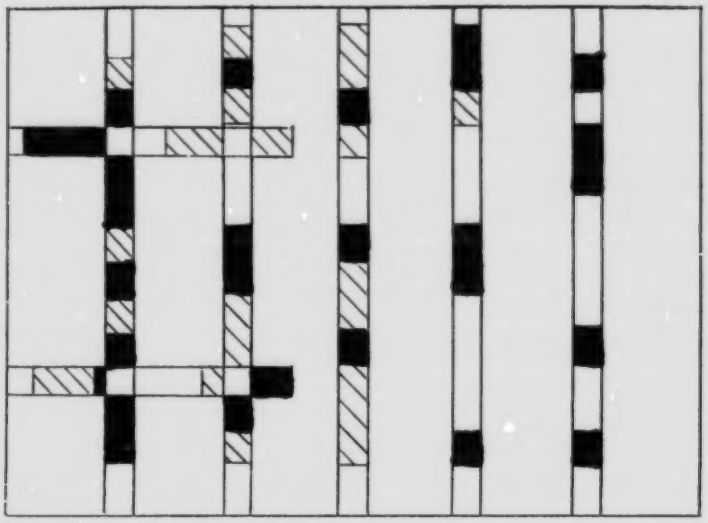

Unreinforced face

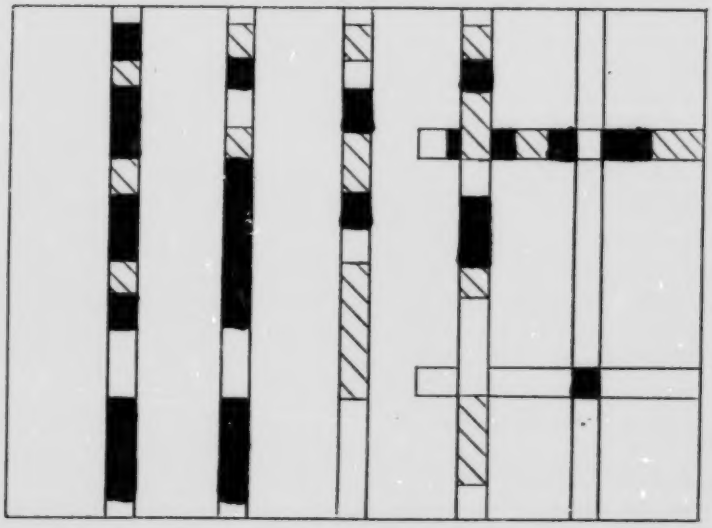

Reinforced face

LEGEND: High confidence that void exists

Indication of void, but less confidence

PLATE 14: LOCATIONS OF VOIDS REPORTED BY NATIONAL BUREAU OF STANDARDS

(c) Some spurious signals were returned, probably due to discontinuities or minor honeycomb in the concrete. This complicated interpretation of the data.

It is noted that the program allowed little opportunity to calibrate the procedure against known conditions and that there is considerable room to refine the procedure. It has been demonstrated that the NBS procedure is capable of locating small voids in grouted ducts. The smallest void (near the bottom of duct E) was located by NBS with relatively high precision.

With the exception of duct A, the survey gave similar results from the reinforced and unreinforced sides. The nature of the procedure allows a signal returned by the rebar to be identified with relatively good precision, hence they could be separated from other signals to assist in the interpretation.

2. U.S. Army Corps of Engineers

Due to the limited penetrating ability of the USACE system, ducts B, C and D could not be seen with the equipment. It was possible to see duct A from the unreinforced side, and duct E from the reinforced side. It was also possible to see duct A from the end of the specimen.

The nature of duct A as reported by USACE is shown on Plate 15, along with the actual conditions. The interpretation of the waveform was that a double peak represented the front and back of a fully-grouted duct, whereas a voided duct would not return a signal from the back interface, giving only a single peak.

The large, flat shape of the transducer faces gave difficulty in areas where the surface of the specimen was not a perfect plywood-formed finish. Along line E on the reinforced face, there was a zone where the concrete had been poorly consolidated and subsequently parged with mortar. The resulting surface could not make complete contact with the transducer, resulting in a severely impaired signal. Similarly, interference of the signal occurred in some areas and was presumed to result from incomplete consolidation or honeycombed zones.

When surveying line E on the reinforced face, the reinforcement could be identified quite readily. The duct could be seen readily through the rebar mat, however, there was strong interference in some areas as described above. Because of this, it could not be determined whether the duct was full or voided.

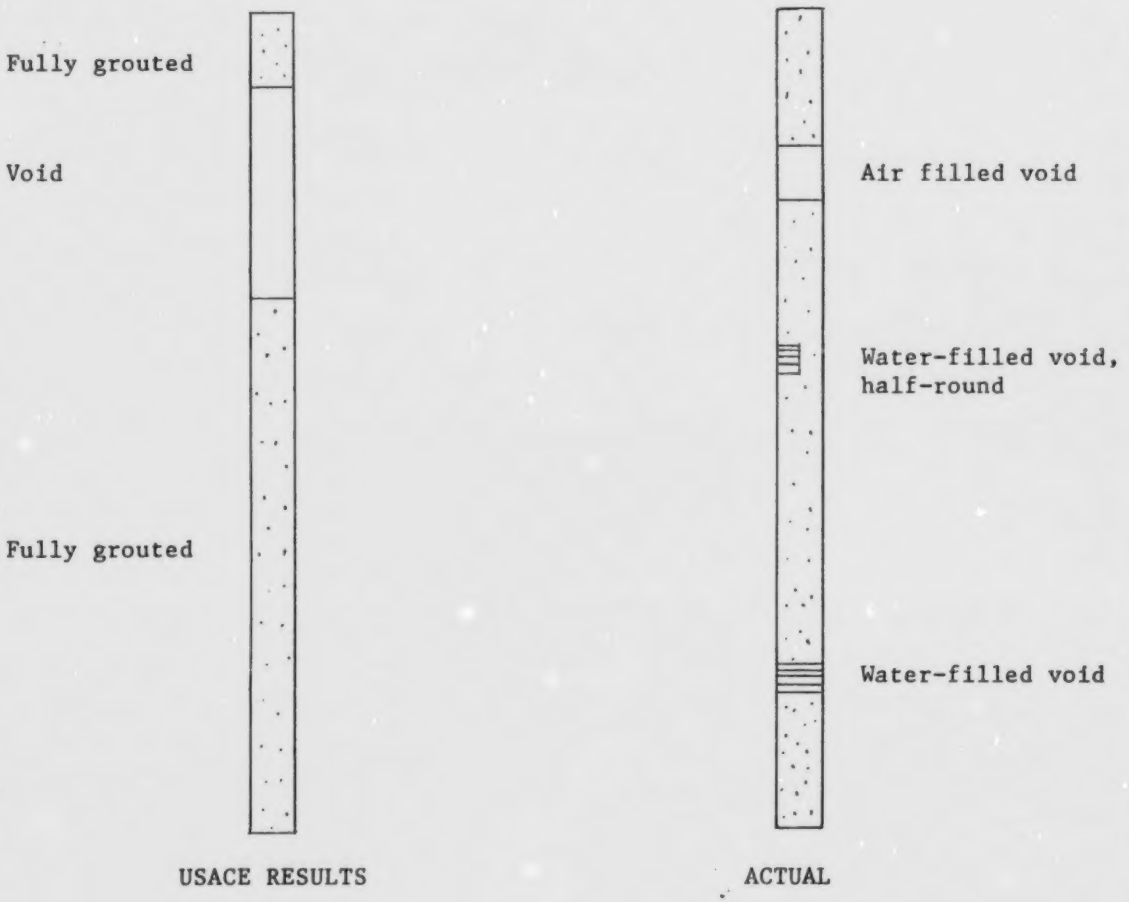

PLATE 15: LOCATION OF VOID IN DUCT A AS REPORTED BY U.S. ARMY CORPS OF ENGINEERS

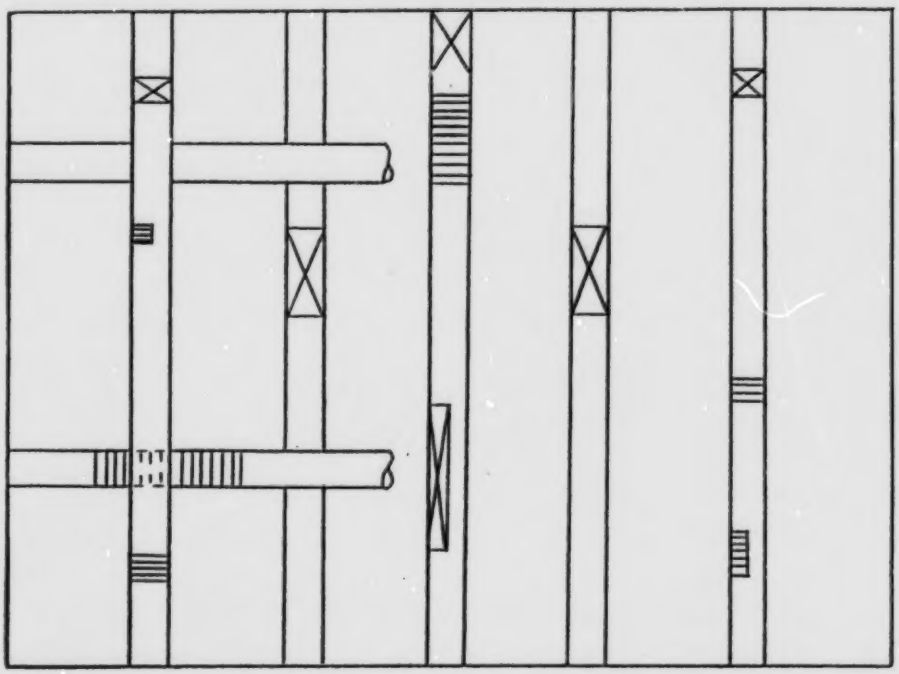

LEGEND

Air-filled void

Water-filled void

PLATE 16A

OVERLAY SHOWING ACTUAL VOID LOCATIONS.

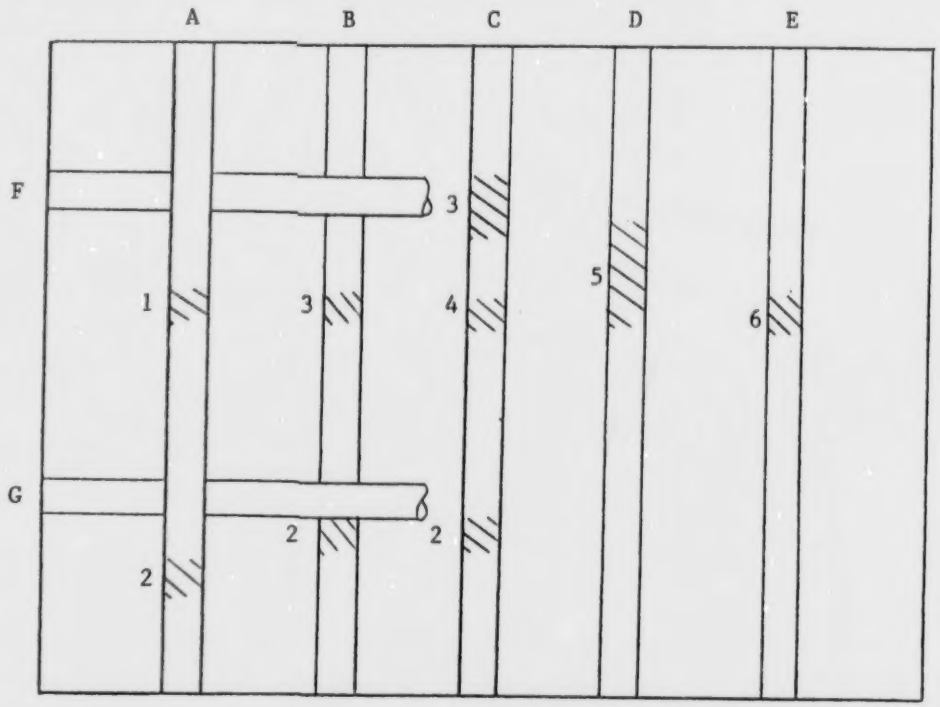

Elevation - viewed from unreinforced side

LEGEND

1) Possible void
2) Possible partly filled void
3) Possible air-filled void
4) Unspecified strong signal
5) Unspecified large reflection
6) Unspecified large echo

PLATE 16: DEFECT LOCATIONS AS REPORTED BY TECHNO SCIENTIFIC INC.

In some areas, peaks in the waveform occurred at depths less than the cover on the duct. These peaks were presumed to represent honeycomb or similar discontinuities.

Duct A was surveyed from the end of the block. The surface was of good quality and a good signal was obtained. A 15M rebar used for a lifting hook occurs between the duct and the end. It could be readily identified in the waveform. As the survey progressed downward along the duct, the end of the rebar was easily identified.

3. Techno Scientific Inc.

The TSI report is included in Appendix 12. Plate 16 shows the locations of the voids reported by TSI with a transparent overlay showing the actual void locations.

Despite the data being presented in a somewhat inconclusive manner, it is apparent that some degree of success was achieved. The proprietor attributes the uncertainty to a lack of time to fully survey the specimen and the lack of an opportunity to calibrate the results to known conditions. In addition, equipment problems during the survey may have contributed.

The writers concur with the conclusion of TSI that with a greater effort the results could be improved. It is noted, however, that the smallest, shallowest voids were not detected, and that some false-positive indications occurred.

With respect to practical application, the manner in which data were acquired and stored was rapid and relatively straight forward, but requires a microcomputer. The need for a gel-based couplant for the transducers is a disadvantage.

E. Conclusions

The following conclusions have been drawn from this research:

1. The NBS impact-echo procedure is capable of identifying relatively small, deep voids in a heavily reinforced concrete wall. Further work is required to refine the process to allow better, easier and more precise interpretation of the data. The ability to identify voids of the critical size and cover identified in Volume I has been demonstrated.

2. The NBS procedure holds the best potential for being adapted to field use. The transducer is small, requires only a pointcontact, and does not require a grease-like couplant. It would be required to make the rest of the hardware more compact for field use.*

* Since this research was completed, NBS has made improvements to both its hardware and software which significantly enhance the system's practicality for use in the field.

3. The ultrasonic technique developed by the USACE was able to identify a small, air filled void at shallow depth. The resolution was relatively poor. The signal was unable to penetrate 0.5 m of the concrete. This technique appears to have limited potential unless a means can be found to improve the resolution of the signal and improve its penetrating ability.

   The large size of the transducers and need for a grease-based couplant present practical difficulties if this equipment were to be adopted for field use.

4. The TSI procedures demonstrated some limited success, but appears to require much refinement and calibration to become practical. The need for a grease-based couplant again limited the practicality.

5. The test specimen was found to contain relatively minor imperfections in the quality of grouting, consolidation of the concrete and surface finish. The success of all three techniques appeared to deteriorate very rapidly when faced with such defects as entrapped air voids, incomplete encapsulation of the duct, and minor shrinkage of the grout. Hence, unless an extremely high quality of concreting and grouting are achieved in a real structure, it may not be possible to obtain useful and meaningful results.

6. Substantial research remains to be done to calibrate the results to known conditions and to further assess the impact of normal construction imperfections on the quality of the test data.

7. The presence of heavy reinforcement did not appear to present a major obstacle to interpretation of the data.

APPENDIX 10

REPORT OF NATIONAL BUREAU OF STANDARDS

LOCATION OF VOIDS IN TENDON DUCTS USING THE IMPACT-ECHO METHOD

INTRODUCTION

This report presents the results of the investigation performed by the research team from the National Bureau of Standards. The fundamental principles of the impact-echo method are reviewed for those who are unfamiliar with the technique. The equipment and test procedures used in the investigation are described, and the approach used in interpreting the data is explained.

The conditions present in this investigation provided a challenge for the impact-echo method. The dimensions of the flaws were small compared with the dimensions of the test specimen, and the depths of the voids were large relative to their size. The nature of the interactions of transient waves with cylindrical shaped voids is not yet fully understood. The presence of voids in adjacent ducts, reinforcing bars, and apparent pockets of honeycombing resulted in complex signals. Time constraints did not permit experimentation to devise an optimum test procedure. Nevertheless, the research team was able to identify many locations where there is a high confidence that voids were present in the ducts.

BACKGROUND

Principle of Impact-Echo Method

The principle of the impact-echo technique is illustrated in Fig. 1. A transient stress pulse is introduced into a test object by mechanical impact on the surface. The stress pulse propagates into the object along spherical wavefronts as P- and S-waves. In addition, a surface wave (R-wave) travels along the surface away from the impact point. The P- and S- waves are reflected by internal interfaces or external boundaries. The arrival of these reflected waves at the surface where the impact was generated produces displacements, which are measured by a receiving transducer. If the receiver is placed close to the impact point, the displacement waveform is dominated by the displacements caused by P-wave arrivals. The displacement waveform can be used to determine the travel time, Δt, from the initiation of the pulse to the arrival of the first P-wave reflection. If the P-wave speed, C_p, in the test object is known, the distance, T, to the reflecting interface can be determined.

An impact-echo test system is composed of three components: an impact source; a displacement transducer; and a waveform analyzer. The force-time history of the impact may be approximated as a half-sine curve, and the duration of the impact is the "contact time". The contact time is an important variable because it determines the size of the defect which can be detected by impact-echo testing. As the contact time decreases, smaller defects can be discerned. However, the penetrating ability of the stress waves is reduced as contact time decreases. Thus the selection of the impact source is a critical aspect of a successful impact-echo test system. For the developmental work performed at NBS [1], contact times on the order of 30 to

60 microseconds have been used. For this investigation, a commercially available impactor was adapted for use as the impact source. The components of the impactor are shown in Fig. 2. The spherically-tipped mass (center) is propelled by the spring-loaded device (left). A 9-mm hardened steel ball was attached to the end of the device. The ball served to increase the repeatability of the input pulse and shorten the contact time of the impact. It is estimated that the impactor produced impacts with contact times ranging from 30 to 50 microseconds, depending on the characteristics of the concrete at the impact point.

The receiving transducer must be capable of accurately measuring surface displacement. A conically-tipped transducer, developed at NBS as a reference standard for calibrating acoustic emission transducers, is used in current work. For this investigation, a special case was built to house the transducer so that it could be used on vertical surfaces. Figure 3 shows the transducer assembly and mechanical impactor used during this investigation.

A waveform analyzer is used to capture the transient output of the displacement transducer, store the digitized waveforms, and perform signal analysis. A suitable waveform analyzer should have a sampling frequency of at least 500 kHz. A pen-plotter is used for hard-copy output of the raw and processed waveforms.

Signal Analysis

During the initial development of the impact-echo technique [1,2,3], interpretation of the recorded waveforms was performed in the time domain. This required establishing the time of impact initiation and the arrival time of the first P-wave echo. While this was feasible, it was found to be time-consuming. An alternative approach is frequency analysis of the displacement waveforms.

The principle of frequency analysis is illustrated in Fig. 4, which shows a solid plate of thickness T subjected to impact. The stress pulse generated by the impact propagates back and forth between the top and bottom surfaces of the plate. Each time the pulse arrives at the top surface it produces a characteristic displacement. Thus the waveform is periodic, and the period, t, is equal to the travel path (2T) divided by the P-wave speed. Frequency is the inverse of the period; thus the frequency, f_p, of the characteristic displacement pattern is:

$$f_p = \frac{C_p}{2\ T} \qquad (1)$$

Thus, if the frequency of P-wave arrivals can be determined, the thickness of the plate (or distance to a reflecting interface) can be calculated:

$$T = \frac{C_p}{2\ f_p} \qquad (2)$$

The frequency content of the recorded waveforms is obtained using the fast Fourier transform (FFT) technique. Appendix A gives additional background

information on digital frequency analysis, and examples of its application may be found in References 1, 4, 5 and 6.

Figure 5 illustrates how frequency analysis works. In Fig. 5(a), an impact-echo test was performed over a solid portion of a 0.5-m thick concrete slab. In the amplitude spectrum, there is a frequency peak at 3.42 kHz. This frequency corresponds to multiple reflections between the bottom and top surfaces of the slab. Using Eq. (1) and solving for C_p, the P-wave speed is calculated to be 3410 m/s. Figure 5(b) shows the amplitude spectrum obtained from a test over a portion of the slab containing a disk-shaped void. The peak at 7.32 kHz results from multiple reflections between the top of the plate and the void. Using Eq. (2), the calculated depth of the void is 3410/(2 * 7320) = 0.23 m, which compares favorably with the known distance of 0.25 m.

Appendix A explains that the resolution in the amplitude spectrum (the frequency difference between adjacent points) is equal to the sampling frequency divided by the number of points in the waveform record. This imposes a limit on the resolution of the depth calculated according to eq. [2]. Because depth and frequency are inversely related, it can be shown that for a fixed resolution in the frequency domain, the resolution of the calculated depth improves as the frequency increases, that is, as depth decreases.

Feasibility Study

The feasibility of using the impact-echo method to detect voids in post-tensioning ducts was demonstrated in a controlled flaw study at NBS [6]. A 100-mm diameter, sheet metal duct was cast into a 0.5-m thick concrete slab. The P-wave speed in the slab was 3910 m/s. The cover over the duct was 150 mm. A portion of the duct was filled with grout and the remainder was hollow. Figure 6 shows the amplitude spectra obtained for tests over the filled and hollow portions of the duct. For the filled portion, the spectrum has a predominant peak at 3.91 kHz. This is the slab thickness frequency produced by multiple reflections between the top and bottom surfaces of the slab. Thus the waves travel through the filled duct. For the hollow portion, there is a significant high frequency peak at 13.7 kHz, which corresponds to multiple reflections between the top of the duct and the top surface of the slab. The depth of the duct is calculated as 3910 / (2* 13700) = 0.14 m, which is in excellent agreement with the known depth of 0.15 m. This limited investigation showed that it is feasible to detect the presence of a void in a tendon duct using the impact-echo method and frequency analysis.

Effect of Reinforcing Bars

The test specimen for this investigation is heavily reinforced on one face. Because of the large bar diameters and the short contact time of the impact, it was anticipated that reflections from the bars would produce peaks in the amplitude spectra [1]. Appendix B gives an explanation of the difference between reflections at a steel/concrete interface compared with a concrete/air interface. Because of these differences, the frequencies due to reinforcing bars occur at one-half the frequencies corresponding to their depths.

PROCEDURE

Scan Lines:

Figure 7 shows elevation views of the wall from the unreinforced and reinforced faces. The letters A-G were used to identify the various ducts in the wall specimen. Ducts A-E are vertical and ducts F and G are horizontal. Impact-echo tests were performed at 100-mm intervals along the centerline of each duct. Test points were identified by a number beginning with 0; these numbers are shown along the perimeter of the elevation views. The receiver was located directly over the test point and the impactor was located adjacent to the receiver on the side of the increasing test point number (see Fig. 7).

At each test location, repeated impacts were performed until a representative amplitude spectrum was obtained. At test points where the surface was in good condition, about three impacts were sufficient. At locations where the concrete surface was rough, 6 to 8 impacts were required to establish a representative spectrum. At each test point, a representative waveform and its corresponding amplitude spectrum were stored on a floppy disk.

A sampling frequency of 500 kHz was used and there were 1024 points in each recorded waveform. Thus the resolution in the amplitude spectrum was 500/1024 = 0.488 kHz. This sampling frequency was chosen because it has been used in most of the NBS laboratory studies. Due to the limited time available to perform the tests, we were not able to experiment with other sampling frequencies, and the value used may not be the optimum.

P-wave Speed:

Two independent approaches were used to establish the P-wave speed for the concrete in the wall. First an impact-echo test was performed on a standard test cylinder cast from the concrete used in the wall. A sampling rate of 100 kHz was used to improve the resolution. The amplitude spectrum had a dominant peak at 6.93 kHz; thus, using Eq. (2), the calculated P-wave speed is 2 * 0.305 * 6930 = 4230 m/s. As a check on this value, the ultrasonic pulse velocity through the wall was measured. The transit time was 213.6 microseconds, which gives a pulse velocity of 4680 m/s. It is has been shown [1,4,5] that the P-wave speed by impact-echo is about 90% of the pulse velocity, that is, 4680 * 0.9 = 4210 m/s. Thus there is excellent agreement between the two independent methods and a P-wave speed of 4230 m/s was used for the investigation.

For the solid 1-m thick wall, the thickness frequency would be 4230/(2*1) = 2.12 kHz. The closest digital values in the amplitude spectrum would be 1.95 kHz and 2.44 kHz.

Data Interpretation:

The locations of the tendon ducts were known. To aid in data interpretation, a table was developed which listed the expected frequency values at different test points assuming there were voids in the ducts directly below the test points. Stress waves generated by impact propagate along spherical wavefronts; therefore, voids in adjacent ducts, as well as a void in the duct directly below the test point, can produce wave reflections. Thus, for test scans along each duct, the frequencies associated with voids in adjacent ducts were also computed. Figure 8 shows the various types of paths that were considered. Along the three diagonal paths (#3, #5, and #7), the S-

wave generated by the point impact is of high amplitude [1,2]. Thus there is the possibility of multiple S-wave reflections from a void, and the frequencies associated with these reflections were also considered. It was assumed that the S-wave speed was 60 percent of the P-wave speed, which is typical of a material having a Poisson's ratio approximately equal to 0.2 [1,7].

The computed frequencies associated with voids in the ducts are shown in the third and fifth columns of Table 1. Since only certain frequency values are possible (multiples of 0.488 kHz in this case) in the digital amplitude spectra, columns 4 and 6 of Table 1 list the digital frequency values closest to the computed values. In most cases, two possible frequency values are shown because the calculated value falls in between the possible values.

Figure 9 shows the reinforcing bar layout. The pattern was verified by means of a covermeter and a radar system. Figure 9 also shows the location of the test points with respect to the center line of the bars. It is seen that the horizontal bars were located directly below the receiver locations. The vertical bars did not generally lie directly below the receiver.

The reinforcement pattern resulted in six different cover distances to be considered in calculating the expected frequencies associated with reflections from the bars. Figure 10 shows plan views of the bar details in different quadrants of the specimen. The quadrant names are assigned as though the specimen were viewed from the reinforced face. The cover dimensions are based on the planned cover of 50 mm and assuming the bars in different layers are in contact with each other. Table 2 lists the expected frequencies associated with P-wave reflections from the bars assuming the tests were performed directly over bar centerlines. As explained in Appendix B, the frequencies are one-half the values that would be associated with reflections from a void at the same depth. The frequencies associated with the inner layer of vertical bars may not be realistic because of the shadowing effect of the outer layer. We have no experience in testing specimens with three layers of steel, so we are not certain whether the inner vertical bars would be discernable.

RESULTS

Waterfall Plots:

The amplitude spectra for each scan line were plotted sequentially to produce "waterfall plots," which are included in Appendix C. The frequency values of the peaks were recorded on these plots. Test point 0 of each scan line is at the bottom of the page for each waterfall plot.

Data Interpretation:

Two examples are provided to illustrate how the waterfall plots were interpreted. Figure 11 shows the waterfall plot for scan line ER (along duct E on the reinforced face). For scan line ER, the reflection path for a void in duct E is a type-2 path as shown in Fig. 8. Referring to Fig. 9, it is seen that this scan line was almost directly over the vertical bars, and test points 1, 4, and 7 through 13 were also located over horizontal bars. Based on the planned depths, the frequencies expected for reflections from various interfaces would be as follows:

Void in duct E:	9.77/10.25 kHz
Outer vertical bar:	20.98 kHz
Horizontal bar:	14.16 kHz
Inner vertical bar (at top):	9.77 kHz
Inner vertical bar (at bottom):	10.74 kHz

Note that the frequency value associated with reflections from the inner vertical bar may lead to interference with the frequency associated with a void. But as was previously mentioned, the inner vertical bar may be shadowed by the outer bar and it may not produce this expected frequency peak. In addition, the inner bar is deeper and would not be expected to produce strong reflections. The waterfall plot for scan line CR was examined, since the test geometry was similar to line ER (Fig. 9). If the inner vertical bar were to produce a frequency peak at 9.77 kHz, this peak would be present in the spectra of every test point along CR. This was not found to be true. Therefore, it was concluded that, for the test geometry along ER, the inner vertical bar would not result in a large peak at 9.77 kHz.

To locate voids in duct E, test points whose spectra had peaks at 9.77 or 10.25 kHz were identified. The points where there was a high confidence that a void was detected are marked with a "Y" (for "yes") on Fig. 11. Test points ER6 and ER11, for example, have large frequency peaks at 9.77 kHz, and these points are classified as "Y". At some points, there was a frequency peak close to the expected value or there was a series of peaks in the vicinity of the expected frequency. These points are marked as "Y?", which signifies that there is an indication of a void, but the results are not as clear as points marked as "Y". For example, points ER1 and ER4 have multiple peaks in the vicinity of 9.77 kHz. Based on the development work at NBS, it is believed that most points marked as "Y?" are above the boundaries of the voids. Test point ER0 has a peak at 8.30 kHz, which is close to the calculated frequency of 8.46 kHz for a half-filled duct. Thus, at point ER0, the duct is believed to be half empty.

Figure 12 shows the waterfall plot for scan line D. In this case the expected frequency for a type-4 path is 4.39 or 4.88 kHz. Test point D1 has a large peak at 4.88 kHz, and points D6 and D12 have peaks at 4.39 kHz. Thus duct D has voids at its ends and center.

Summary:

The above procedure was used to interpret the waterfall plots for all the scan lines. Table 3 summarizes the results for each test point. In Fig. 13, test points marked as "Y" are shown shaded and those points marked as "Y?" are shown cross-hatched. In drawing the extent of voids, it was assumed that, at each point where a void was detected, the void extended 5 cm to either side of the transducer location.

As can be seen in Fig. 13, the results obtained from the reinforced and unreinforced faces were not identical; however, in most cases there was sufficient agreement. The following summarizes the conditions of the ducts:

Duct A: The test results from the unreinforced face indicate large voids at the two ends and a smaller void at the center. From the reinforced face, only a portion of the void at the bottom of the duct could be identified.

Duct B: From the unreinforced face, voids were identified at the ends and center of the duct. The existence of these voids was confirmed from the reinforced face, except that the void at the bottom was difficult to positively identify.

Duct C: The results were similar to duct B.

Duct D: Voids were positively identified at the ends and middle of the duct. The results from the unreinforced and reinforced faces were in good agreement.

Duct E: Based on the results from the reinforced face, it appears that there are extensive voids in the duct. It is remarkable, that positive indications of these voids were obtained from the unreinforced face despite the large depth.

Duct F: It was known that this duct was hollow. The test results were more conclusive from the reinforced face.

Duct G: The results from the unreinforced face, indicate the presence of two voids. Time constraints did not permit tests from the reinforced face.

DISCUSSION

This investigation represents the most challenging application to date of the impact-echo method. The test program included difficult conditions: the voids were small compared with their depth; the close spacing of the ducts, crossing of ducts, and reinforcing bars resulted in complex signals; the condition of the concrete surface at test points was highly erratic; and time constraints did not allow optimization of the test procedure. In addition, past analytical studies at NBS have been limited to axisymmetric problems [1,6,8-11], therefore, we do not have a clear understanding of the interaction of transient waves with cylindrical-shaped voids.

Based on the amplitude spectra, it appears that the specimen contained voids in addition to those present within tendon ducts. For tests from the reinforced face, the highest peak frequency associated with a void is 9.77 or 10.25 kHz along scan line A. However, examination of the waterfall plots in Appendix C reveals many instances of significant peaks at frequency values greater than those associated with voids in the ducts. From our understanding of the impact-echo method, these peaks must be caused by other discontinuities, such as honeycombing. For tests from the reinforced face, high frequency peaks exist in the spectra at points near the top and near the bottom of the wall.

For tests from the reinforced face the expected highest frequency peak is 21.15 kHz, which is associated with the outermost layer of reinforcement. As in the case of the unreinforced face, there were many test points with significant peaks at frequencies greater than 21.15 kHz. In heavily reinforced structures, honeycombing defects at the location of the steel are probable if care is not taken to vibrate the concrete. If honeycombing were located in the specimen at depths equal to the cover over the reinforcing bars (see Fig. 10), the following frequencies would be observed in the waterfall plots:

Depth (m)	Frequency (kHz)
0.050	42.3
0.075	28.2
0.085	24.9
0.100	21.2
0.110	19.2
0.120	17.6

The most likely depth of the honeycombing would be at the location of the horizontal bars, and the expected frequency would be between approximately 25 and 30 kHz. Significant peaks within this frequency range were observed at many tests points, such as AR4, AR8, AR11, BR1, BR4, BR5, BR6, BR8, CR0, CR3, CR4, CR7, CR8, CR12, DR3, DR4, DR9, DR10, DR13, ER3, and ER10. If possible, cores should be drilled at some of these test locations to verify whether honeycombing exists.

As mentioned, this investigation was a challenge for the impact-echo method. Many questions were raised that should be investigated through further research. For example, the impact-echo response due to voids in adjacent ducts needs to be understood. By performing a test along one tendon duct, it may be possible to reliably detect voids in adjacent ducts, thereby reducing the amount of testing. The impact-echo response of different types of discontinuities and the effects of voids within intersecting ducts need study. The relationships between void size, contact time, and void depth need to be understood. Aside from a better understanding of the wave propagation process, improved techniques for data reduction are needed.

POSTSCRIPT

After the above report was submitted to B.H. Levelton & Associates (BHL), the investigators were given a sketch showing the planned locations of the flaws. In addition, two cores were drilled from the specimen. Photographs and descriptions of the cores were also given to the investigators. The following discussion compares the impact-echo results with the planned locations of the flaws.

Figure 14 is a scale drawing of the planned flaw locations according the sketch provided by BHL. A comparison with Fig. 13 shows that the presence of all the defects was detected. However, there are two differences between the impact-echo results and the actual flaw configuration: 1) the size of the flaws tended to appear greater in the impact-echo results; and 2) more flaws were detected by impact-echo than those shown in the drawing of the planned locations of flaws (Fig. 14). Explanations for these differences follow.

In impact-echo testing, the stress pulse penetrates into the test object along spherical wavefronts. As a result, points within the object which are not directly below the test point will interact with the propagating waves. In addition, the boundaries of a defect will diffract incident waves. This means that the edge of a defect will reflect waves in all direction as shown by the P_d wavefront in Fig. 15. The presence of the defect can be detected without being directly above the defect. This is an inherent characteristic of impact-echo testing, and it is both an advantage and disadvantage of the method. The advantage is that the presence of a defect can be detected when

the test point is not located directly over the flaw. This means that it is possible to detect the presence of defects which are smaller than the spacing between the test points. The disadvantage is that the boundaries of a defect are not precisely determined.

Some of the impact-echo tests gave positive indications of voids at locations which did not contain preformed voids. For example, in duct D there appeared to be voids at the top and bottom ends; whereas, according to the plans, the ends were fully grouted. A possible explanation for this was provided by the description of a core drilled 390 mm from the top of the specimen along duct A. This core was 275 mm long, and it penetrated duct A where it was fully grouted. The description provided by BHL stated that "shrinkage of grout has caused a separation of 0.05 mm between the grout and inside wall of the duct around 20 percent of the circumference." Such a shrinkage crack introduces an air gap between the grout and tendon duct, and the duct will respond to propagating waves as through it was empty. Thus it is entirely possible that such shrinkage occurred in other ducts. Another possible reason for the larger number of flaw locations which were detected by the impact-echo method is poor consolidation of the concrete adjacent to the ducts. Lack of consolidation was noted at the exposed end of duct F. The core taken along duct A cut through the duct. The core broke at the far side of the duct. The photograph of the fractured face of the core showed significant voids adjacent to the duct. Thus it is believed that the impact-echo results indicated more voids because of the presence of shrinkage cracks between the grout and ducts or because of poor consolidation adjacent to the ducts.

REFERENCES

1. Sansalone, M., and Carino, N.J., "Impact-Echo: A Method for Flaw Detection in Concrete Using Transient Stress Waves," NBSIR 86-3452, National Bureau of Standards, Sept., 1986, 222 pp.

2. Carino, N.J., "Laboratory Study of Flaw Detection in Concrete by the Pulse-Echo Method," in In Situ/Nondestructive Testing of Concrete, V.M. Malhotra, Editor, ACI SP-82, American Concrete Institute, 1984, pp. 557-579.

3. Carino, N.J., Sansalone, M., and Hsu, N.N., "A Point Source - Point Receiver Technique for Flaw Detection in Concrete," Journal of the American Concrete Institute, Vol. 83, No. 2, April, 1986, pp. 199-208.

4. Carino, N.J., Sansalone, M., and Hsu, N.N., "Flaw Detection in Concrete by Frequency Spectrum Analysis of Impact-Echo Waveforms," International Advances in Nondestructive Testing, 12th Edition, W.J. McGonnagle, Ed., Gordon & Breach Science Publishers, New York, 1986, pp. 117-146.

5. Sansalone, M., and Carino, N.J., "Laboratory and Field Study of the Impact-Echo Method for Flaw Detection in Concrete," to be published by the American Concrete Institute, 1988.

6. Sansalone, M., and Carino, N. J., "Detecting Honeycombing, the Depth of Surface-opening Cracks, and Ungrouted Ducts Using the Impact-Echo Method," accepted for publication in Concrete International, 1987.

7. Carino, N.J., and Sansalone, M., "Pulse-Echo Method for Flaw Detection in Concrete," NBS Technical Note 1199, Gaithersburg, Maryland, July, 1984.

8. Sansalone, M., Carino, N.J., and Hsu, N.N., "A Finite Element Study of Transient Wave Propagation in Plates," Journal of Research of the National Bureau of Standards, Vol 92, No. 4, July-August, 1987, pp 267-278.

9. Sansalone, M., Carino, N.J.,and Hsu, N.N., "A Finite Element Study of the Interaction of Transient Stress Waves with Planar Flaws," Journal of Research of the National Bureau of Standards, Vol 92, No. 4, July-August, 1987, pp 279-290.

10. Sansalone, M., and Carino, N.J., "Transient Impact Response of Thick Circular Plates," Journal of Research of the National Bureau of Standards, Vol 92, No. 6, Nov.-Dec., 1987, pp 355-367

11. Sansalone, M., and Carino, N.J., "Transient Impact Response of Plates Containing Flaws," Journal of Research of the National Bureau of Standards, Vol 92, No. 6, Nov.-Dec., 1987, pp 369-381.

Table 1 Expected Frequencies for Various Paths from Test Points to Voids

Path Number	Distance m	Frequencies (kHz) P-Wave Calculated	P-Wave Possible	S-wave Calculated	S-wave Possible
1	0.340	6.22	5.86/6.35		
2	0.215	9.84	9.77/10.25		
3	0.572	3.70	3.42/3.91	2.23	1.95/2.44
4	0.465	4.55	4.39/4.88		
5	0.787	2.69	2.44/2.93	1.61	1.46/1.95
6	0.715	2.96	2.93		
7	0.396	5.34	5.37	3.20	2.93/3.42
8	0.590	3.58	3.42/3.91		

C_p = 4230 m/s
C_s = 2540 m/s

Table 2 Expected Frequencies Associated with P-wave Reflections from Bars

Cover Distance (m)	P-Wave Frequencies (kHz) Calculated	Possible
0.050	21.15	20.98
0.075	14.10	14.16
0.085	12.44	12.21
0.100	10.58	10.74
0.110	9.61	9.77
0.120	8.81	8.79

C_p = 4230 m/s

Table 3 Results of data interpretation

Test Point	Void	Test Point	Void	Test Point	Void	Test Point	Void
A0	No test	AR0		B0	Y?	BR0	Y?
A1	Y?	AR1		B1	Y	BR1	Y
A2	Y	AR2		B2	Y?	BR2	Y?
A3	Y?	AR3		B3		BR3	Y?
A4	Y	AR4		B4		BR4	
A5	Y	AR5		B5		BR5	Y
A6	Y?	AR6		B6	Y	BR6	Y
A7	Y	AR7		B7	Y	BR7	Y?
A8	Y?	AR8		B8	Y?	BR8	
A9	Y	AR9		B9	Y?	BR9	
A10	Y?	AR10	Y	B10		BR10	
A11	Y	AR11		B11	Y	BR11	Y?
A12	Y	AR12		B12	Y?	BR12	Y?
A13						BR12.5	Y?
C0	Y?	CR0	Y?	D0	Y	DR0	Y?
C1	Y?	CR1		D1	Y	DR1	Y
C2	Y	CR2	Y	D2	Y?	DR2	
C3	Y?	CR3	Y?	D3		DR3	Y?
C4		CR4	Y?	D4		DR4	Y
C5		CR5	Y	D5		DR5	Y
C6	Y	CR6		D6	Y	DR6	Y
C7	Y?	CR7	Y?	D7	Y	DR7	Y
C8	Y?	CR8	Y?	D8		DR8	Y
C9	Y	CR9	Y?	D9		DR9	
C10	Y?	CR10	Y?	D10		DR10	
C11	Y?	CR11		D11		DR11	Y
C12	Y?	CR12		D12	Y	DR12	Y
						DR13	Y
E0		ER0	Y(1/2)	F0	Y	FR0	Y?
E1	Y	ER1	Y?	F1	Y	FR1	Y
E2		ER2	Y	F2	Y	FR2	Y
E3	Y	ER3	Y	F3		FR3	Y
E4	Y	ER4	Y?	F4	Y?	FR4	Y?
E5		ER5	Y	F5	Y?	FR5	Y
E6		ER6	Y	F6	Y?	FR6	Y?
E7		ER7	Y?	F7	Y?	FR7	
E8		ER8	Y	F8		FR8	
E9	Y	ER9		F9		FR9	
E10		ER10					
E11		ER11	Y				
E12	Y	ER12	Y				
		ER13	Y				

Table 3 Results of data interpretation (Continued)

Test Point	Void
G0	Y?
G1	Y?
G2	Y
G3	
G4	
G5	Y(1/2)?
G6	Y(1/2)
G7	Y(1/2)
G8	Y(1/2)?
G9	

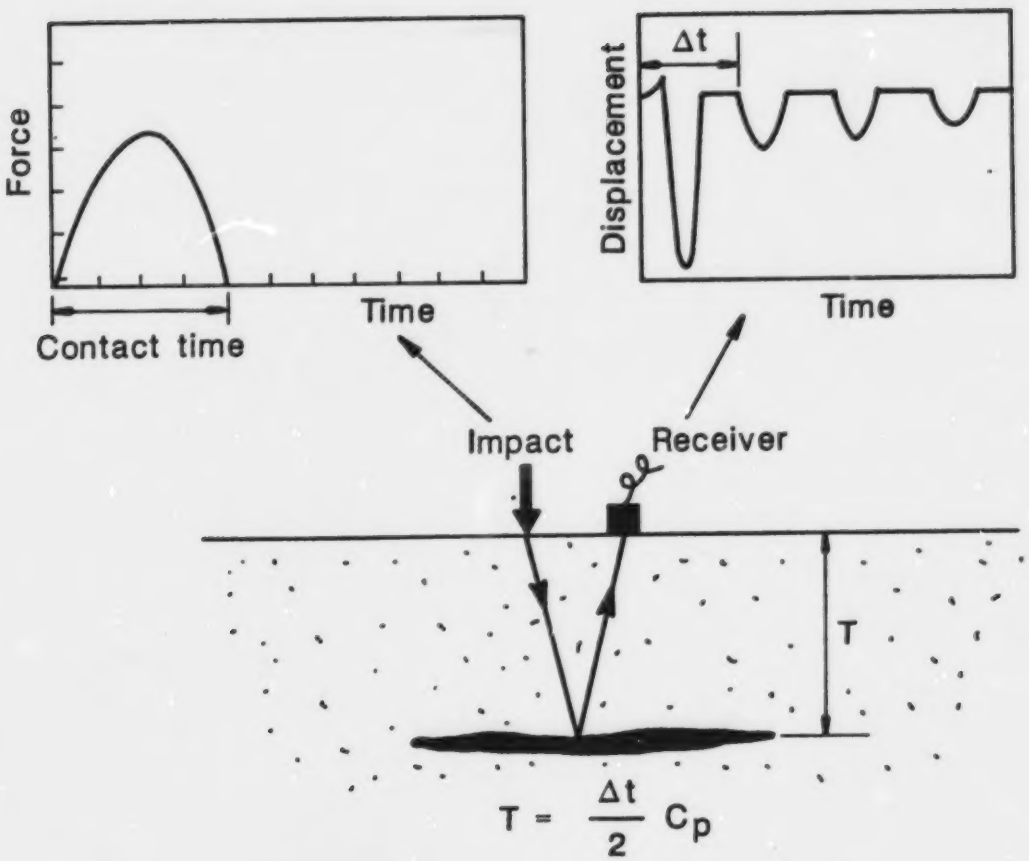

Figure 1 Principle of the impact-echo method.

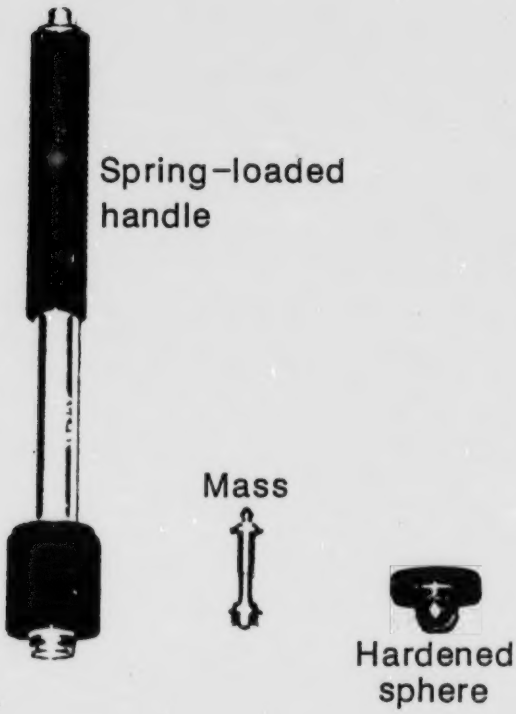

Figure 2 Modified mechanical impactor used in investigation

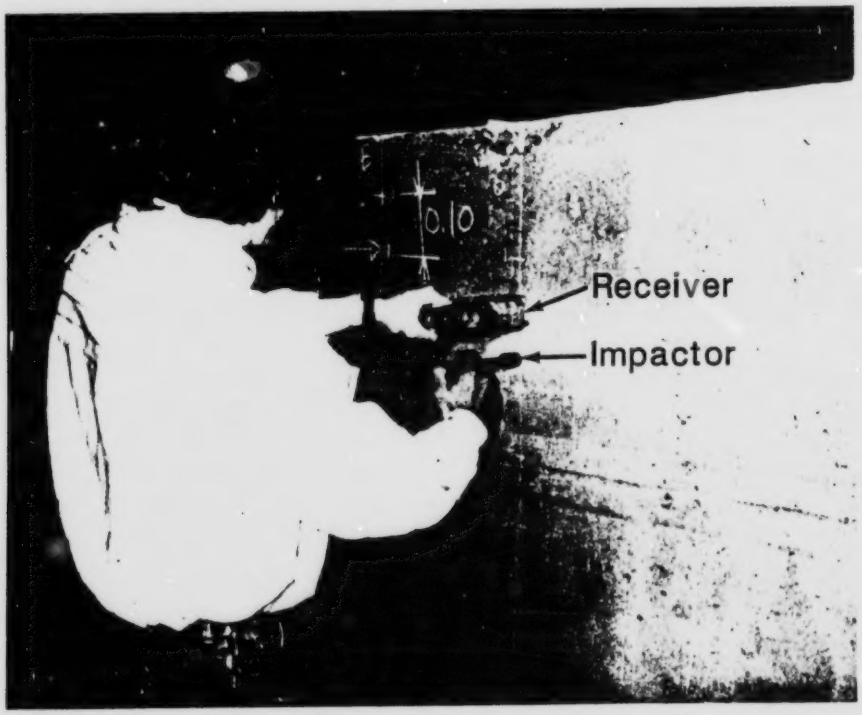

Figure 3 Impact-echo test being performed on test specimen

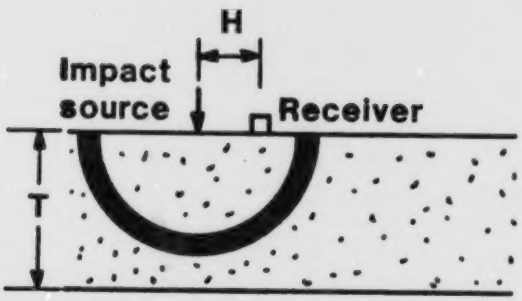

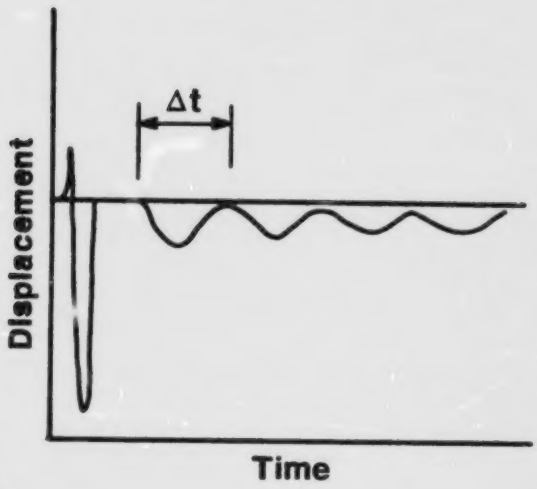

For small H:

$$\Delta t = \frac{2T}{C_p}$$

$$f = \frac{1}{\Delta t} = \frac{C_p}{2T}$$

$$T = \frac{C_p}{2f}$$

Figure 4 Principle of frequency analysis

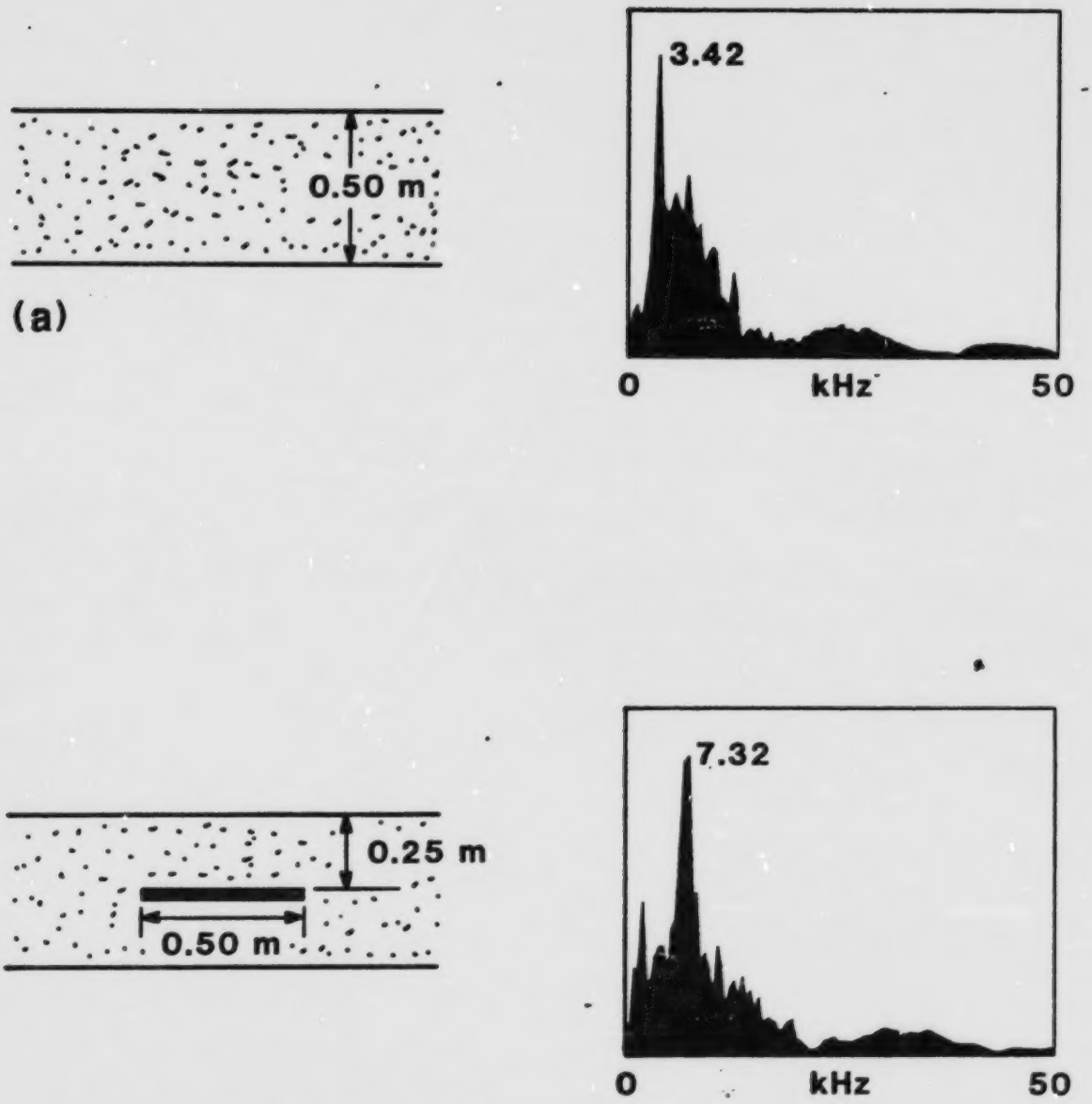

Figure 5 Examples of amplitude spectra: a) for test over a solid portion of a 0.5-m thick concrete slab; b) for a test over a disk-shaped void embedded in another portion of the same slab.

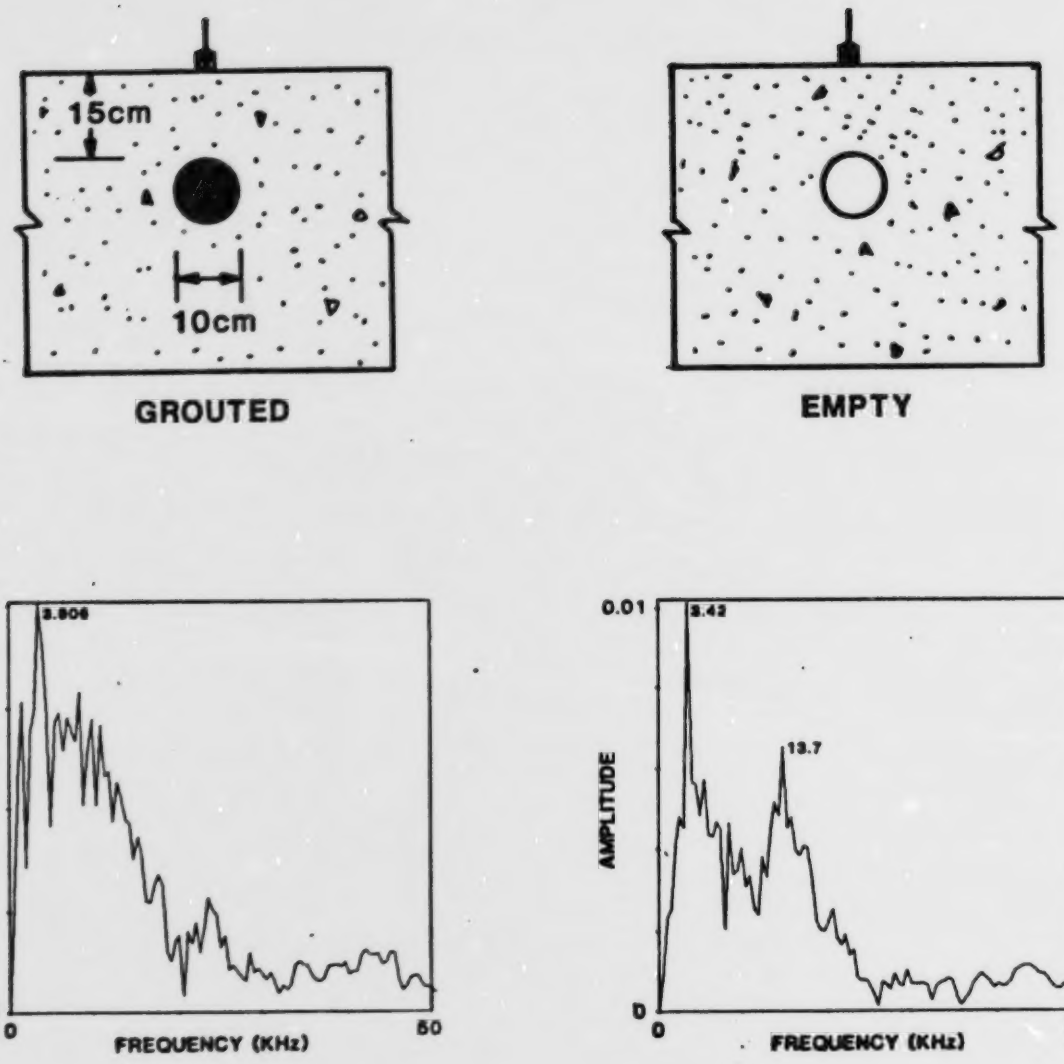

Figure 6 Results from feasibility study of voids in a duct: a) amplitude spectrum for test over grouted portion of duct; b) spectrum for test over hollow duct.

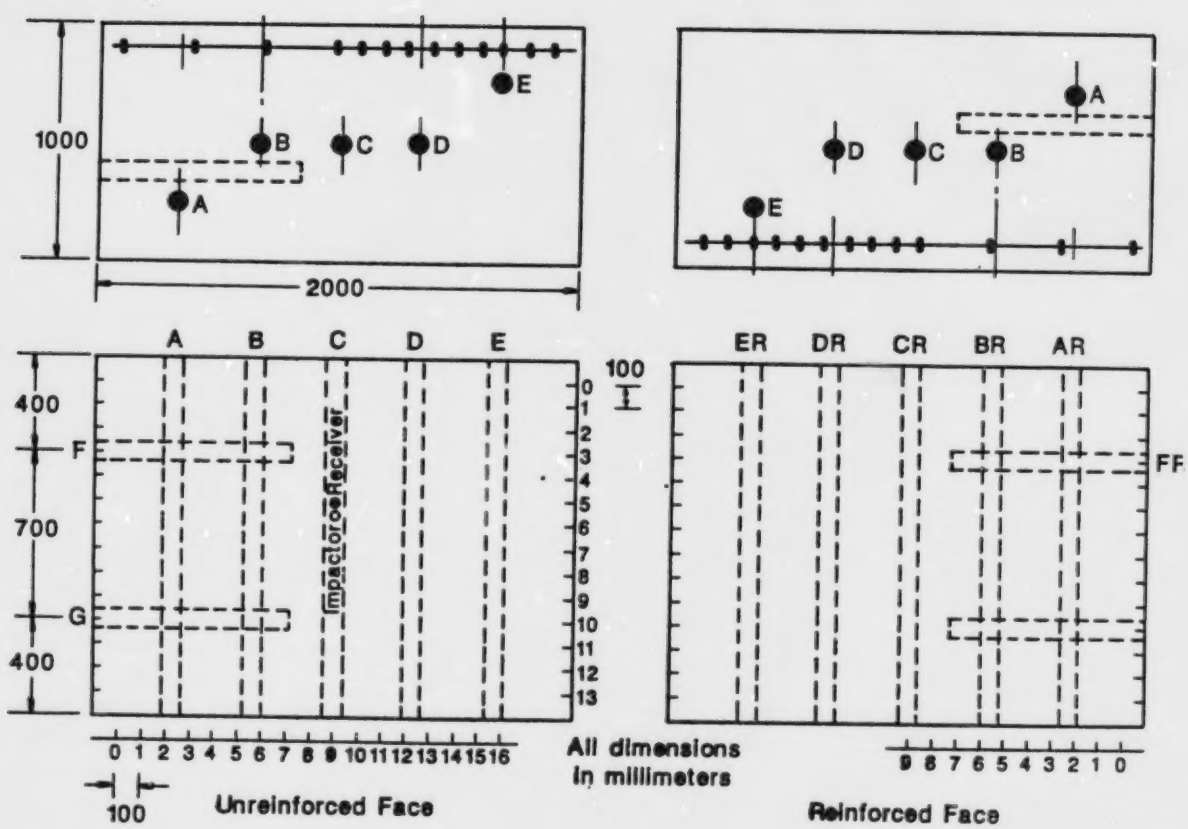

Figure 7 Duct designation and location of test points on faces of specimen

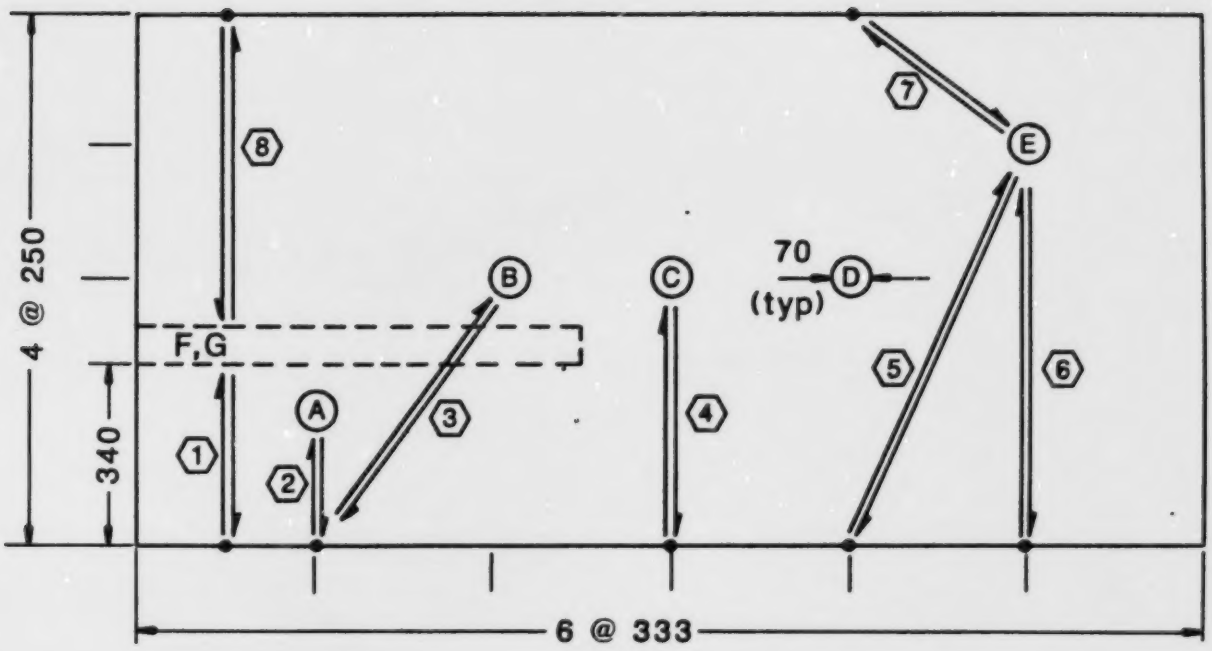

All dimensions in millimeters

Figure 8 Reflection paths

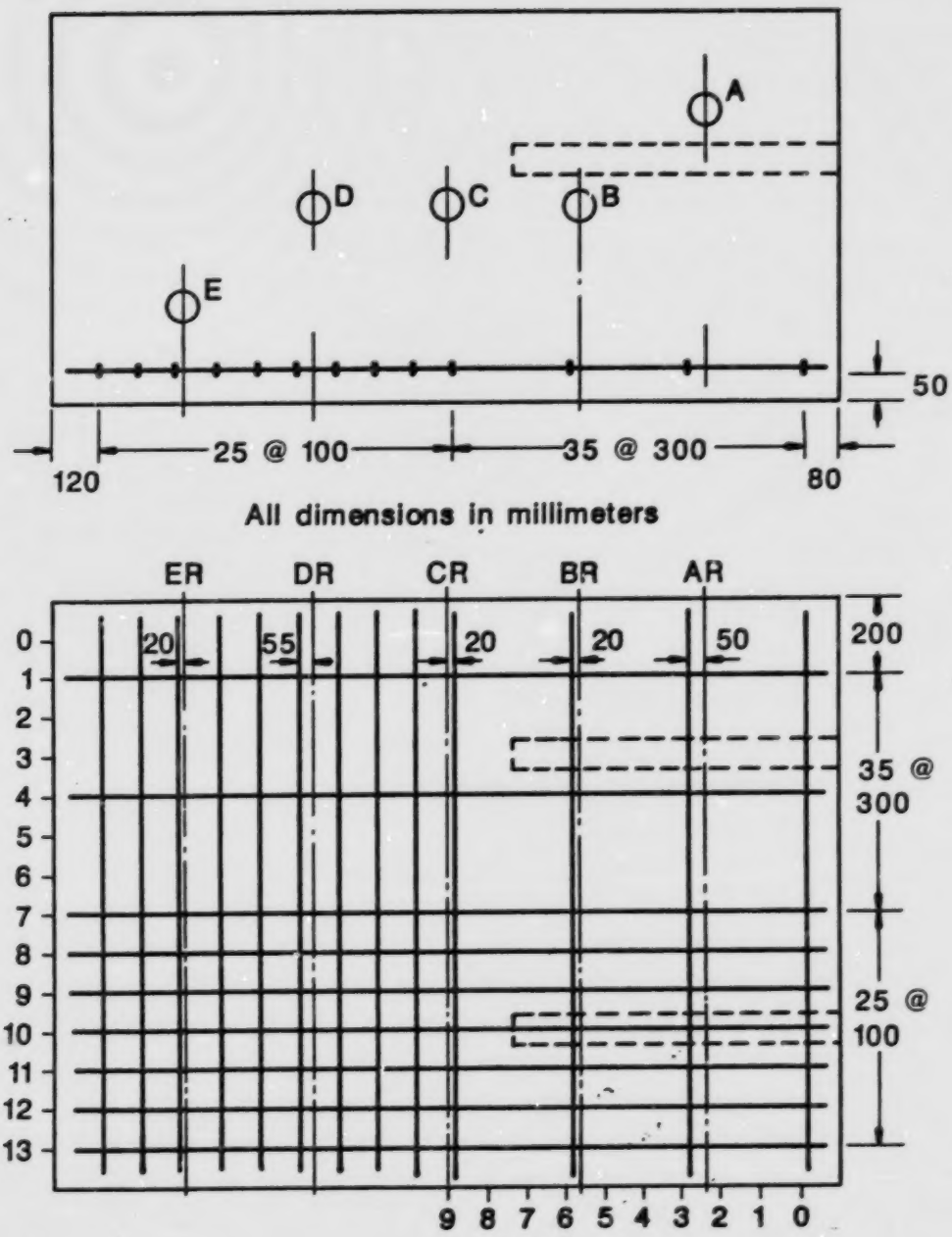

Figure 9 Reinforcement pattern and locations of scan lines on reinforced face

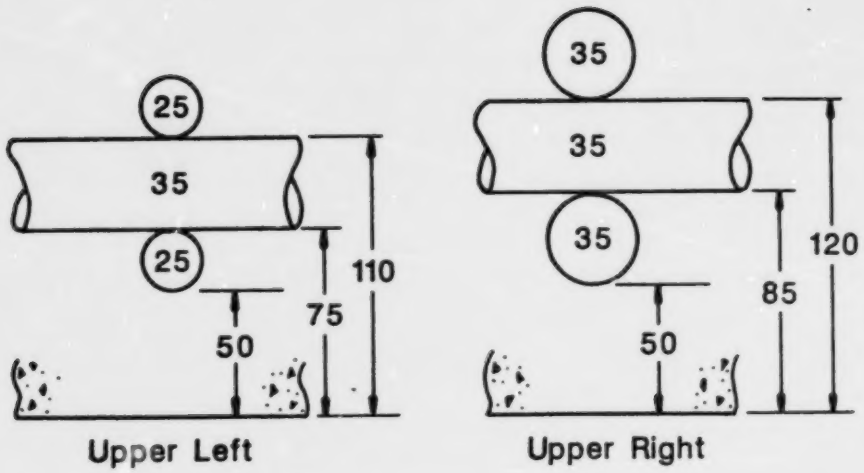

All dimensions in millimeters

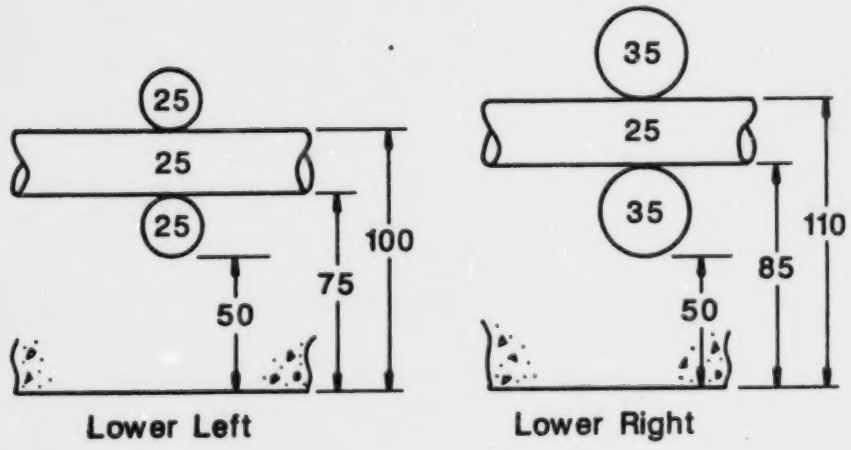

Figure 10 Depth of cover to bar layers in different quadrants

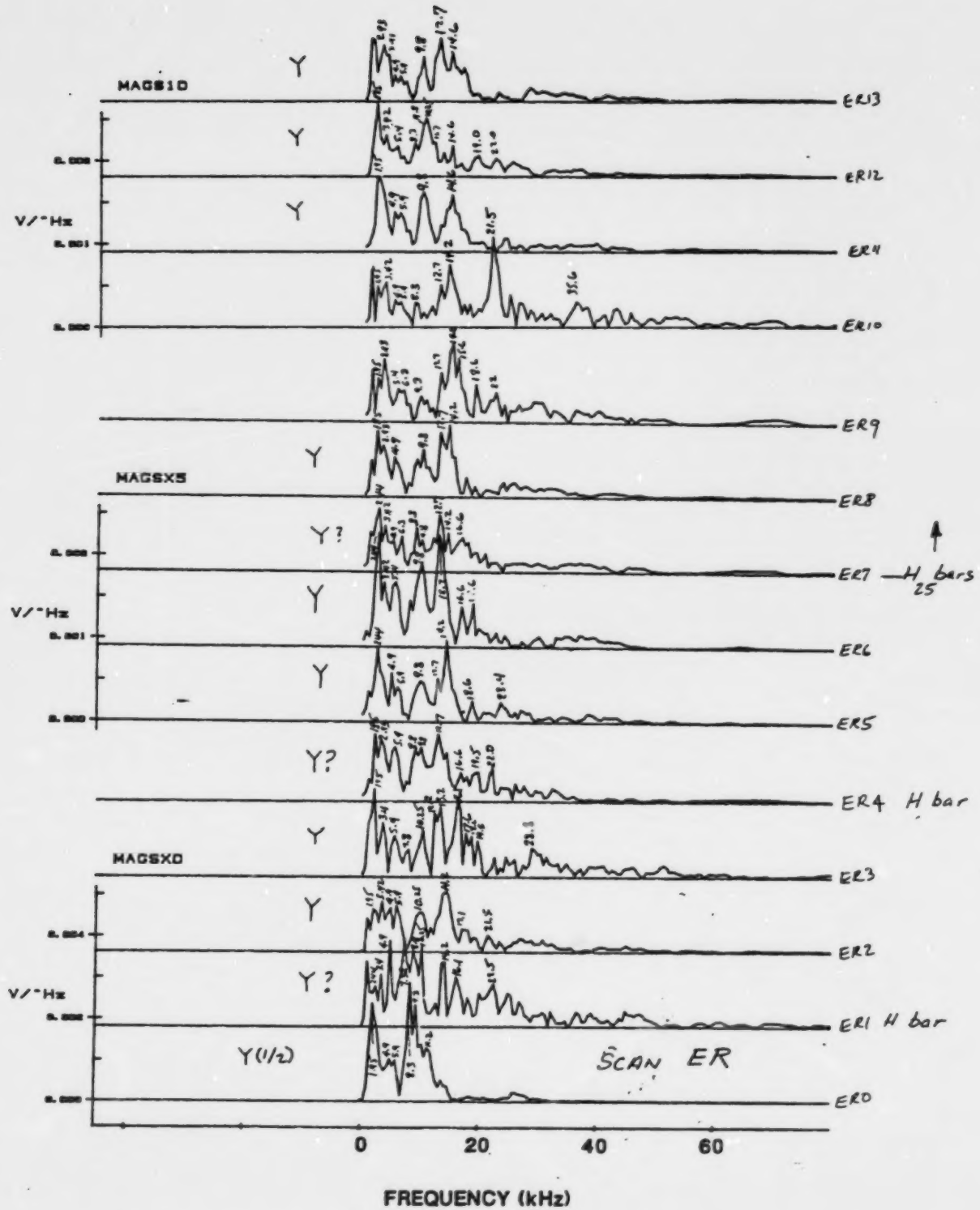

Figure 11 Waterfall plot for scan line ER

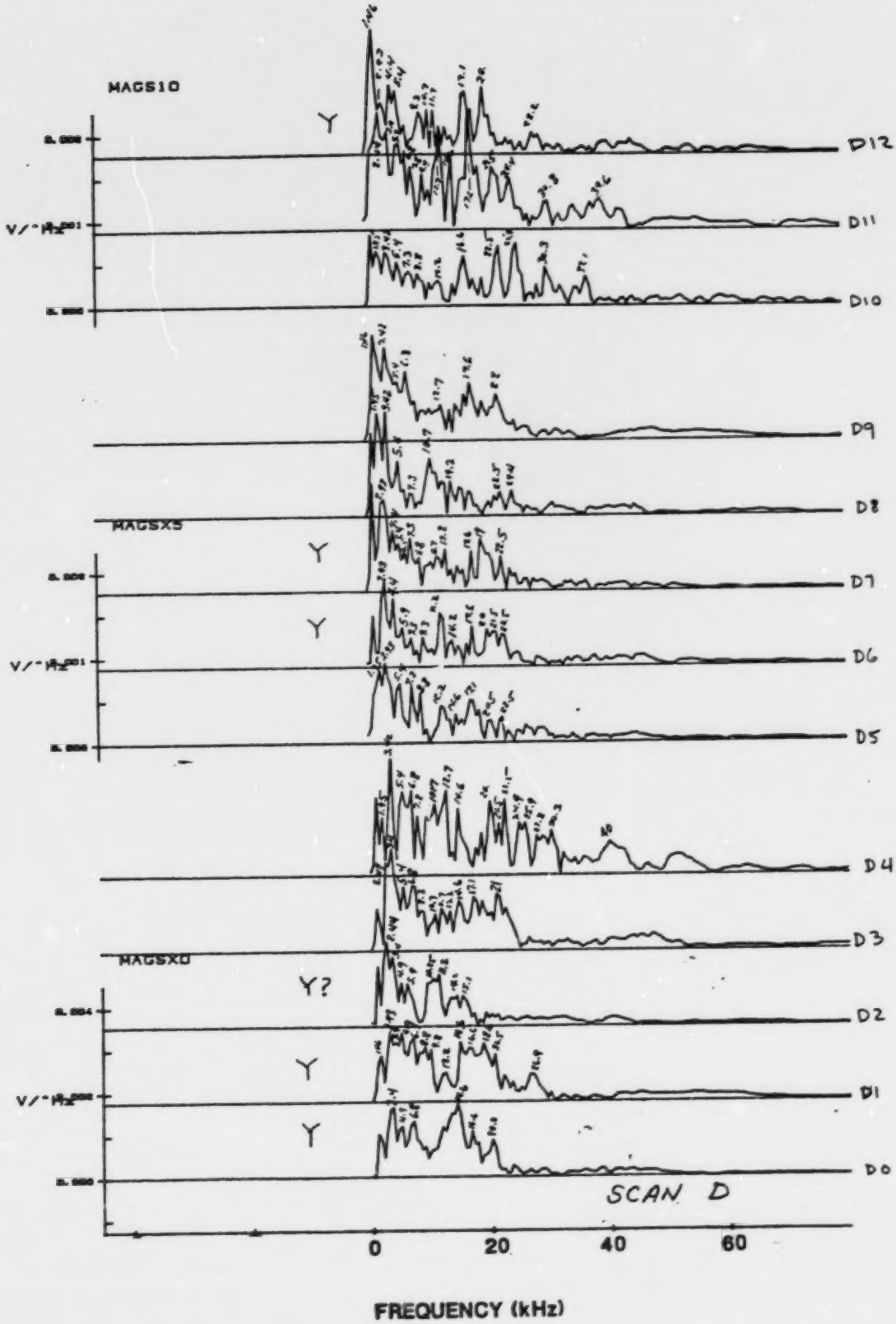

Figure 12 Waterfall plot for scan line D

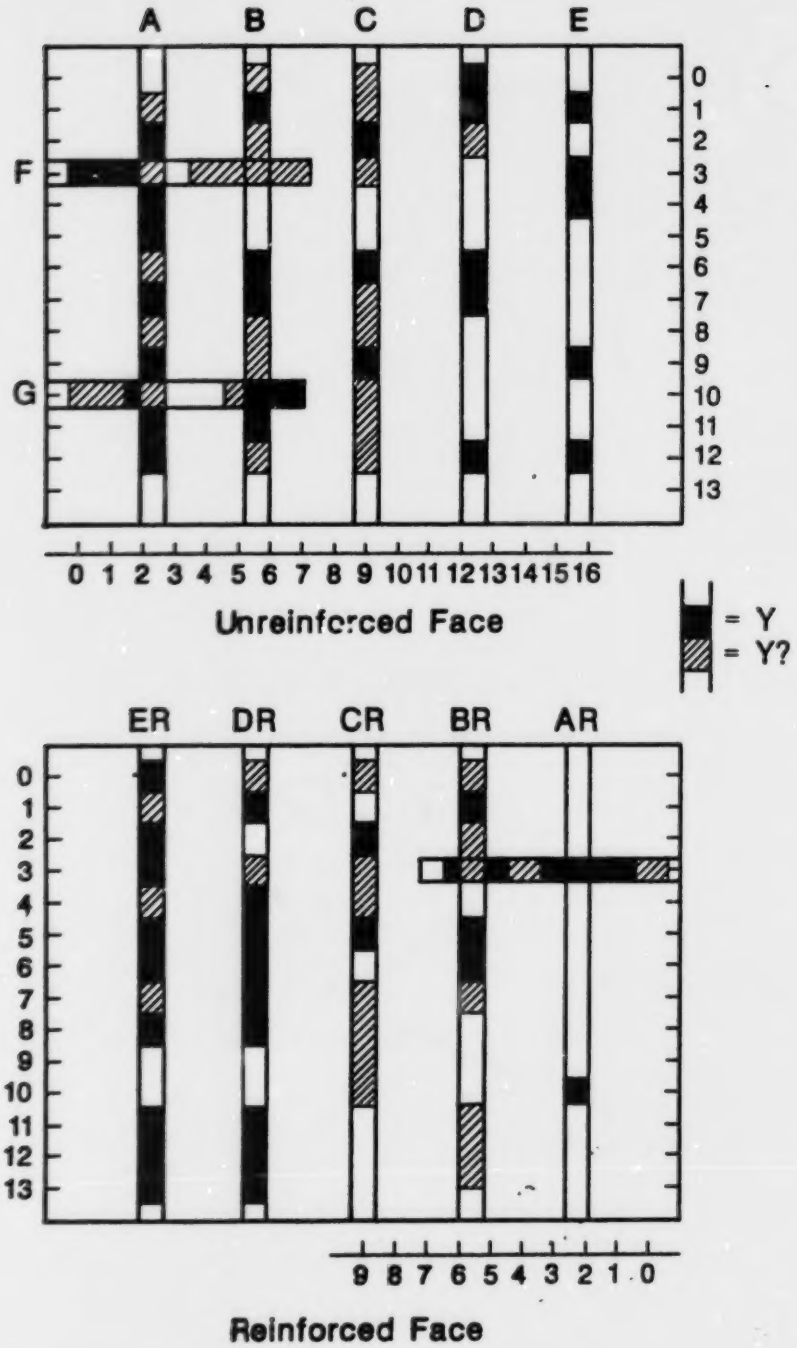

Figure 13 Test points marked as "Y" and "Y?"

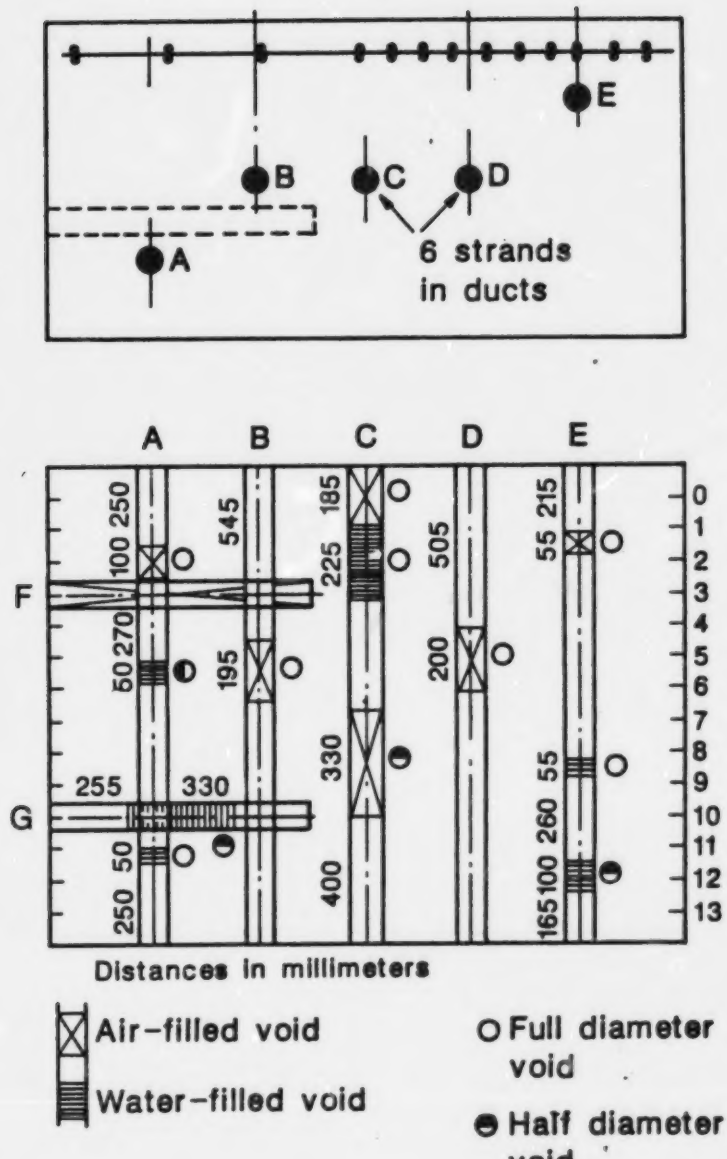

Figure 14 Planned locations of the voids in the tendon ducts

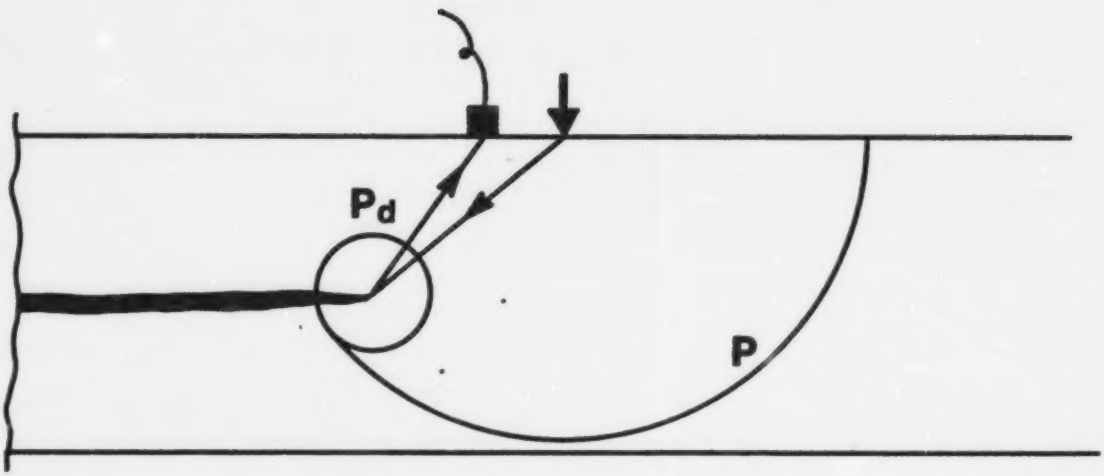

Figure 15 Diffraction of a wave at the edge of a defect

APPENDIX A

Frequency Analysis

An impact on the top surface of an infinite plate results in multiple reflections of stress waves between the top and bottom surfaces. The multiple reflections give a periodic character to the displacement response at points close to the impact point. In finite solids containing flaws, multiple reflections occur between a variety of interfaces and free boundaries. As a result, time domain waveforms become complex and difficult to interpret. However, if the waveforms are transformed into the frequency domain, multiple reflections from each interface become dominant peaks in the amplitude spectrum - at frequency values corresponding to the frequency of arrival of reflections from each interface. These frequencies can be used to calculate the location of each interface. It has been found that, for impact-echo testing, data interpretation is much simpler and quicker in the frequency domain than in the time domain.

The transformation from the time to the frequency domain is based on the idea that any waveform can be represented as a sum of sine curves, each with a particular amplitude, frequency, and phase shift. This transformation is carried out using the principles of the Fourier transform. As an example, Fig. A1(a) shows the digital time domain waveform, g(t), given by the function:

$$g(t) = \sin 2\pi(20)t + 2 \sin 2\pi(40)t + 3 \sin 2\pi(60)t \qquad (A.1)$$

where t = time, s.

This function is composed of three sine curves of different amplitudes having frequencies of 20, 40, and 60 Hz.

The digital sample in Fig. A1(a) is made up of 256 discrete points. The time interval between points is 0.001 seconds; this is equivalent to a sampling frequency of 1000 Hz.

The objective of frequency analysis is to determine the dominant frequency components in the digital waveform. This is most easily accomplished by using the fast Fourier transform (FFT) technique. The FFT results can be used to construct the amplitude spectrum, which gives the amplitudes of the various frequency components in the waveform. The amplitude spectrum obtained by the FFT contains half as many points as the time domain waveform, and the maximum frequency in the spectrum is one-half the sampling rate, which for this example is 500 Hz. Figure A1(b) shows the initial portion of the computed amplitude spectrum; the peaks occur at 20, 40, and 60 Hz. Each of the peaks corresponds to one of the component sine curves in Eq. [A.1].

With the FFT technique, the frequency interval in the spectrum is equal to the sampling frequency divided by the number of points in the waveform. For this example, the interval is equal to 1000 Hz divided by 256, or 3.9 Hz. Since the frequency interval is proportional to the sampling frequency, a slower sampling rate enhances resolution in the frequency domain. However, to avoid errors in frequency analysis, the sampling frequency should be greater than twice the maximum frequency that appears in the time domain waveform.

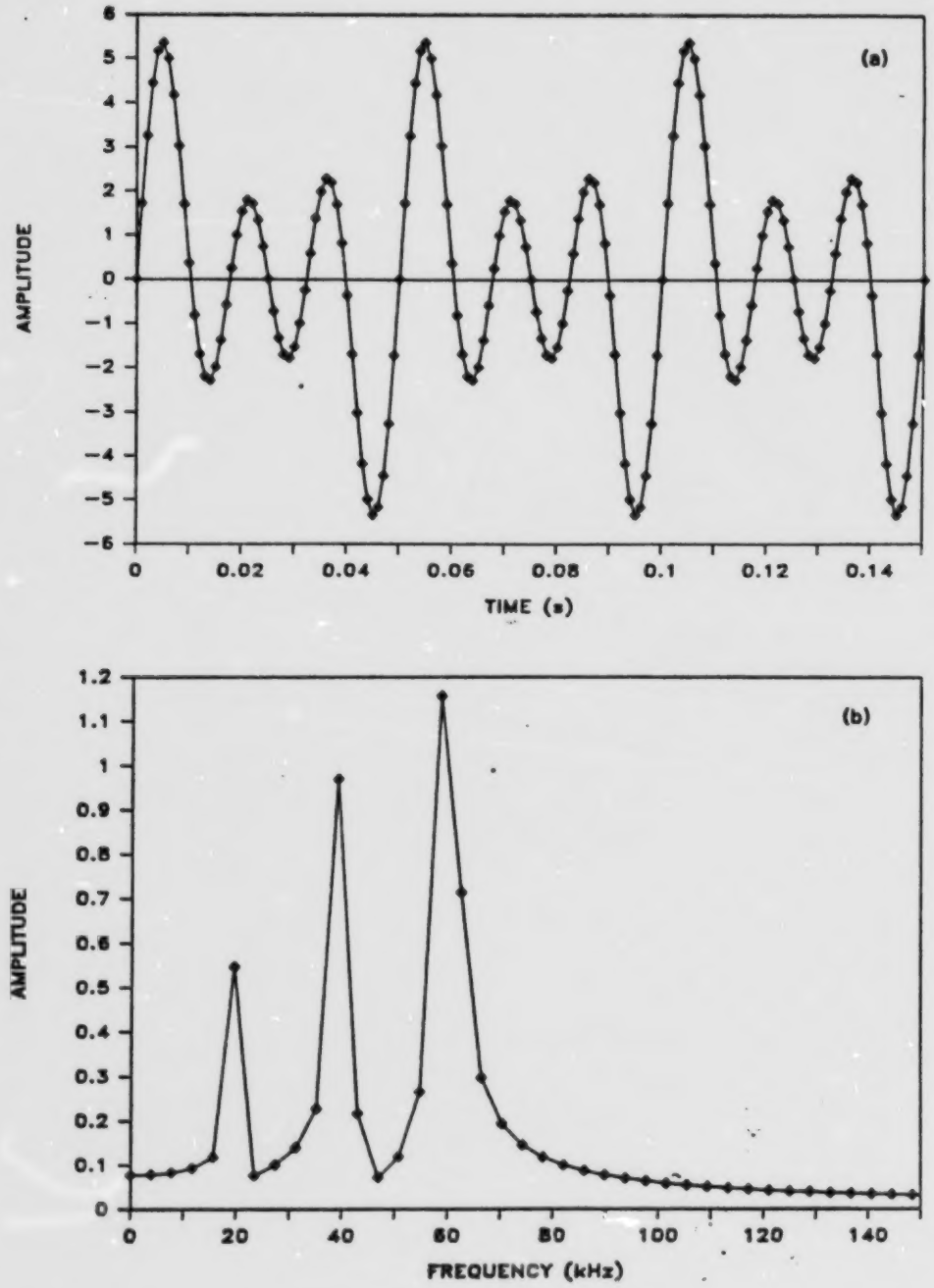

Figure A1 Example of frequency analysis using the fast Fourier transform technique: a) digital waveform, b) initial portion of corresponding amplitude spectrum.

APPENDIX B

Wave Reflection from a Concrete/Steel Interface

When a stress wave is incident upon an interface between dissimilar materials both reflection and refraction occur at the interface. The portions of the incident energy that are reflected and refracted depend upon the angle of the incident wave and the acoustic impedance (product of wave speed and density) of the two materials. At a stress free interface, such as concrete/air, and for normal incidence, almost total reflection occurs because the acoustic impedance of air is negligible compared with that of concrete.

If steel is embedded in concrete, wave reflections occur at the concrete/steel interface because the acoustic impedance of the steel is about 5 times that of concrete. However, the higher acoustic impedance of steel causes a difference in the nature of wave reflection at a concrete/steel interface compared with that at a concrete/air interface. This difference is explained qualitatively in Fig. B1, which shows an infinite concrete plate bounded by air (Fig. B1(a)) and an infinite concrete plate bounded on the bottom by steel and on the top by air (Fig. B1(b)).

First, consider the case where impact occurs on a surrounded by air (Fig. B1(a)). The P-wave generated by the impact is a compression wave (the particles are pushed together). When this wave is incident upon the bottom surface of the plate, it is reflected as a tension wave (the particles are pulled apart). This tension wave propagates back up through the plate to be reflected at the top surface as a compression wave, and the cycle begins again. Each P-wave arriving at the top of the plate is a tension wave which causes a downward displacement of the surface. The period between successive downward dips in the waveform is the time between successive P-wave arrivals, that is, the time for a P-wave to travel twice the thickness of the plate. Thus, if an amplitude spectrum were computed, the frequency value of the peak in the spectrum would be associated with twice the plate thickness.

Next, consider impact on the top surface of a concrete plate which is in contact with a thick layer of steel at its bottom surface (Fig. B1(b)). When the initial compression wave generated by the impact is incident upon the concrete/steel interface it does not change sign because the steel has a higher acoustic impedance than the concrete. Thus the incident wave is reflected as a compression wave. When this compression wave reaches the top surface of the plate it causes an upward displacement of the surface. However, since the top surface of the plate is a concrete/air, the incident compression wave is reflected as a tension wave. This wave propagates down through the plate and is reflected at the concrete/steel interface unchanged. When this tension wave reaches the top surface of the plate it causes a downward displacement of the surface. The incident tension wave is reflected as a compression wave and the cycle begins again. Therefore, in the surface displacement waveform (Fig. B1(b)), the periodicity of displacements (time between successive upward or downward displacements) is twice as long as in waveform obtained from the plate with free boundaries (Fig. B1(a)). This explanation has been verified by a finite element analysis of a layered concrete/steel plate.

The period in the waveform shown in Fig. B1(b) is equal to the time it takes for a wave to travel four thicknesses of the plate. Therefore, the value of the peak in the amplitude spectrum obtained by transforming this

waveform is associated with four plate thicknesses. For equal thicknesses of the concrete plates, the peak frequency value in Fig. B1(b) will be half that obtained from the waveform shown in Fig. B1(a).

Based on this qualitative analysis, the frequency peak associated with reflections from steel bars would be expected to occur at a frequency value that is approximately one-half the value that would be obtained for reflections from a concrete/air interface at the same depth as the bars. Therefore, to determine the depth of a concrete/steel interface from the peak in an amplitude spectrum, Eq. (2) (derived for a plate with stress free boundaries) can be modified:

$$T = \frac{C_p}{2\ (2f_p)} \qquad (B.1)$$

Figure B.2 shows the results of an impact-echo test on concrete slab containing a disk-shaped void and reinforcing bars. From tests over solid portions of the slab, the P-wave speed was found to be 3910 m/s. The large peak at 7.81 kHz corresponds to a depth of 0.25 m, which agrees with the planned distance to the void of 0.26 m. The high frequency peaks at 14.6 and 21 kHz are due to reflections from the bars. Using Eq. B.1, the corresponding depths are 0.07 m and 0.05 m, which agree with the planned depths of the bars. Thus the applicbility of Eq. B.1 has been verified.

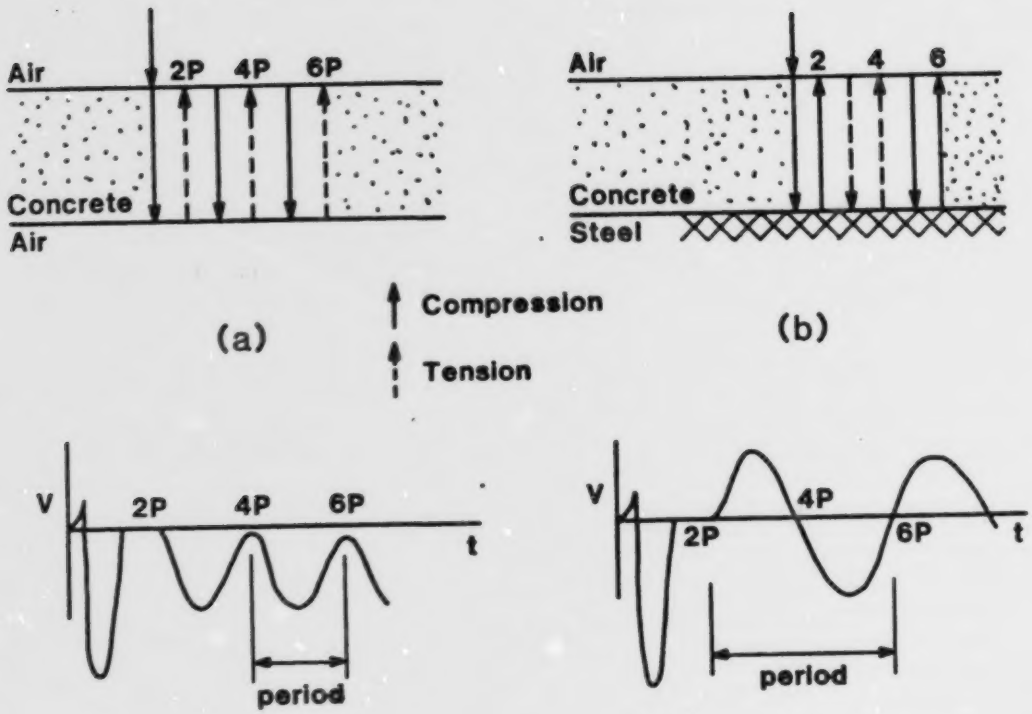

Figure B1 Effect of nature of the bottom interface of a plate on the resulting waveform recorded at the top surface: a) concrete/air interface, b) concrete/steel interface.

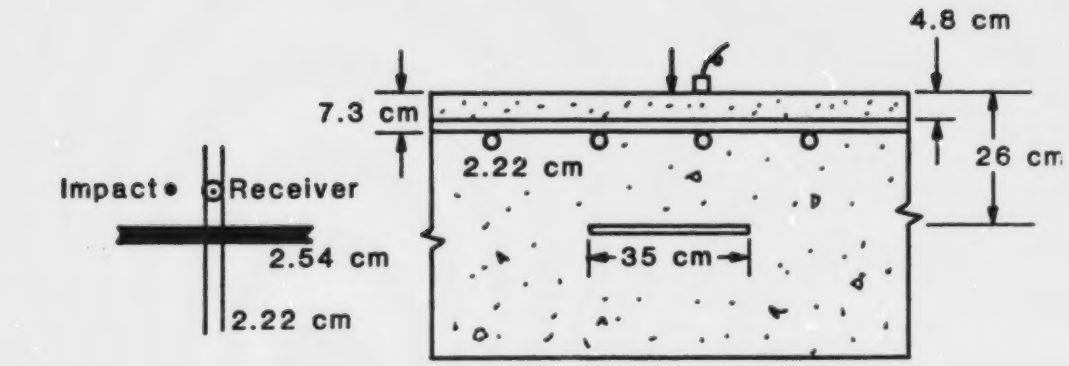

(a)

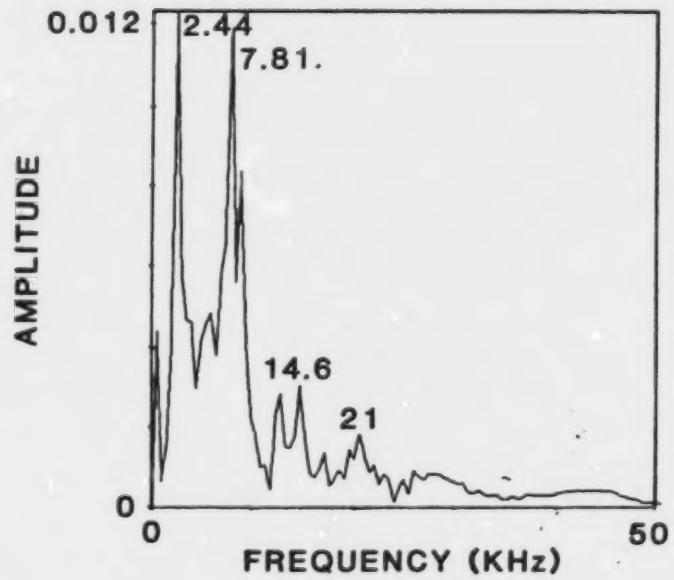

(b)

Figure B.2 Results of an impact-echo test on reinforced concrete slab: a) test geometry; b) resulting amplitude spectrum.

APPENDIX C

Waterfall Plots

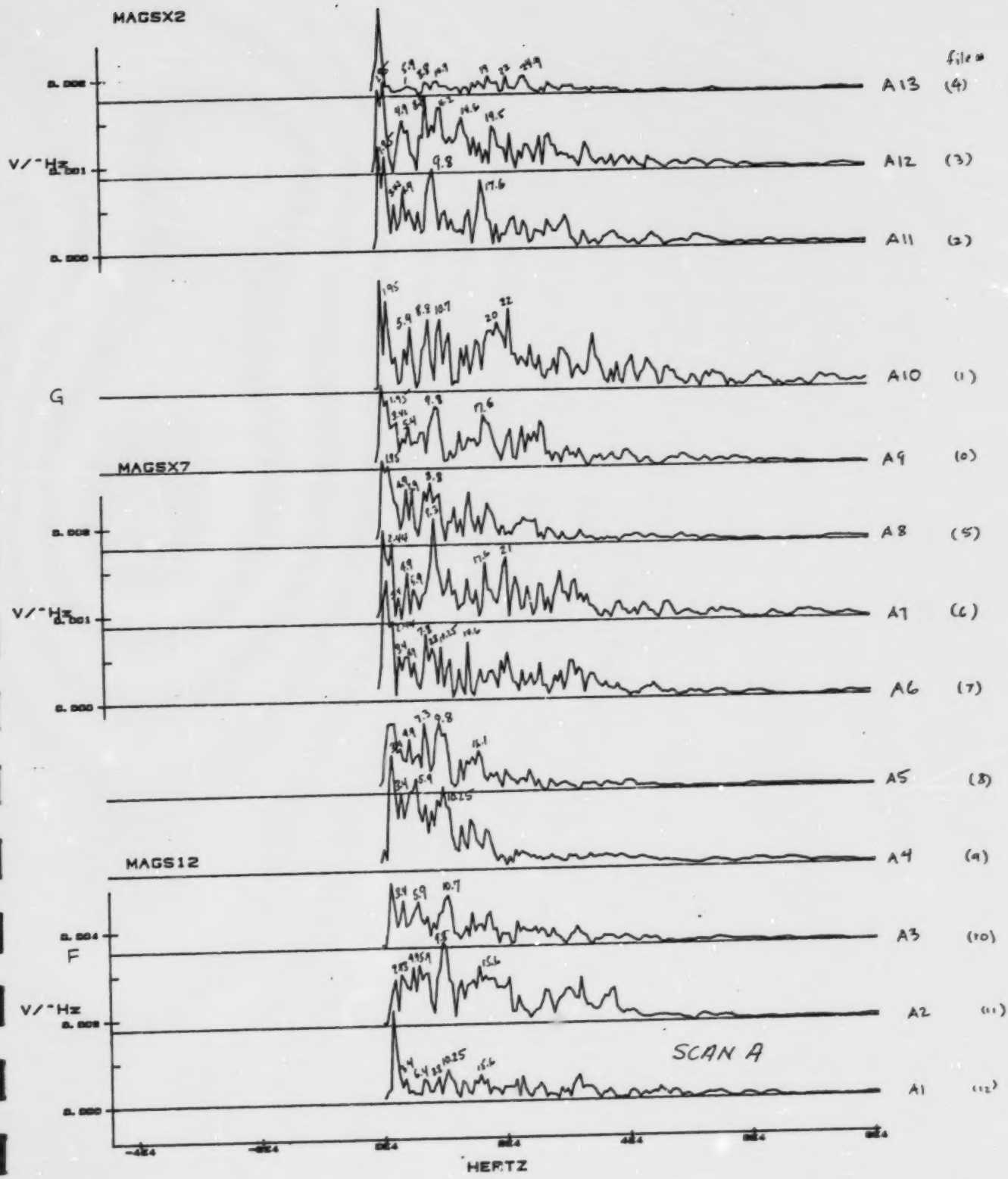
MAGSX2
MAGSX7
MAGS12
V/√Hz
G
F
A13 (4)
A12 (3)
A11 (2)
A10 (1)
A9 (0)
A8 (5)
A7 (6)
A6 (7)
A5 (8)
A4 (9)
A3 (10)
A2 (11)
A1 (12)
file #
SCAN A
HERTZ

Y = 0.45
kHz max

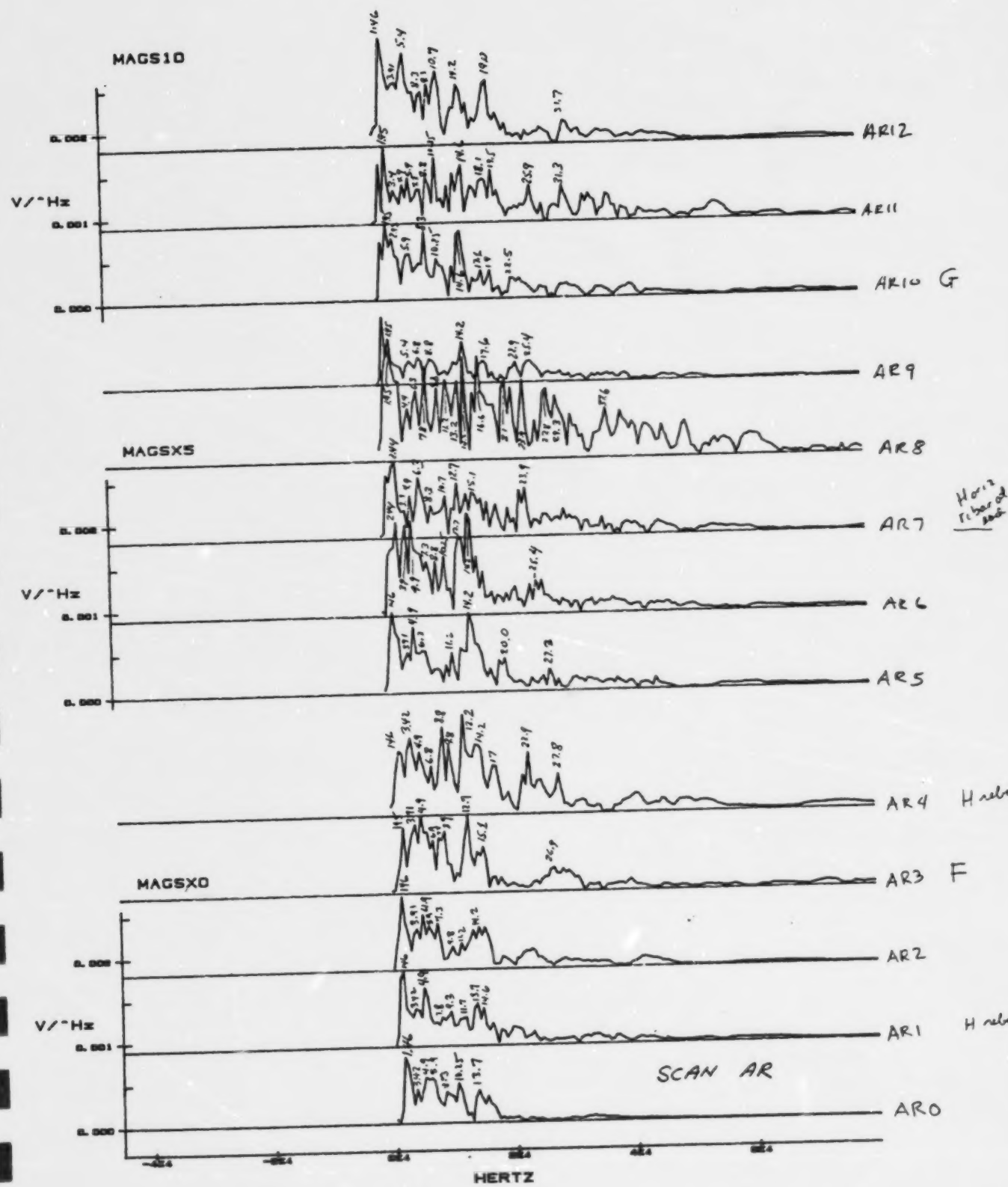
MAGS10
MAGSX5
MAGSX0
V/√Hz
0.008
0.001
0.000
AR12
AR11
AR10
AR9
AR8
AR7
AR6
AR5
AR4
AR3
AR2
AR1
AR0
G
F
SCAN AR
HERTZ

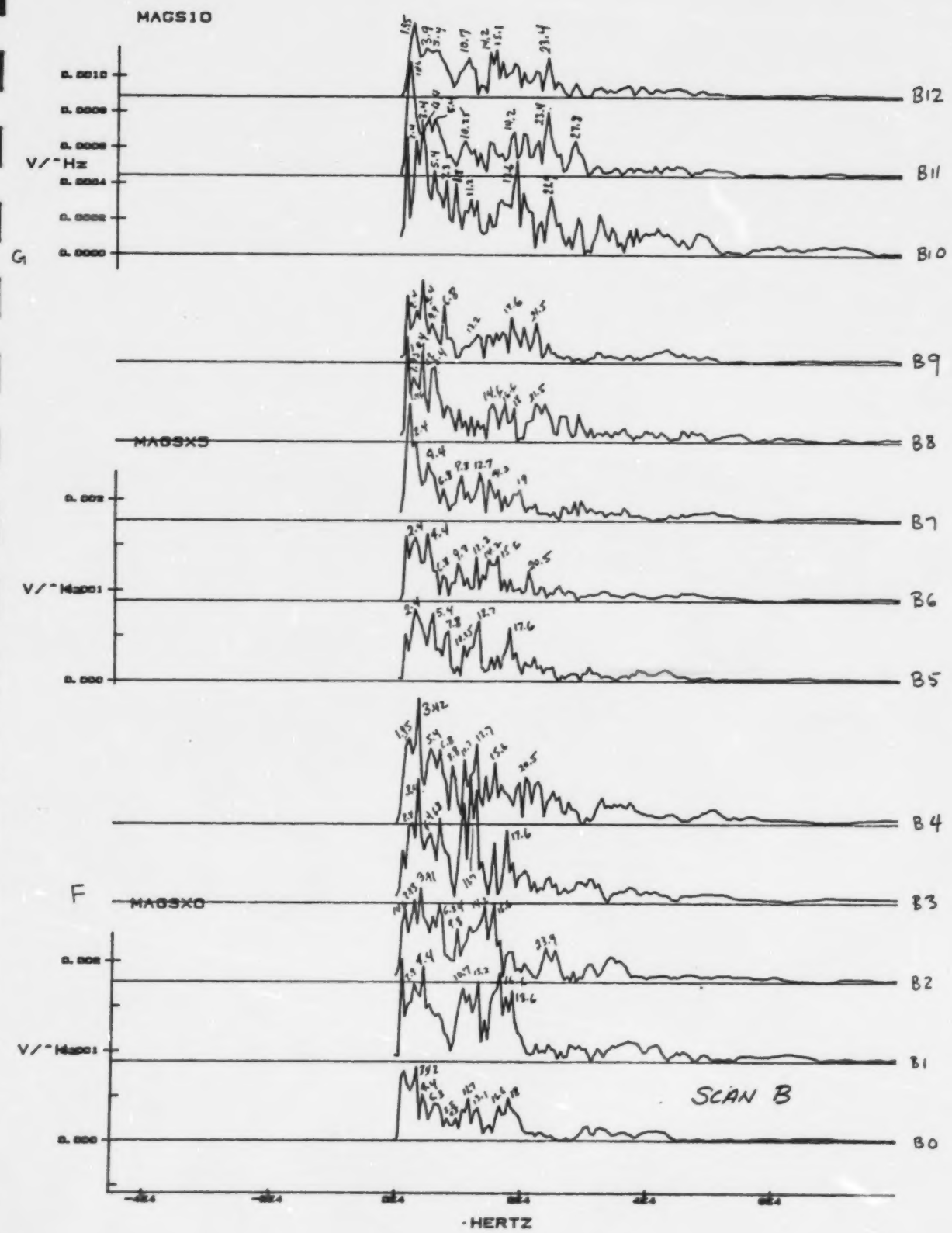
MAGS10
B12
B11
B10
G
MAGSX5
B9
B8
B7
B6
B5
B4
F
MAGSX0
B3
B2
B1
B0
SCAN B
HERTZ

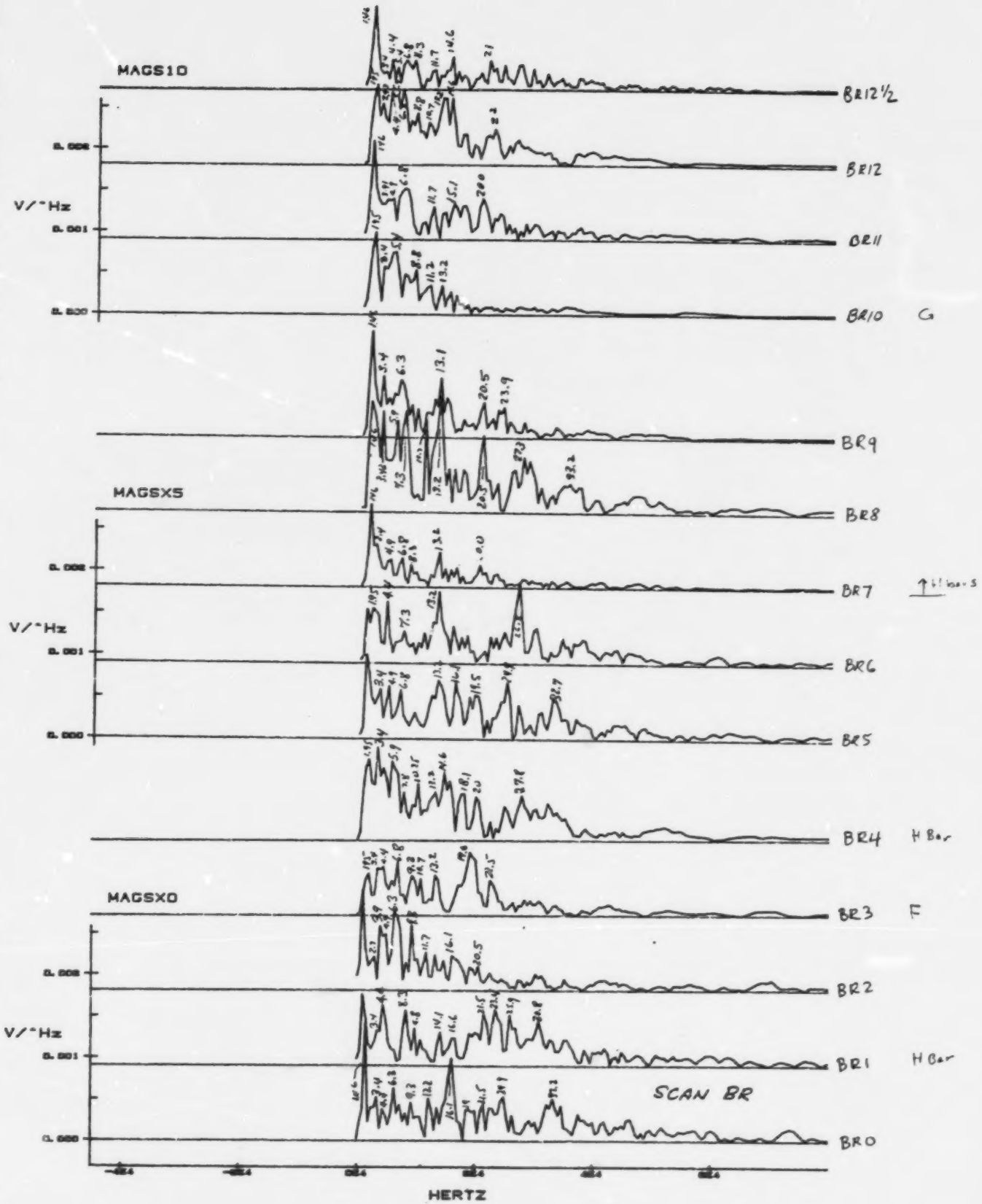
MAGS10
BR12½
BR12
BR11
BR10
G
MAGSX5
BR9
BR8
BR7
BR6
BR5
BR4
H Bar
MAGSX0
BR3
F
BR2
BR1
H Bar
BR0
SCAN BR
V/√Hz
HERTZ

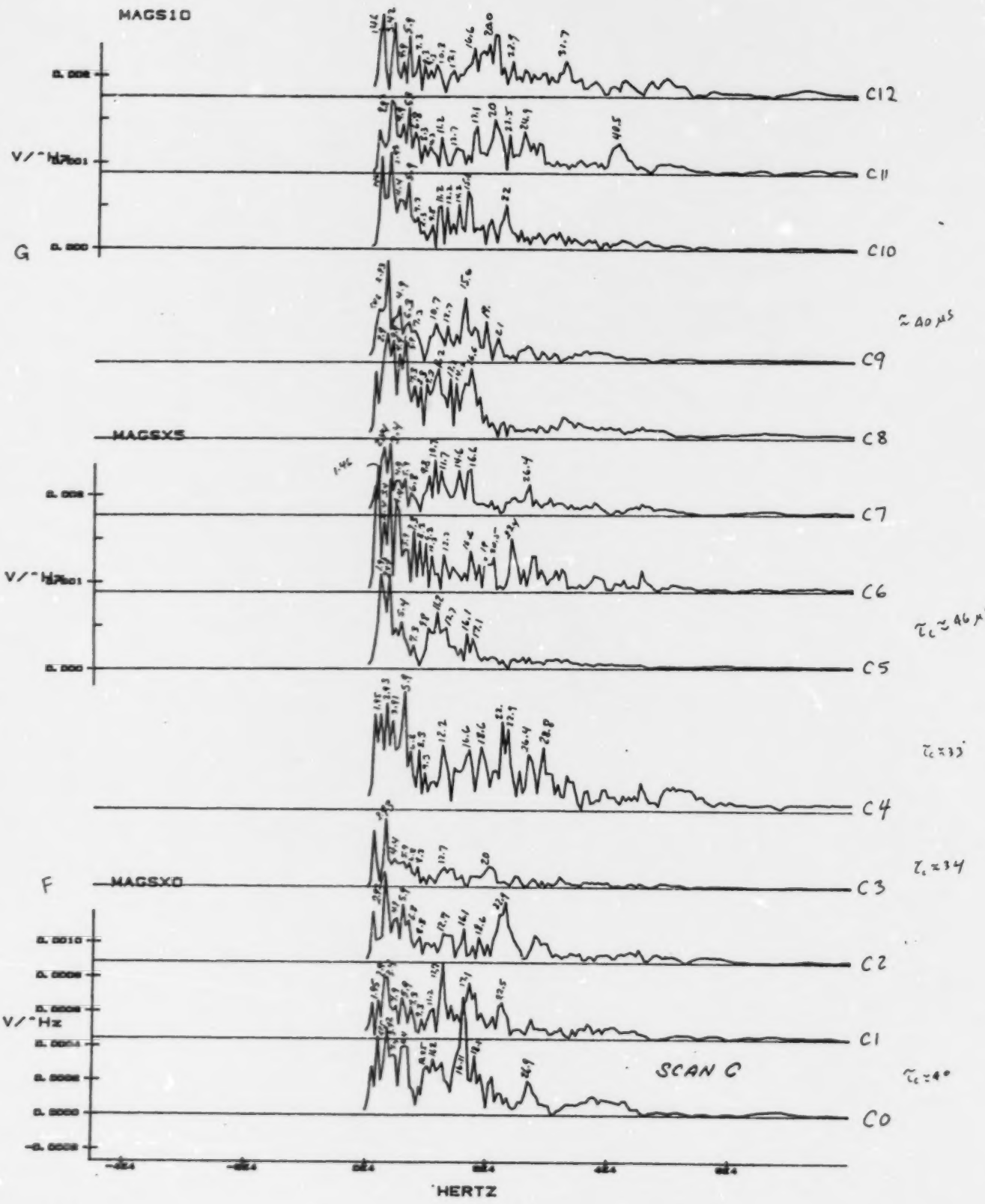
MAGS10
C12
C11
C10
G
≈ 40 μs
C9
C8
MAGSX5
C7
C6
C5
C4
C3
F
MAGSX0
C2
C1
C0
SCAN C
HERTZ

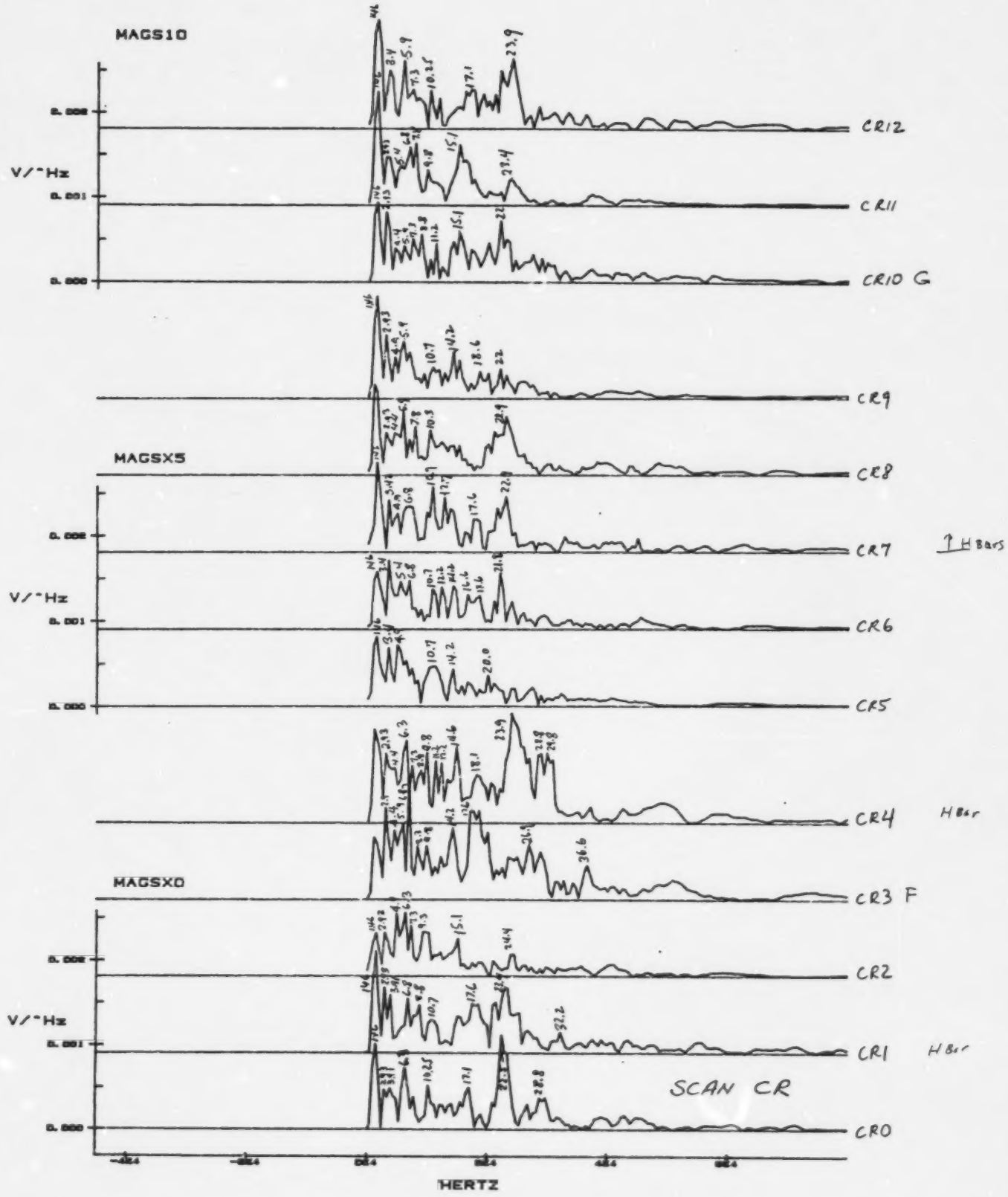
MAGS10
MAGSX5
MAGSX0
V/√Hz
0.002
0.001
0.000
CR12
CR11
CR10 G
CR9
CR8
CR7
CR6
CR5
CR4
CR3 F
CR2
CR1
CR0
↑ H Bars
H Bar
H Bar
SCAN CR
HERTZ

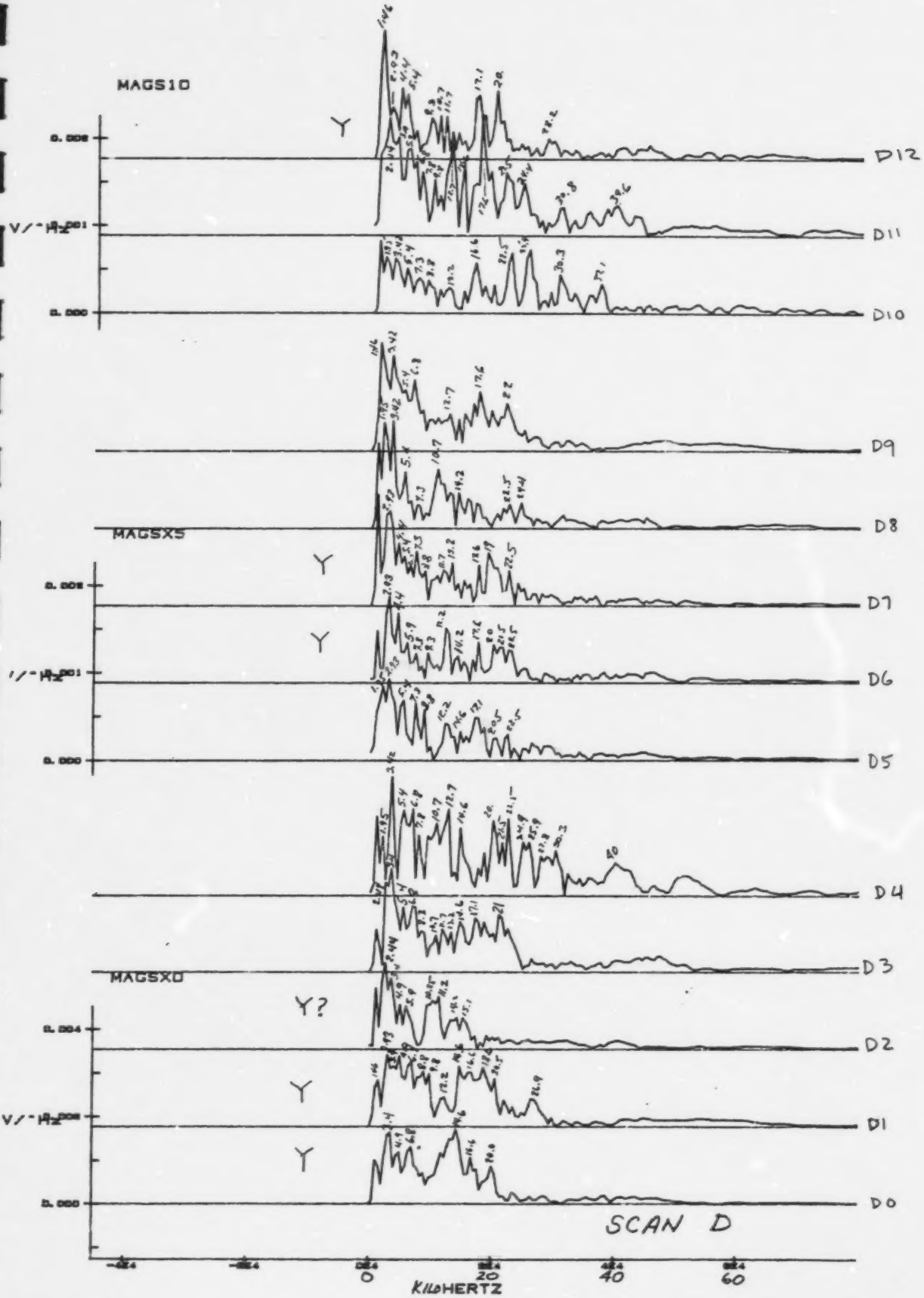
MAGS10
Y
D12
D11
D10
D9
D8
MAGSX5
Y
D7
Y
D6
D5
D4
D3
MAGSX0
Y?
D2
Y
D1
Y
D0
SCAN D
KILOHERTZ
0
20
40
60

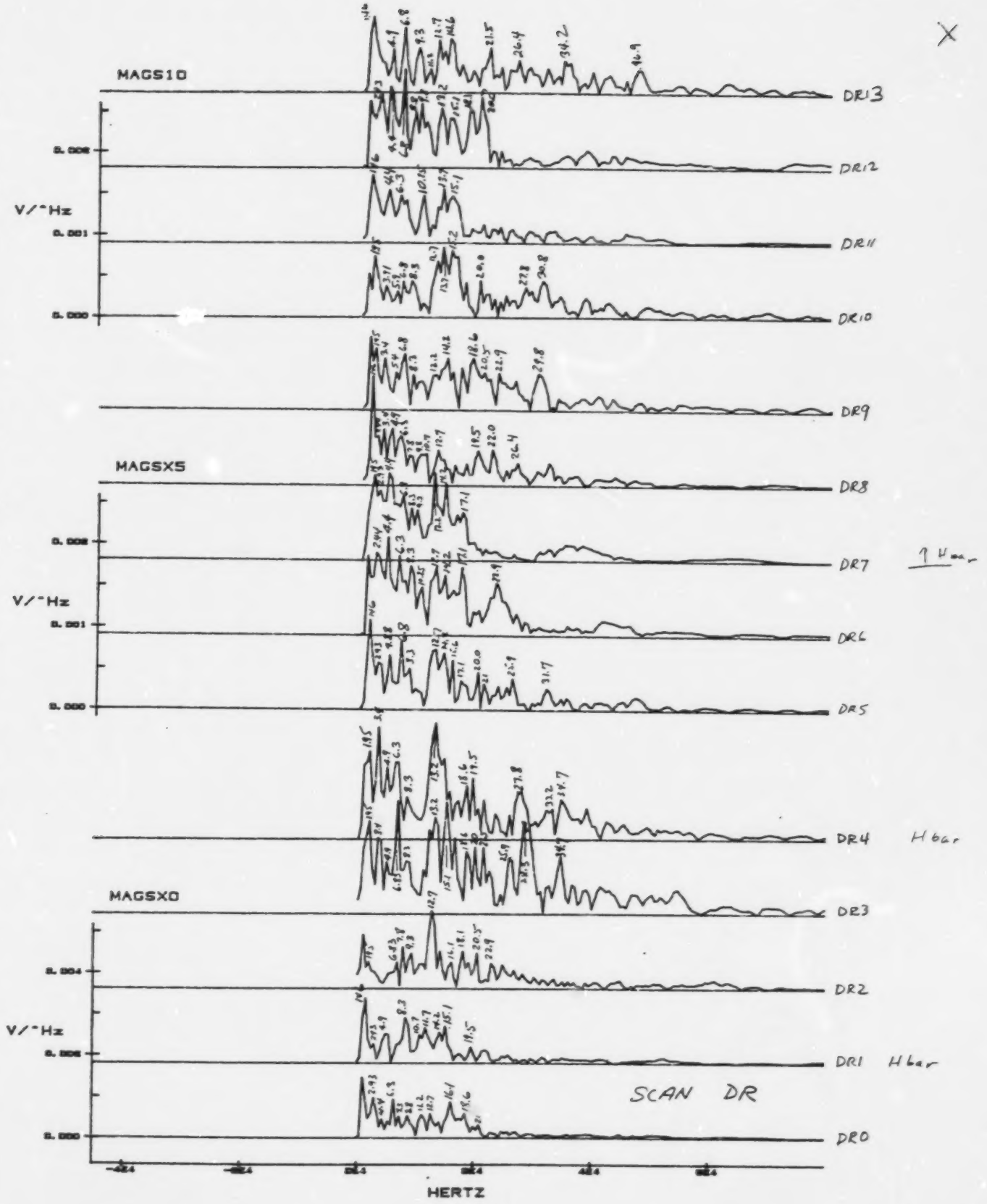
MAGS10
DR13
DR12
DR11
DR10
V/√Hz
0.000
0.001
MAGSX5
DR9
DR8
DR7
DR6
DR5
0.002
0.001
0.000
DR4
DR3
MAGSX0
DR2
DR1
DR0
0.004
0.002
0.000
SCAN DR
HERTZ

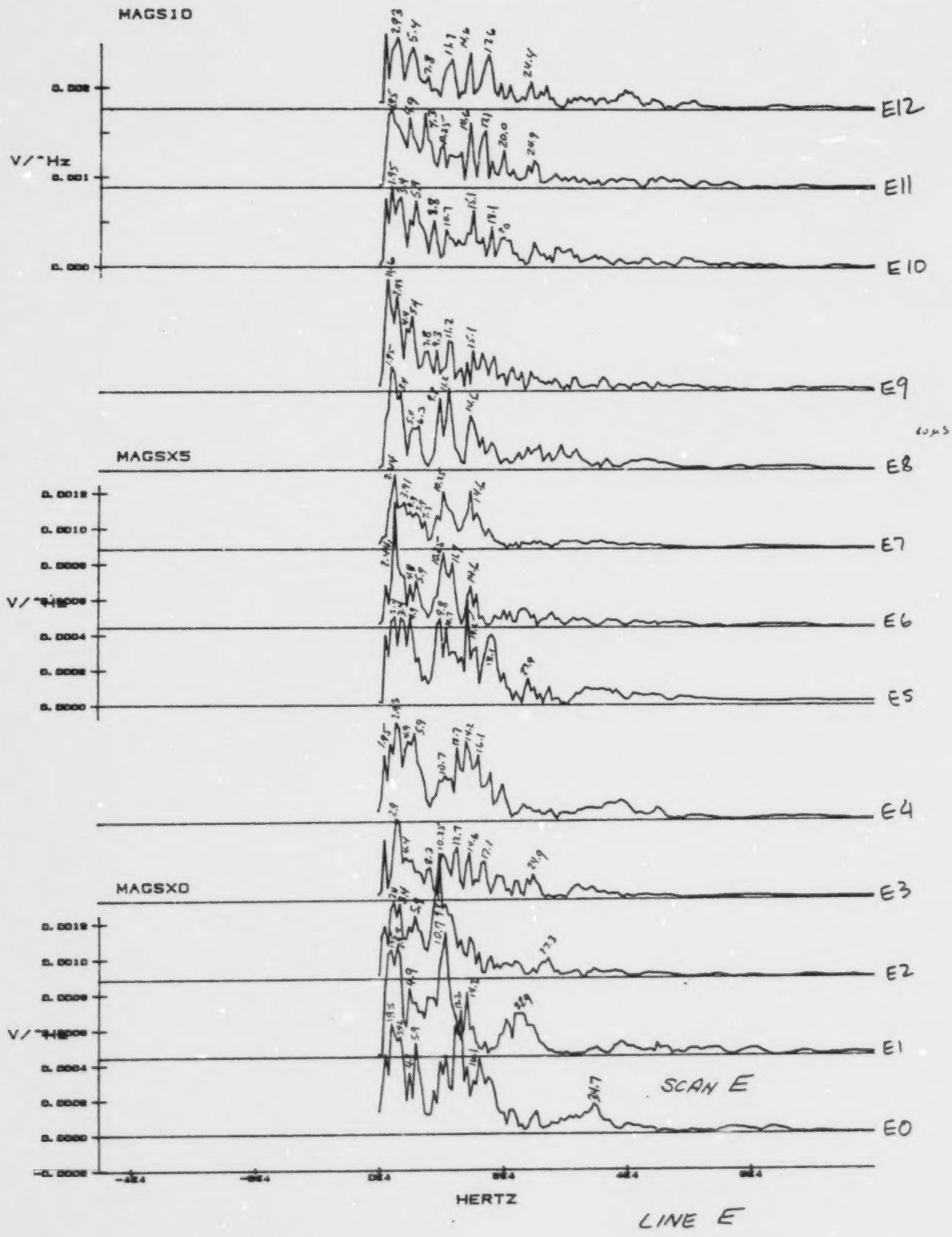
MAGS10
MAGSX5
MAGSX0
V/√Hz
E12
E11
E10
E9
E8
E7
E6
E5
E4
E3
E2
E1
E0
SCAN E
HERTZ
LINE E

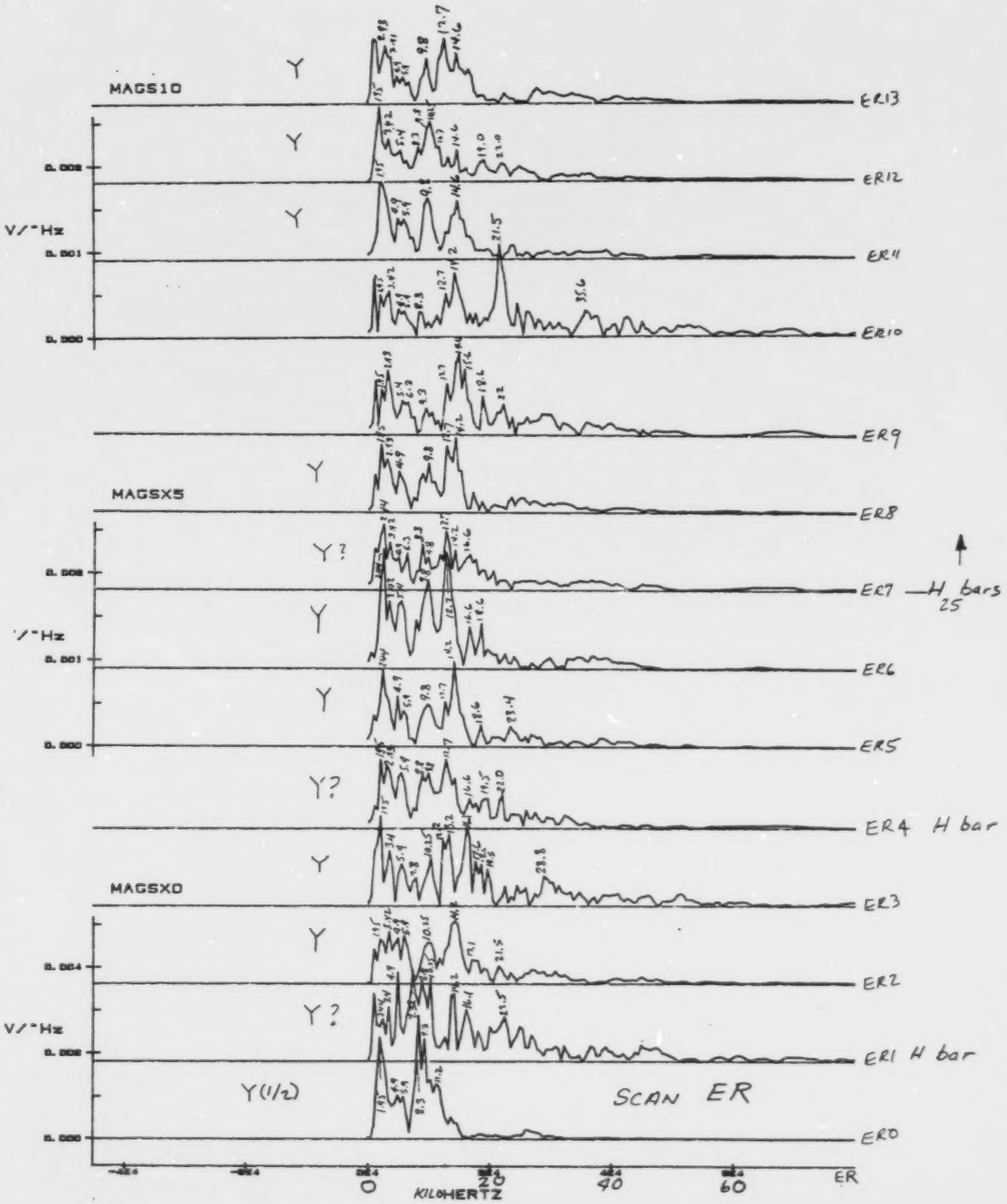
MAGS10
MAGSX5
MAGSX0
ER13
ER12
ER11
ER10
ER9
ER8
ER7
ER6
ER5
ER4
ER3
ER2
ER1
ER0
H bars 25
H bar
H bar
SCAN ER
V/√Hz
KILOHERTZ
0
20
40
60
ER

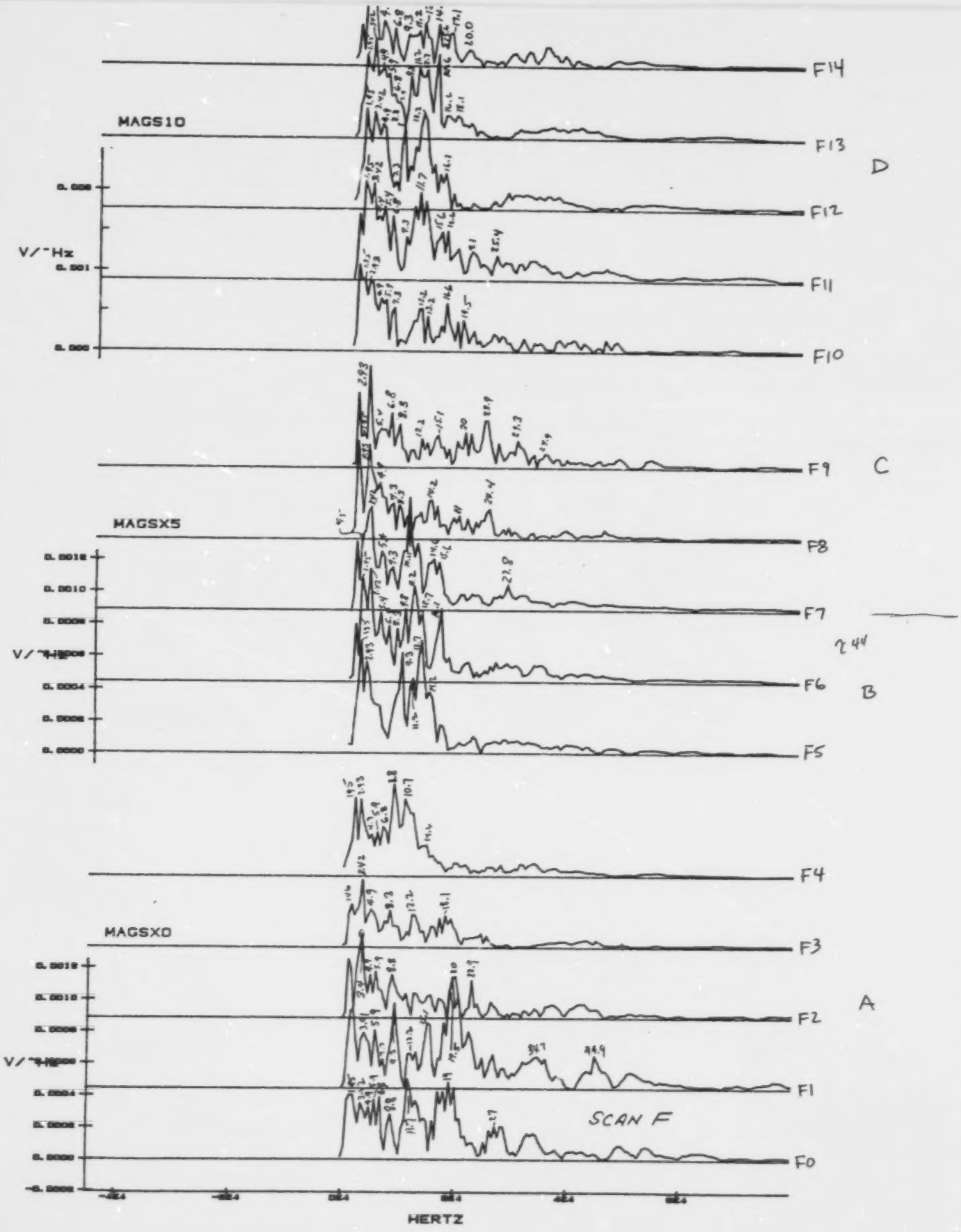
MAGS10
F14
F13
F12
F11
F10
D
V/√Hz
MAGSX5
F9
F8
F7
F6
F5
C
B
MAGSXO
F4
F3
F2
F1
F0
A
SCAN F
HERTZ

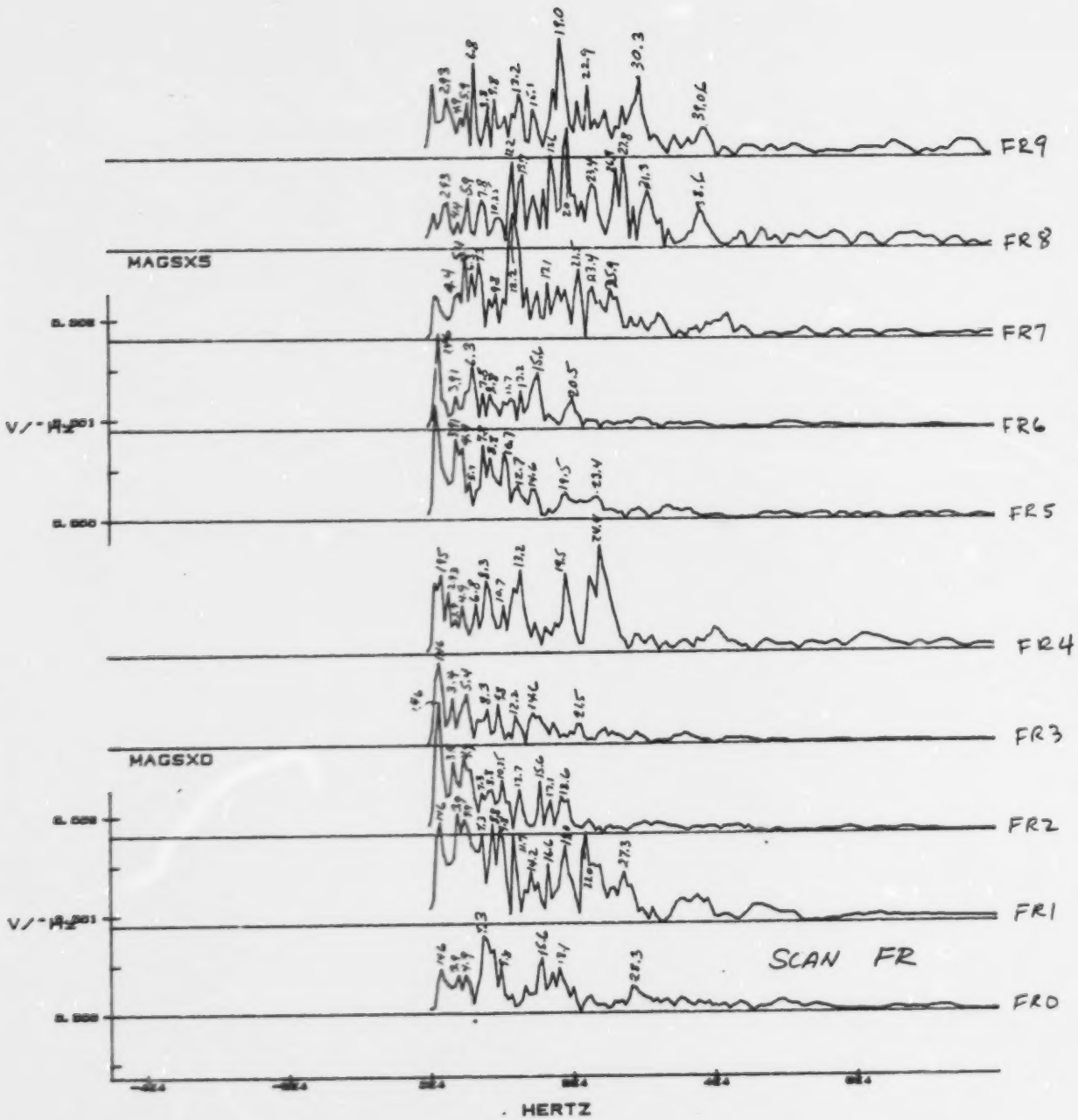
MAGSX5
MAGSXO
FR9
FR8
FR7
FR6
FR5
FR4
FR3
FR2
FR1
FR0
END
VBAR
VBAR
SCAN FR
HERTZ

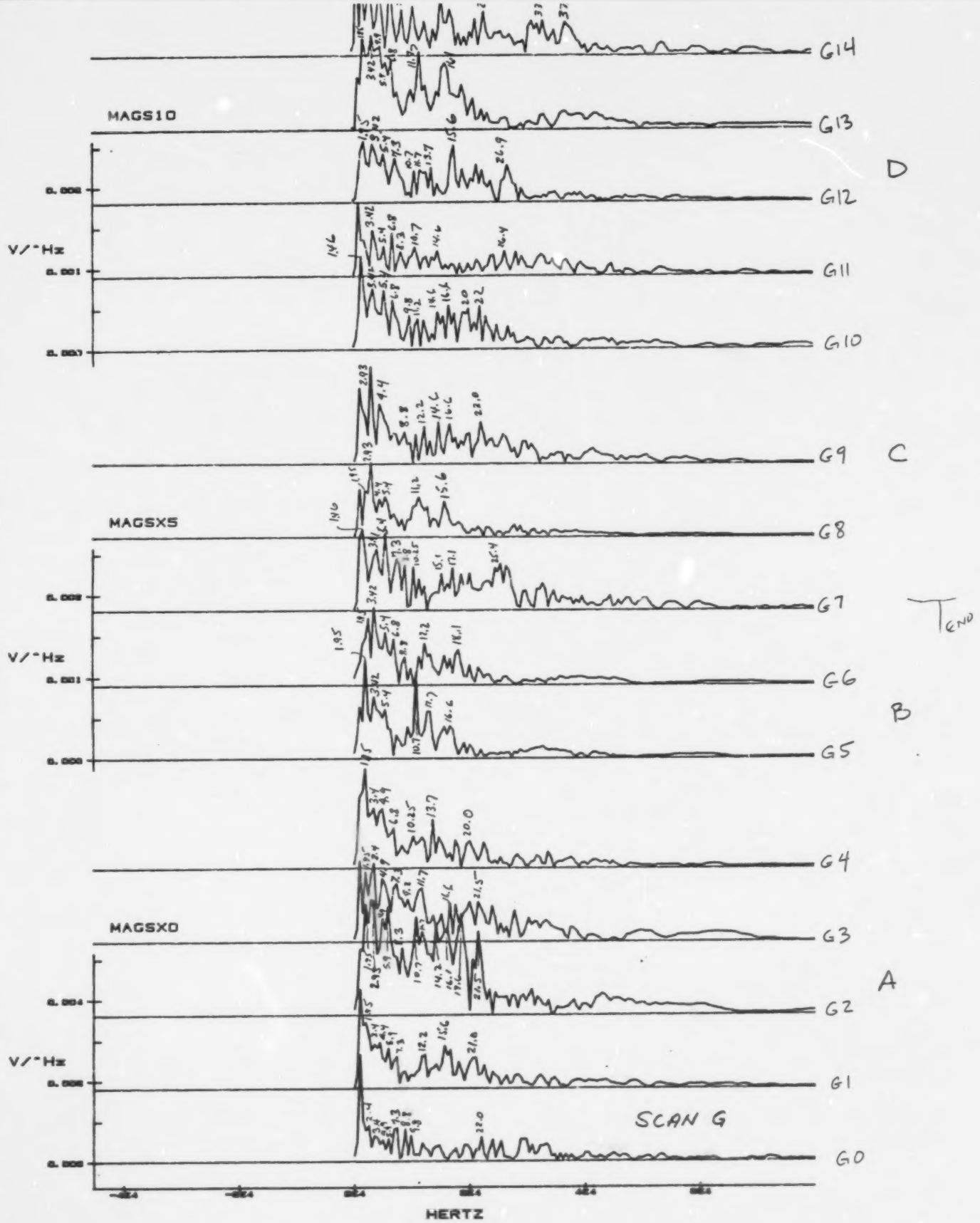
MAGS10
MAGSX5
MAGSXO
V/√Hz
G14
G13
G12
G11
G10
G9
G8
G7
G6
G5
G4
G3
G2
G1
G0
D
C
B
A
TEND
SCAN G
HERTZ

APPENDIX 11

ULTRASONIC PITCH-CATCH AND PULSE-ECHO MEASUREMENTS IN CONCRETE

Paper by: A. Michel Alexander and Henry T. Thornton, Jr.
U.S. Army Corps of Engineers
Waterways Experiments Station
Vicksburg, Mississippi

Ultrasonic Pitch-Catch and Pulse-Echo Measurements In Concrete

A. Michel Alexander and Henry T. Thornton, Jr.

Synopsis: A new improved prototype ultrasonic pitch-catch (two-transducer) and pulse-echo (one-transducer) system has been developed for concrete. Signal generation and detection is done with piezoelectric crystals. A literature search revealed that no pulse-echo system had been developed and that pitch-catch measurements needed further development. No commercial system could be found on the market for making pitch-catch measurements. Only about 10 references that deal directly with ultrasonic pitch-catch measurements in concrete were located, the earliest of which is Bradfield (1948). There are none that deal with pulse-echo.

Although investigators have made progress in understanding the problems associated with the development of pulse echo for concrete the heterogeneous nature of concrete and the state-of-the-art of ultrasonic materials and techniques prior to the present have prevented the development of a practical system like that used for homogeneous materials. The literature revealed that resolution was poor due to long pulse lengths (high Q value) for the transducers. Investigators had problems with interfering Rayleigh waves at low frequencies. Signal-to-noise ratios (SNR) ranged from only about 2 to 6. The latest state-of-the art transmitter (Ohio State University) had a diameter of 18 in. (457 mm) and a mass of 40 lbs (18 kg). Measurements showed extraneous signals other than the desired longitudinal mode due to mode conversion in the transducers. Also transducers lacked the proper focal length, directivity, and sensitivity.

Research by the U.S. Army Engineer Waterways Experiment Station (WES) has resulted in the development of a 200-kHz pitch-catch system with a signal to noise ratio of 18 and a pulse-echo system with a SNR of 8. The mass and dimensions of the improved system have been reduced 90% from the prior state-of-the-art system. The WES system has the lowest Q (shortest ringing time and widest bandwidth) and therefore the shortest pulse length on record. The present system works well for making thickness measurements of portland-cement concrete pavement and can indicate the presence of voids.

A. Michel Alexander is a research physicist with the Structures Laboratory, U.S. Army Engineer Waterways Experiment Station.

Keywords: Nondestructive tests; ultrasonics; pulse echo; pitch-catch; concrete evaluation; pavement thickness measurements; piezoelectric transducers.

He has worked for 20 years in concrete research and in development of nondestructive testing techniques for evaluation of concrete structures.

Henry Thornton is Chief, Evaluation and Monitoring Unit, Concrete Technology Division, Structures Laboratory, U.S. Army Engineer Waterways Experiment Station. He is a member of ACI Committee 228, Nondestructive Testing, and has worked in the field of concrete durability and evaluation of concrete structures by means of nondestructive testing for 25 years.

INTRODUCTION

Ultrasonic measurements in concrete structures with two accessible sides in which a transducer is mounted on each side is a well-established technique, but no system is known to the authors to be commercially available for making measurements of velocity from one side to the other where only one surface is accessible. Work done by various investigators since 1948 has contributed to the development of knowledge and expertise in this area. The inherent heterogeneous nature of portland-cement concrete (PCC) has complicated the development of a system. A practical ultrasonic pulse-echo nondestructive testing (NDT) system would increase the available means for evaluation of the condition of concrete structures, especially those accessible from only one surface. All of the references located by the authors prior to 1985 deal with two-transducer systems (pitch-catch) rather than pulse-echo (one-transducer) systems. Only pulse techniques are referred to in this report because continuous wave techniques do not have the potential for operator simplicity.

Bradfield (1948) first reported measuring the thickness of 1-in. (25-mm) and 2-in. (50-mm) thick concrete plates with a 2.5-ft (0.75-m) magnetostriction nickel rod. A transmitter coil developed the wideband acoustic pulse and another coil picked up the echo. The longitudinal pulse generated was about 12 microseconds in width and had the shape of one cycle of a sine wave. The center frequency was near 80 kHz. The signal to noise ratio (SNR) was very low and the acoustical mismatch of the nickel rod to the concrete was inefficient in the transfer of energy. This represents the first report of an ultrasonic pitch-catch measurement made on concrete known to the authors.

Jones (1953) reported that Bradfield encountered three main difficulties; (1) scattering by aggregate at higher frequencies, (2) surface-wave interference at low frequencies, and (3) a small number of wavelengths present in the total path length making it necessary to produce a short, highly damped pulse (wide bandwidth). He also noted an upper frequency limit of 200 kHz for concrete when the thickness is 2 ft (0.6 m) or

less and when the nominal maximum size of the aggregate is 3/4 in. (19.0 mm) and the wavelength is about 1 in. (25 mm).

Bradfield and Woodroffe (1953) reported a significant advance in pitch-catch measurements in concrete using 100-kHz barium titanate longitudinal mode mosaic transducers. Both transmitter and receiver were normal to the concrete surface. By smoothing the surface and applying a layer of grout flattened by a sheet of glass they were able to measure thru 18 in. (0.46 m) of concrete with a SNR of about 5 to 6. The measurement is shown in Figure 1. The transmitter and receiver dimensions were about 2.5 by 4 in. (64 by 102 mm) each. The height was 1 in. (25 mm). Large area transducers are required for the low frequencies in concrete to give directivity to the ultrasonic beam. Therefore mosaic transducers were constructed from smaller standard elements. The expense of manufacturing large pieces is prohibitive. The long ring time of the transmitter ruled out the possibility of using a common transducer. The Q of the barium titanate was 90 in air and 5 on the concrete. The pulse length determines the least distance that can be resolved in a material. It will be several wavelengths long depending on the Q of the transducer. The pulse length (distance) in a material is equal to the input pulse width (time) multiplied by the wave velocity in the material. An input pulse width of 50 μs. (5 wavelengths of a 100 kHz signal) would correspond to a pulse length and hence resolution of 8-in. (203 mm) in concrete. The location of the first discontinuity can be resolved to within one wavelength. However subsequent discontinuities must be separated by the resolution distance of 8-in. or they will be obscured by the ringing caused by the first-returning echo. No electrical or acoustical matching was done. Although this reference represents the first recorded pulse-echo measurement (pitch-catch) made on concrete using piezoelectric materials, the report lacks significant detail for other investigators to follow with ease.

Bradfield and Gatfield (1964) reported thickness measurements with a set of variable-angle longitudinal mode transducers. One hundred-kHz transducers of barium titanate were mounted on Perspex shoes covering a total area of 3.5 by 4.5 in. (89 by 114 mm) for each transducer. The height of the transducers was about 10 in. (252 mm). The ceramic was loaded on the back face with litharge (lead oxide, PbO) and rubber to reduce the Q. Lateral ringing of the transducer however created unwanted interference. They obtained an error of 2% on a 12-in. (300-mm) thick layer of concrete. See Figure 2. However the signal was preceded by unwanted surface waves almost equal in magnitude to the desired longitudinal wave. The transmitter pulse precedes the first timing mark (10 μs each) by 150 μs. The large dimensions of the driving mechanism necessary to vary the angle of the transducers prevented use of the system outside the laboratory.

Canfield and Moore (1967) reported that the difficulty of building a pulse-echo system lay with the transducer development. They were able to measure the thickness of a 5-in. (127-mm) concrete plate with pitch-catch transducers but no practical instrument was perfected. They also met with difficulties of surface-wave interference and high Q (narrow bandwidth) transducers that rang for an excessive time. They used lead zirconate titanate (PZT) which resonated at 83 kHz. It is difficult to damp crystals at low frequencies as the attenuation of damping materials decreases as the frequency is decreased.

Howkins (1968) reported the results of about 4 years of research by the Illinois Institute of Technology Research Institute on the development of an ultrasonic pulse-echo system for concrete. Their final pitch-catch system was used to measure the thickness of a 7-in. (178-mm) thick concrete plate using two epoxy discs with barium-titanate ceramic rods (100 kHz) embedded in the epoxy and mounted on fixed-angle wedges (see Figure 3). About 44 rods were in each epoxy disc and both transmitter and receiver were mounted on fixed-angle wedges. Each transducer was 3 in. (75 mm) in diameter. A sharp onset for the echo was present with a SNR of about 5 to 6. However the Q was about 20 or more and since the period of each cycle is 10 μs for a 100 kHz signal the pulse length would be over 200 μs. This created too much blind time for detecting echoes that are closely spaced. For a 15,000-ft/sec (4573 m/s) velocity in concrete this would cover 3 ft (3.28 m) in concrete.

Howkins (1968) made a significant contribution by explaining the physics involved in making an ultrasonic pulse-echo measurement in a composite material like concrete. Although he found 150 references on ultrasonic measurements in concrete only 6 of them had information about pitch-catch measurements in concrete. He also noted that the common nondestructive measuring techniques used for homogeneous materials were not applicable to concrete. With few exceptions investigators had relied upon direct application of transducers designed for homogeneous and fine-grained materials such as aluminum and steel. He suggested going back to fundamental principles.

McMaster led a research program at Ohio State University over a period of 8 years and developed the first field system (Golis et al., 1966; Golis, 1968; Mailer et al., 1970; Mailer, 1972). Golis built an 18-in. (457-mm) diameter ring transducer (200 kHz) for measuring pavement thickness. The 3-in. (75-mm) diameter receiver was placed into a 5-in. (125-mm) diameter hole in the center of the transmitter. Again, the surface wave energy prevented flaw detection measurements, but the SNR(5) was sufficient to measure pavement thickness within 2 or 3 percent. The system had a low Q(3) and used lithium sulfate for the receiver. Barium titanate was used initially for the transmitter, but this was later changed to PZT. A concentrated

effort by the Ohio State University (OSU) team was made to document their work that permitted others to follow up with less effort. No commercial unit was ever marketed although a patent was obtained on the system. Typical signals (Golis et al., 1971) in Figure 4 show a high frequency pip (small circle) on a larger amplitude lower frequency waveform.

The U.S. Army Engineer Waterways Experiment Station (WES) obtained one set of the transducers built by OSU. The Pennsylvania State Highway Department donated one of their transmitters that was in need of repair. Two lithium-sulfate receivers were also received but could not be repaired. After restoration of the transmitter and the purchase of a new receiver the system was restored to operation. However, low-frequency energy obscured the higher frequency echo energy. A strong 40-kHz frequency was present probably due to a resonance in the housing. By using a high-pass filter with cutoff at 100 kHz the signal shown in Figure 5 was obtained (Thornton and Alexander, 1987). The center frequency of 180 kHz became the dominant energy and echoes were obtained on a 9-1/4 in. (235-mm) thick concrete slab. The SNR was about 4 to 5 and the Q of the transmitter is about 4. However, the calculated near-field length is several feet. For pavement thickness of about 9 in. (230 mm) a smaller diameter transmitter of about 4 to 8 in. (100 to 200 mm) would reduce the near field length and be more efficient. Also the mass of over 40 lb (18 kg) for the transmitter and the need to use about 500 mL of couplant liquid suggests a new design.

Claytor and Ellingson (1984) measured the thickness of a refractory concrete slab 12 in. (300 mm) thick using two 250-kHz PZT-5A (Q=75) transducers with a liquid buffer between the ceramic and the concrete to reduce surface wave energy. Each mosaic transducer was 7.0 in. (178 mm) in diameter. Seven 2-in. diameter discs were embedded in a 20% tungsten/epoxy mixture by volume for each transducer. The transducer rang for about 300 μs at 96 kHz. This represents a Q of over 20 (see Figure 6). They noted that progress had been hampered in developing acoustic techniques for concrete due to (1) poor characterization of test materials, (2) lack of calibration and response curves for transducers, and (3) the difficulty of experimental tests on large structural objects.

DEVELOPMENTAL WORK

In 1983 Thornton and Alexander made a literature search to determine the state-of-the-art of ultrasonic pulse echo in concrete. The results of this study (Thornton and Alexander, 1986) confirmed the findings of previous investigators, i.e., that the main effort in pulse-echo development should be in the area of transducer development and the reduction of the Q of the transducer.

It was found that tungsten-loaded epoxy will provide better damping for piezoelectric materials such as PZT. The high acoustic impedance of the tungsten matches that of the PZT and a backing made of a 2:1 mixture of tungsten and epoxy by mass (Washington, 1961) will produce a minimum of reflections returning from the backing to the piezoelectric crystal. This is necessary to produce a wide bandwidth transducer. In the lower frequency range, suitable for working in concrete, piezoelectric materials fail to damp as well and it becomes difficult to design a transducer with the necessary bandwidth. The damping naturally lowers the sensitivity but a significant reduction in the sensitivity is due to the fact that the sound pressure generated from a transmitter is directly related to the square of the frequency. For this reason impacts are sometimes used to generate sonic and ultrasonic energy in the low frequency spectrum required for concrete (Carino, et al., 1985; Thornton and Alexander, 1987). However we discuss here only information about the generation and detection of ultrasonic signals with piezoelectric materials.

Although a number of transducers were fabricated using the tungsten-loaded epoxy, the sensitivity was reduced too much for the transducers to function as a transmitter. Also, the PZT material had too much mode conversion to generate a pure longitudinal mode. In studying the various properties of piezoelectric materials it was found that lead metaniobate had a much lower Q than PZT. PZT-5H has a Q of 65 in air; lead metaniobate (EC-82) has a Q of 11 in air. Also the transverse mode coupling coefficient was much lower for lead metaniobate (0.066 compared with 0.65 for PZT). The transverse mode acts as noise and interferes with the generation of a pure longitudinal mode. Surface waves therefore are suppressed because of the increased directivity.

The final transducer was constructed of four piezoelectric plates (2.35 by 2.35 by 0.28 in. (60 by 60 by 7 mm)) of lead metaniobate (EC-82). All four were bonded to a 1/4-in. (6-mm) thick sheet plastic plate to form a square pattern of 4.7 in. (120 mm). A thin copper sheet was inserted between the piezoelectric elements and the plastic faceplate to provide a ground connection. The combination was adhesive bonded with Loctite 326. On the top side of the crystals all the element electrodes were joined with a lead wire using solder and the positive lead connected to the ground to form a parallel electrical connection for all four elements.

The undamped longitudinal resonant frequency was 200 kHz in air. It dropped to 190 kHz after being attached to the plastic faceplate. The Q in air was 11 and dropped to about 2-1/2 when the plastic plate was in contact with the concrete. Since the Q was such a desirably low value there was no need to provide external damping on the back face. When the EC-82 was used as the transmitter and the PZT-5H used as a receiver, a SNR ratio

of 18 was obtained when measuring the thickness of a 9-1/4-in. thick (235-mm) concrete plate element (air-backed) with 3/4-in. (19.0-mm) nominal maximum size aggregate. No surface preparation was done and castor oil was used for the couplant (see Figure 7). An inductor was placed in parallel with the receiver to cancel out the static capacitance (tune the receiver). This increased the SNR ratio by 50% (12 to 18). A series inductor was added in the transmitter circuit which increased the sensitivity of the system but did not improve the SNR. Shock excitation was provided with a Model 5055 Panametrics pulser. The total system is shown in Figure 8.

A 1-3/4-in. deep (45-mm), 24-in. long (0.6-m) saw cut was made in the concrete plate to test for the presence of surface waves. When the transducers were placed on opposite sides of the cut no appreciable change occurred in the amplitude of the energy preceding the echo signal. Also, a through-transmission measurement made on the concrete plate revealed the SNR to be about 300. Therefore the noise in front of the echo is apparently due to backscattering from the 3/4-in. (19.0-mm) nominal maximum size aggregate in the concrete. The mass and dimensions of the prototype system were reduced from those of the OSU device by about 90%. The SNR was increased by 200%.

When the lead metaniobate was used in the pulse-echo configuration, i.e., using one transducer as the transmitter and receiver, an echo was received from the bottom of a 6-in. (150-mm) concrete plate. (See Figure 9.) The small number of periods which elapse before the echo returns is a large percentage of the time required for the receiving amplifier to recover from its paralysis after being excited. Therefore it remains to be seen whether or not one transducer can be used successfully for pulse-echo measurements in concrete as is common in fine-grained materials.

WES contracted with Argonne National Laboratories to determine the potential of the new mechanically flexible piezoelectric material polyvinyldene fluoride (PVDF). Figure 10 shows the results of a pulse-echo measurement made with a 10-by-10 in. 200-kHz transducer on a 12-in.-thick section of portland-cement concrete. (Private communication from Claytor and Ellingson March, 1986). The SNR of the received signal to precursor noise was about 3. The onset of the echo is not well defined due to the presence of surface waves. However, the surface waves have been reduced somewhat by signal processing. The PVDF material is a poor transmitter but one of the best receiver materials.

Lower frequencies were made possible by bonding 40 sheets of 40-μm thick PVDF film. While the transducer was designed for 200 kHz, it was operated at 60 kHz on concrete to obtain penetration. This, of course, lowered the efficiency of the transmitter in the pulse-echo mode.

CONCLUSION

An ultrasonic pulse-echo system (Figure 8) for use in concrete requires large area transducers to collimate the ultrasonic beam, produce a near-field length (focal length) shorter than the thickness of the concrete being tested, and suppress interfering surface waves. The piezoelectric material should match the acoustic impedance of the concrete as closely as possible or the faceplate should have an intermediate impedance between that of the material and the concrete. The piezoelectric materials should be chosen to have high activity constants for the transmitter and receiver because of the high attenuation of the concrete. The piezoelectric material should have a low Q to reduce ringing or it will require a proper backing of tungsten loaded epoxy to reduce the Q. The piezoelectric material should have low mode conversion like lead metaniobate to prevent generation of signals other than the desired longitudinal mode. Concrete requires that a transducer operate at 200 kHz or below. This means that in thicknesses of 1 ft (300 mm) or less the concrete thickness is only equivalent to a few wavelengths so that the pulse can only be 1-2 cycles in length. The high capacitance of the mosaic transducer and the accompanying low impedance generally require shock excitation rather than a sinusoidal burst in order to introduce enough energy. The pulser should be designed to have a pulse width that matches the center frequency of the transmitter. At the present state-of-the-art, pitch-catch measurements rather than pulse-echo should be made to gain full efficiency. Finally both transmitter and receiver should be tuned electrically with inductors to improve SNR and sensitivity. WES future plans are to test the effects of the degree of backscatter on specimens of varying deterioration. Although the activity that precedes the back wall echo appears to be noise, it is acoustical (not electrical interference) energy and may reveal the degree of microcracking in deteriorated surfaces. Presently the system has a sufficiently large SNR to detect back-wall reflections successfully and can be useful for making pavement and floor slab thickness determinations. Continuing improvements in the SNR should make it possible to detect cracks, voids, and discontinuities.

ACKNOWLEDGEMENT

The tests described and the resulting data presented herein, unless otherwise noted, were obtained from research conducted under the Concrete Research Program, for which the technical monitor is Mr. Fred Anderson, Headquarters, United States Army Corps of Engineers (HQUSACE), the Repair, Evaluation, Maintenance, and Rehabilitation (REMR) Research Program for which the technical monitors are Messrs. John R. Mikel (DAEN-CWD-M), Tony C. Liu (DAEN-ECE-D), and Bruce L. McCartney (DAEN-CWH-D) all of HQUSACE, and the US Bureau of Reclamation Program Related Engineering and Scientific Studies (PRESS), directed by

Dr. Francis G. McLean, Chief, Division of Research and Laboratory Services. All work was conducted by the U.S. Army Engineer Waterways Experiment Station except a part contracted to Argonne National Laboratory. We gratefully acknowledge permission from the Chief of Engineers to publish this paper.

The work was conducted under the general supervision of Mr. Bryant Mather, Chief, Structures Laboratory, and John M. Scanlon, Chief, Concrete Technology Division, U.S. Army Engineer Waterways Experiment Station.

COL Dwayne G. Lee was Commander and Director of WES during the preparation and publication of this paper. Dr. Robert W. Whalin was Technical Director.

REFERENCES

Bradfield, G. 1948. "New Electro-Acoustic Transducer Operating with Short Pulses," Electronic Engineering, Vol 20, No. 241, pp 74-78.

Bradfield, G., and Gatfield, E. N. 1964. "Determining the Thickness of Concrete Pavements by Mechanical Waves: Directed-Beam Method," Magazine of Concrete Research, Vol 16, No. 46.

Bradfield, G., and Woodroffe, E. P. H. 1953. "Determination of Thickness of Concrete Pavements by Mechanical Waves," Report No. PHYS/U5, Teddington National Physical Laboratory, Dept. of Scientific and Industrial Research, Great Britain.

Canfield, Joe R., and Moore, Willard H. 1967. "Development of Instrument for Nondestructive Measurement of Concrete Pavement Thickness," Research Project No. 1-9-63-61, Materials and Test Division, Texas Highway Department in Cooperation with the US Department of Transportation, Federal Highway Administration, Bureau of Public Roads.

Carino, N. J., Sansalone, M., and Hsu, N. N. 1985. International Advances in Nondestructive Testing, W. J. McGonnagle, Editor, (Gordon and Breach Science Publishers, New York). To be published.

Claytor, T. N., and Ellingson, W. A. 1984. State-of-the-Art Review of Acoustic Techniques for Application to the Nondestructive Evaluation of Refractory Concrete for Coal Gasification, ANL/FE-83-23, Argonne National Laboratory, Argonne, Illinois.

Golis, M. J. 1968. "Pavement Thickness Measuring Using Ultrasonic Pulses," Highway Research Record No. 218, pp 40-48, Highway Research Board, Washington, D.C.

Golis, M. J., McMaster, R. C., and Cooper, G. L. 1971. Patent 3,616,682 "Ultrasonic Nondestructive Thickness Gauge."

Golis, M. J., McMaster, R. C., Toth, L., and Cooper, G. 1966. "The Development of Ultrasonic Nondestructive Testing Instrumentation to Measure Pavement Thickness," Report No. 208-3, Engineering Experiment Station, Ohio State University, Columbus, Ohio.

Howkins, S. D. 1968. "Measurement of Pavement Thickness by Rapid and Nondestructive Methods," NCHRP Report 52, 82 pp, Highway Research Board, NRC, NAS, Washington, D.C.

Jones, R. 1953. "Testing of Concrete by Ultrasonic-Pulse Technique," Proceedings of the 32nd Annual Meeting, Highway Research Board, Washington, D.C., pp 258-275.

Mailer, H. 1972. "Pavement Thickness Measurement Using Ultrasonic Techniques," Highway Research No. 378, pp 20-28, Highway Research Record, Washington, D.C.

Mailer, H., Golis, M. J., McMaster, R. C., and Raab, T. J. 1970. "The Development of Ultrasonic Nondestructive Testing Instrumentation to Measure Pavement Thickness," Final Report EES 208, Engineering Experiment Station, Ohio State University, Columbus, Ohio.

Thornton, H. T., Jr., and Alexander, A. M. 1987. "Development of Nondestructive Testing Systems for In-Situ Evaluation of Concrete Structures," Technical Report REMR-CS- , US Army Engineer Waterways Experiment Station. (In press).

Washington, A. B. G. 1961. "The Design of Piezoelectric Ultrasonic Probes," British Journal of Nondestructive Testing, Vol 3, pp 56-63.

CAPTIONS

Figure 1. Pitch-catch measurements on PCC with 100 kHz barium titanate transducers from Bradfield Woodroffe, 1953.

Figure 2. Pitch-catch measurements on PCC with 100 kHz barium titanate transducers from Bradfield and Gatfield 1964.

Figure 3. Pitch-catch measurements on PCC with 100 kHz barium titanate transducers from Howkins, 1968.

Figure 4. Pitch-catch measurements on PCC with 200 kHz lead zirconate titanate transmitter and a broadband receiver of lithium sulfate from Golis et al., 1971.

Figure 5. Pitch-catch measurements on PCC with 180 kHz lead zirconate titanate transmitter and broadband lithium sulfate receiver from Thornton and Alexander, 1987.

Figure 6. Pitch-catch measurements on refractory concrete with 250 kHz transducers of lead zirconate titanate from Claytor and Ellingson, 1984.

Figure 7. Pitch-catch measurements on PCC with 190 kHz lead metaniobate transmitter and lead zirconate titanate receiver from Thornton and Alexander, 1987.

Figure 8. Ultrasonic pitch-catch system: transmitter, receiver, pulser/filter/amplifier, oscilloscope, 9.25" thick PCC slab.

Figure 9. Pulse-echo measurement (one-transducer) on PCC with 190 kHz lead metaniobate transducer from Thornton and Alexander, 1987.

Figure 10. Ultrasonic pulse-echo measurement on PCC with 200 kHz polyvinyldene fluoride (PVDF) transducer operating at 60 kHz from Claytor and Ellingson, 1986.

Alpha-Transmitter Pulse
(0.0 μs)

Beta-Reflected Longitudinal
Wave (226.0 μs)

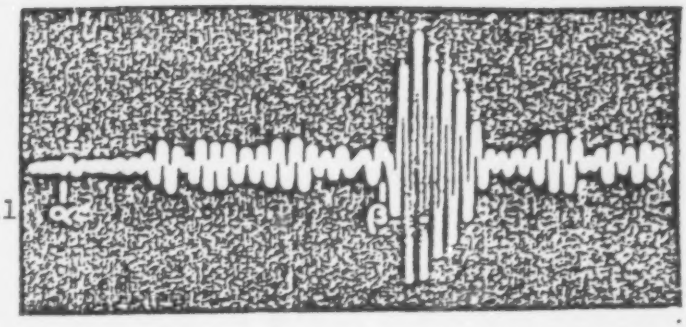

Figure 1. Pitch-catch measurements on PCC with 100 kHz barium titanate transducers from Bradfield, Woodroffe, 1953.

and

A-Time Mark 150 μs after
Transmitter Pulse

B-Surface Wave (185 μs)

C-Reflected Longitudinal
Wave (281 μs)

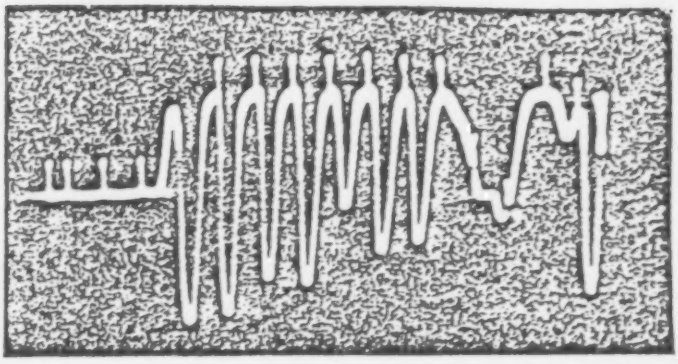

A B C

Figure 2. Pitch-catch measurements on PCC with 100 kHz barium titanate transducers from Bradfield and Gatfield, 1964.

A-Transmitter Pulse
(0 μs)

B-Surface Wave
(110 μs)

C-Reflected Longitu-
dinal Wave (188 μs)

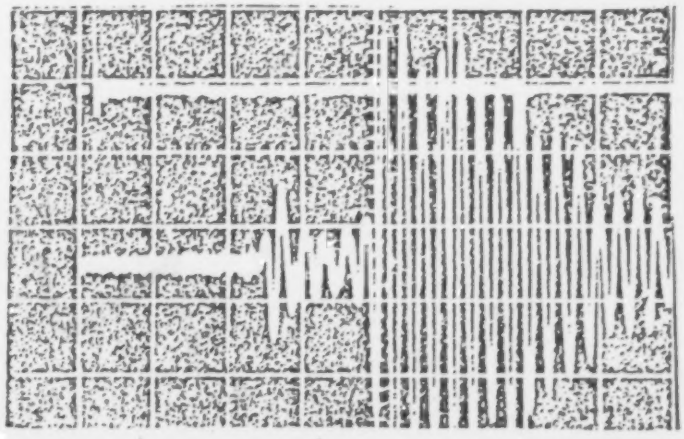

A B C

Figure 3. Pitch-catch measurements on PCC with 100 kHz barium titanate transducers from Howkins, 1968.

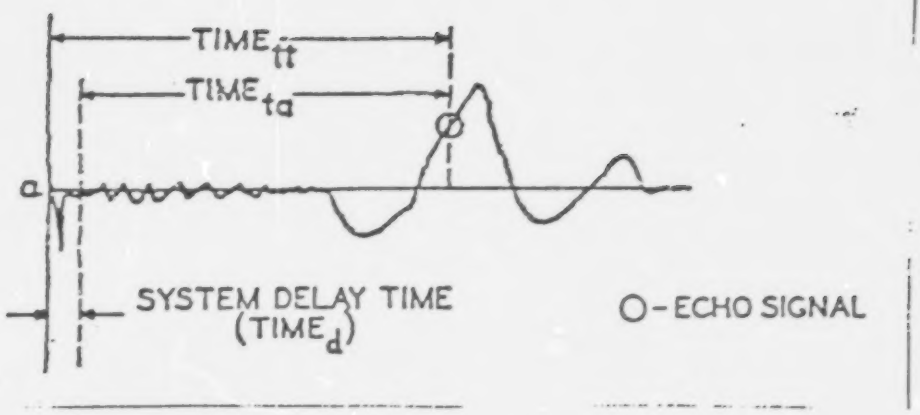

Figure 4. Pitch-catch measurements on PCC with 200 kHz lead zirconate titanate transmitter and a broadband receiver of lithium sulfate from Golis et al., 1971.

A-Transmission Pulse
(0 us)

B-Surface Wave (50 us)

C-Reflected Longitudinal
Wave (130 us)

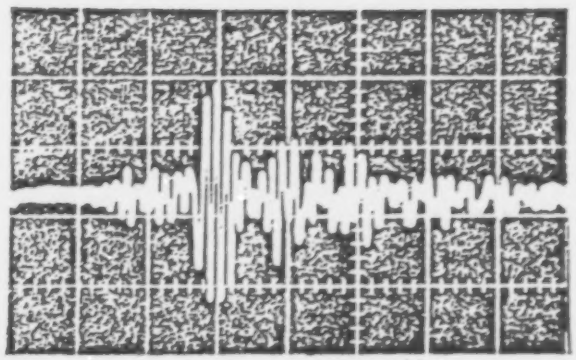

A B C

Figure 5. Pitch-catch measurements on PCC with 180 kHz lead zirconate titanate transmitter and broadband lithium sulfate receiver from Thornton and Alexander, 1987.

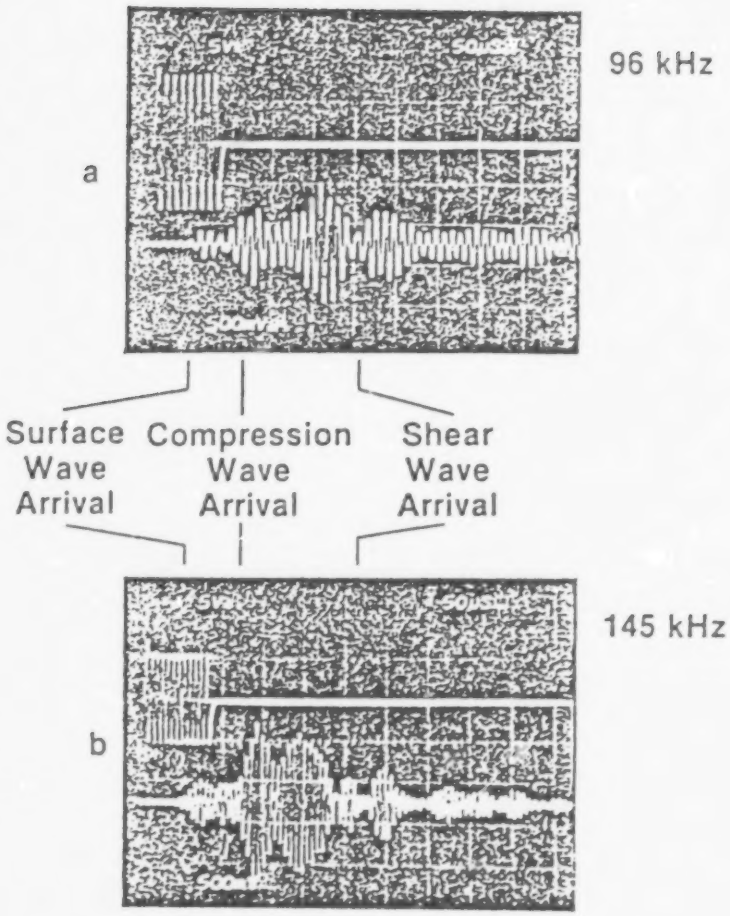

Figure 6. Pitch-catch measurements on refractory concrete with 250 kHz transducers of lead zirconate titanate from Claytor and Ellingson, 1984.

A-Transmitter pulse
(0 μs)

B-Backscattering
(35 μs)

C-Reflected Longi-
tudinal Wave
(106 μs)

S/N - 18
9/18/85

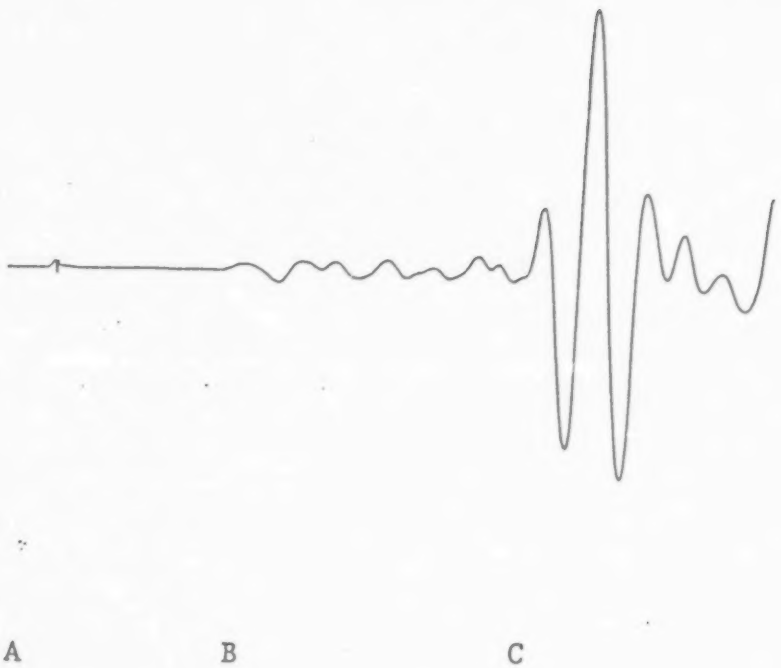

Figure 7. Pitch-catch measurements on PCC with 190 kHz lead metaniobate transmitter and lead zirconate titanate receiver from Thornton and Alexander, 1987.

A-Receiver (PZT-5H)

B-Lead Metaniobate
Transmitter (EC-82)

C-Pulser

D-Oscilloscope

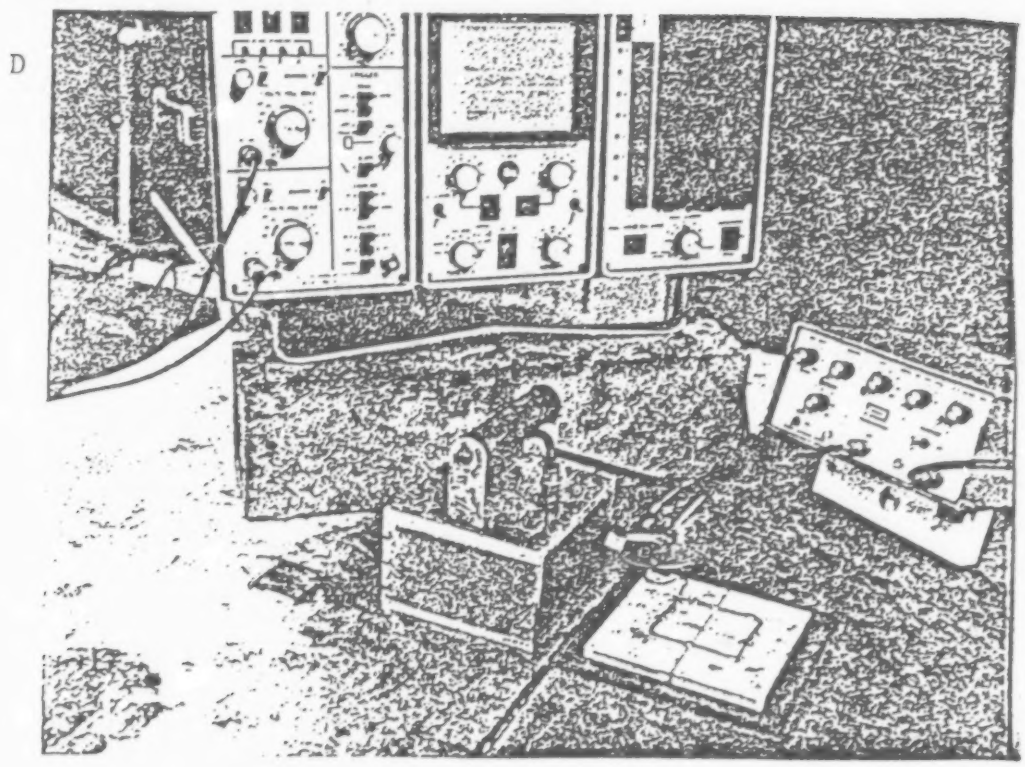

Figure 8. Ultrasonic pitch-catch system: transmitter, receiver, pulser/filter/amplifier, oscilloscope, 9.25" thick PCC slab.

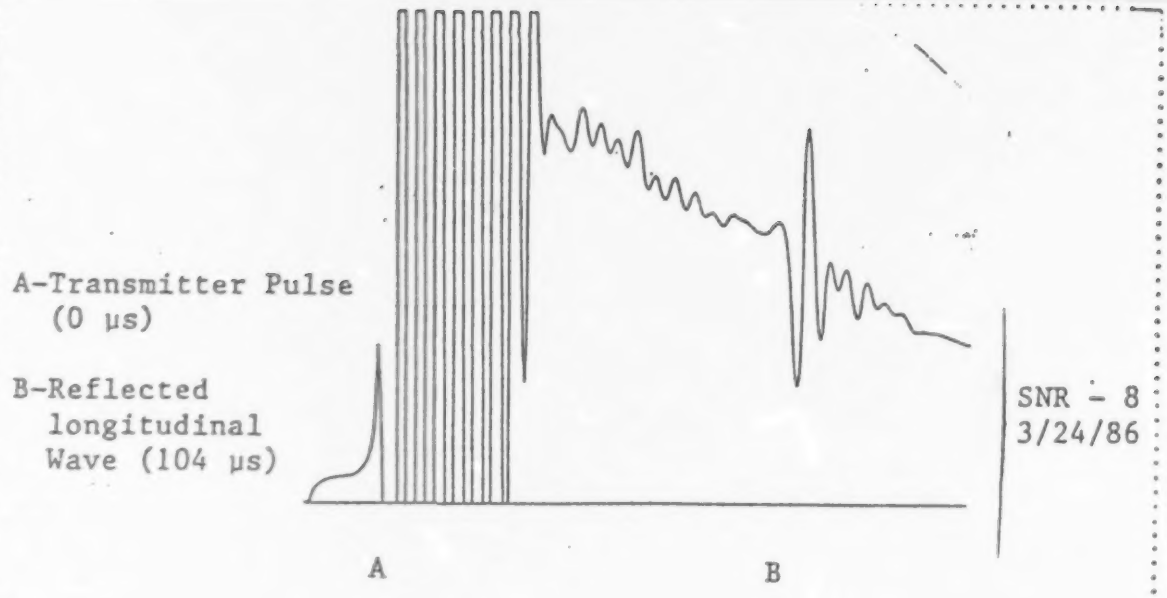

Figure 9. Pulse-echo measurement (one-transducer) on PCC with 190 kHz lead metaniobate transducer from Thornton and Alexander, 1987.

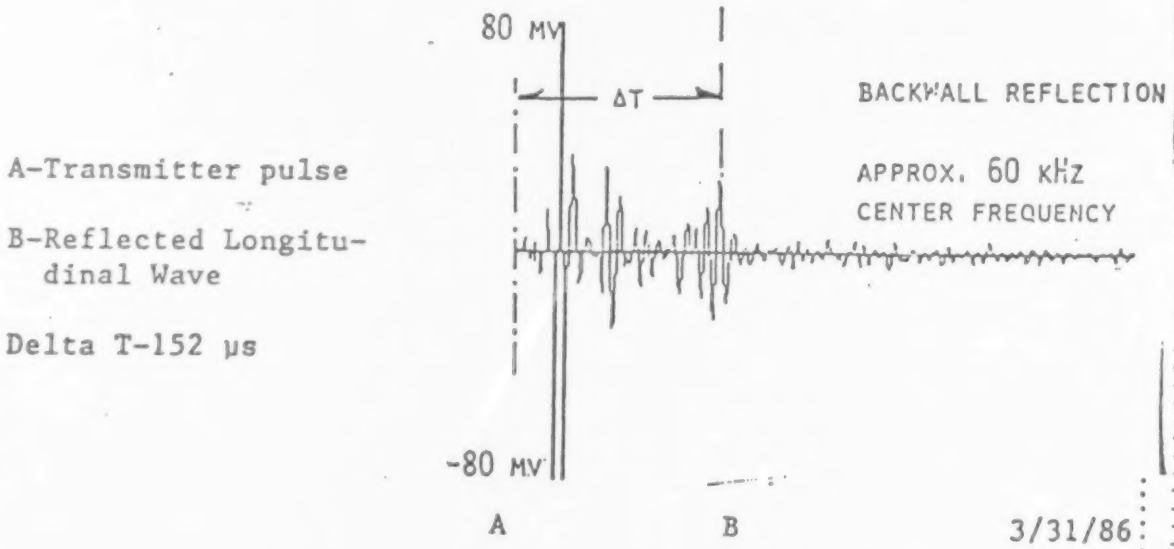

Figure 10. Ultrasonic pulse-echo measurement on PCC with 200 kHz polyvinyldene fluoride (PVDF) transducer operating at 60 kHz from Claytor and Ellingson, 1986.

APPENDIX 12

REPORT OF TECHNO SCIENTIFIC INC.

TECHNO SCIENTIFIC INC.
60 Caster Ave., Woodbridge, Ontario, L4L 4X2 (416) 851-9958, Telex 06-986766 TOR

PULSE ECHO TESTING OF ARCTIC STRUCTURE MOCK-UP

Report to

B.H. Levelton and Associates Ltd.

R8801

December 1987

Prepared by: M.Macecek
C.Jaikaran

INTRODUCTION

Techno Scientific Inc. (TSI) was approached by Levelton and Associates to participate in informal trials of ultrasonic testing of reinforcing ducts filled with grout. A short test was carried out at the University of Ottawa attended by three teams, i.e. TSI, National Bureau of Standards, and U.S. Corps of Engineers, each team with its own technology. TSI used the pulse-echo technique with transducers developed at TSI and some advanced signal processing techniques.

BACKGROUND

In the ultrasonic testing of concrete, difficulties arise from two problems, the greater an isotropy of physical properties of concrete and its variability due to the aggregates, its high attentuation of ultrasound and mode conversion at each boundary. Consequently, signals are very complex and the material is very difficult to penetrate. The project deals with the ducts for reinforcing material which are partly filled with grout. The objective of the exercise is two-fold, to detect the grout ducts and to detect if they are filled with grout or empty. The concrete test block prepared was 1 m X 1 1/2 m X 2 in size and it is shown in Figure 1. Seven ducts were prepared by the manufacturer of the block and TSI had prior knowledge of their location but not of the degree of filling or location of cavities. In addition, one side of the block had a grid of reinforcing bars of two sizes 35mm and 20mm.

METHOD AND PHILOSOPHY

TSI was previously involved in ultrasonic concrete testing projects which were initiated by EMR and jointly funded by EMR and TSI. We addressed the basic physical problems. We believe that the main and foremost objective of the exercise is to obtain sufficient signals. This was the thrust of our original research work (1) and we produced transducers which reliably isonified concrete blocks in the pulse-echo mode up to the depths of 40feet. The transducer is characterized by its frequency, beam spread and damping. An optimized transducer should be chosen for the application at hand. By varying the frequency we can vary the attentuation. The beam can be restricted by focusing or by choosing the size of the transducer.

EXPERIMENTAL MEASUREMENTS

The ultrasonic pulse-echo technique from one side of the wall was used. Experimental measurements were carried out with a simple experimental set-up shown in Figure 2. Velocity in the block was first established for 1 m and 2 m sides using a transmit-receive technique which not only established the velocity but electronic delays in the instrumentation as well. The ultrasonic velocity yielded was 4,380 m per second. Figure 3 shows the signal which was received and depicts the amplitude versus the time of arrival of the signal. The typical geometry of testing was shown in Figure 4. The measurements consisted of placing the transducers separated by a constant distance i.e. 150mm and recording the

signal in a digital form. Analog signals were also observed on the attached Tektronix 2445 scope. A sample of the signal with some relevant features is shown in Figure 5. However, we had some difficulties with triggering the signals and therefore we had to use a surface wave as a trigger signal for a digitizing computer. One-hundred to hundred and fifty points were taken and these signals were stored. Examples of a signal are shown in Figures 6 - 11. The evaluation consisted of allocating the peaks, evaluation of amplitudes of the signal and its normalization. This takes into account the variable quality of the concrete where the back wall was used as the best reflector. Some signals were evaluated in the frequency domain. The evaluation logic is shown by the flow chart in Figure 12.

Some difficulties were encountered in signal quality because of the rough surface of the block. At times the quality of coupling varied. Lithium white grease was used as the couplant and the surface roughness at times prevented good contact between the transducer and the concrete wall. Evaluation consisted of plotting the signals and its echoes along the time basis to give a two-dimensional B-scan equivalent plot. Some examples of the plots are shown in Figure 13. As mentioned before, the problem with triggering led to some variation in the trigger pulse so in some instances the absolute travel times were not obtained. However, the back wall was reliably established and based on the velocity calculated on the first two measurements, the thickness of the block was calculated to be 1m up to 1.06, within 6 % error which is considered a very good agreement.

Echo evaluation of the signals for these features can be seen in Figure 14. A typical plot displays the amplitude of the echo-signals normalized to the back wall (BW) along the length of the duct. Variations of the amplitude are caused both by the variations in coupling which were hopefully eliminated by normalization to the back wall signal amplitude and changes in the duct. An air cavity filled duct will have a stronger signal then the one filled with the grout. A partially filled cavity will fit in between the two cases whereas a water filled cavity will have its backwall appearing later due to the lower velocity in water. In some instances no BW signals were received because of the additional duct crossing. The effect off the bar reinforcements was not detrimental as can be seen in Figure 15. While there were signal variations, the echo could be clearly resolved. The comparison of signals from the clean and the reinforced side is shown in Figure 15. In many locations, signals were identical from both sides. In the presence of the interfering duct, rebar, poor surface or a different distance to the duct, the two signals differ noticeably.

(The original plan for this round robin experiment involved taking measurements on the first day and then being told about internal features of the block.The method could be trained then on these features. However, this never materialized so we had no positive confirmation of any signal from the duct.)

OBSERVATIONS

Duct A

-no backwall in positions 2 and 3, probably due to Duct F
-no backwall in position 6, could be due to an air filled void
-strong duct signal in position 12, could indicate a partially filled void or it could be a bottom reflection

Duct B

-no backwall in position 2, could be due to duct F
-no backwall in position 6, could be an air filled void
-strong duct signal in position 11, could be due to a partly filled void

Duct C

-large reflection in position 3, could indicate air filled cavity
-no backwall position 4, could indicate same
-strong direct signal position 11, could indicate partially filled cavity
-also strong in position 6

Duct D
-large duct reflection around positions 4,5,and 6

Duct E
-large duct echo in position 6

Duct F
-nil

Duct G
-nil, completely filled

UNCERTAINTIES

The major difficulties arose from the following:

1) poor concrete surface

2) variable signal amplitudes in two neighboring spots

3) appearance of extra echoes probably caused by the aggregates

4) variation in the rising edge of the echo pulse which would require careful experiments to see the reflection from the duct.

5) normalization routines were subjective and did not yield enough accuracy.

6) knowledge of energy defect interaction is the most important factor in the evaluation of ultrasonic signals.

CONCLUSIONS

The short test carried out in the round robin experiment revealed that TSI's pulse-echo technique produced sufficient ultrasonic signals. Optimum working frequency was found to be 40 - 150 KHz with the higher end giving more distinct echoes over shorter distances. The evaluation routines were subjective and were not verified or correlated with the true state of the test piece. Some proposed interpretations of signals were put forward. These are therefore probabilistic in nature. In combination with the verification of each case and some advanced signal processing and signal evaluation routines, the method could achieve the objective of this exercise. Also, some two or three dimensional displays of results would give a clear overall view and would be most helpful.

B.H. LEVELTON & ASSOCIATES LIMITED
8805 Oster St., Vancouver, B.C. V6P 4G1 ■ (604) 266-1411 ■ Telex 04-55581
Fax 266-0130

PROJECT: VOIDS IN GROUTED DUCTS
SUBJECT: CONFIGURATION OF TEST WALL

PAGE: 1
DATE: 87/10/22
FILE: 184-612

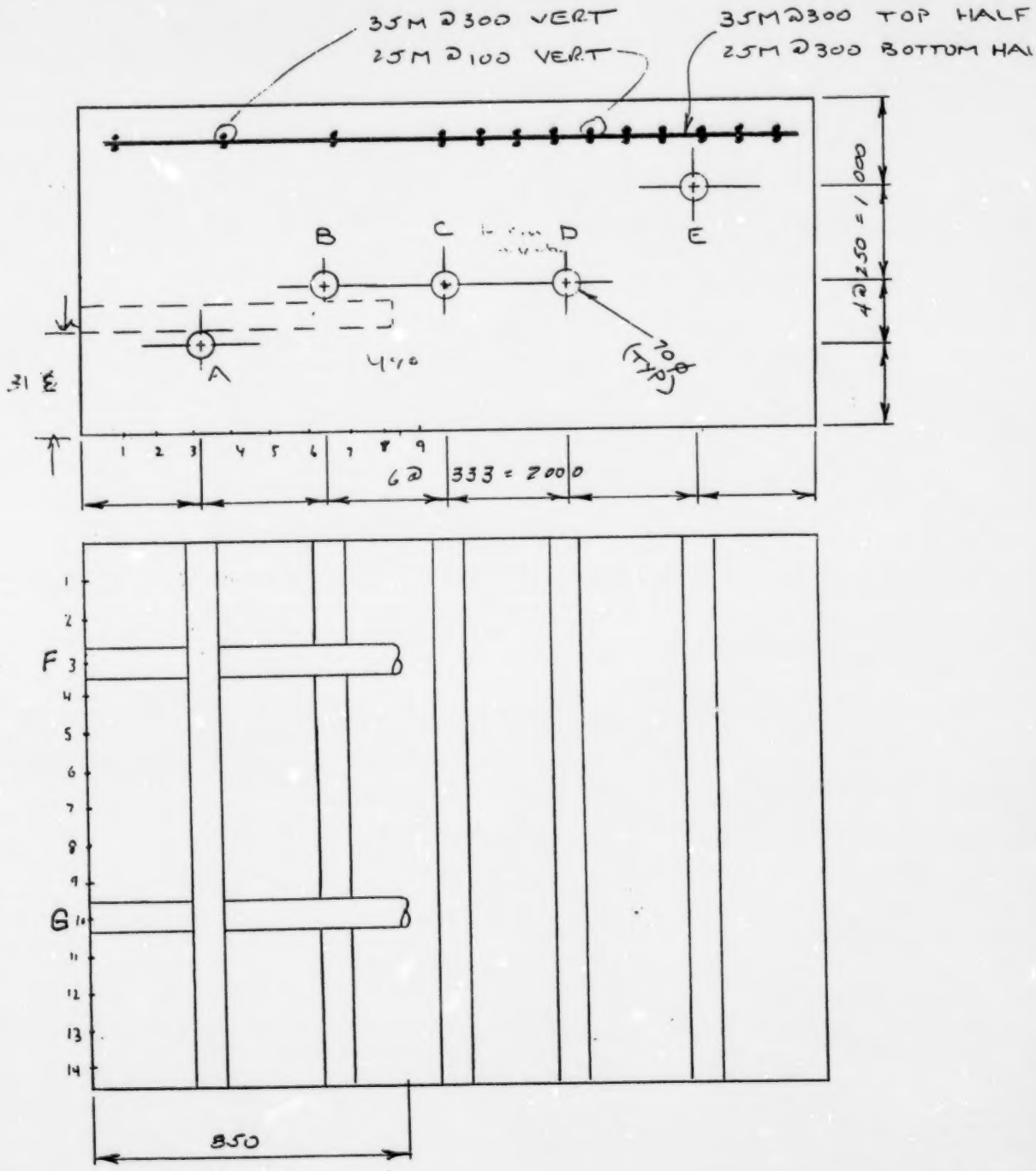

FIGURE 1. Layout of the concrete test block containing vertical and horizontal ducts and reinforcing bars.

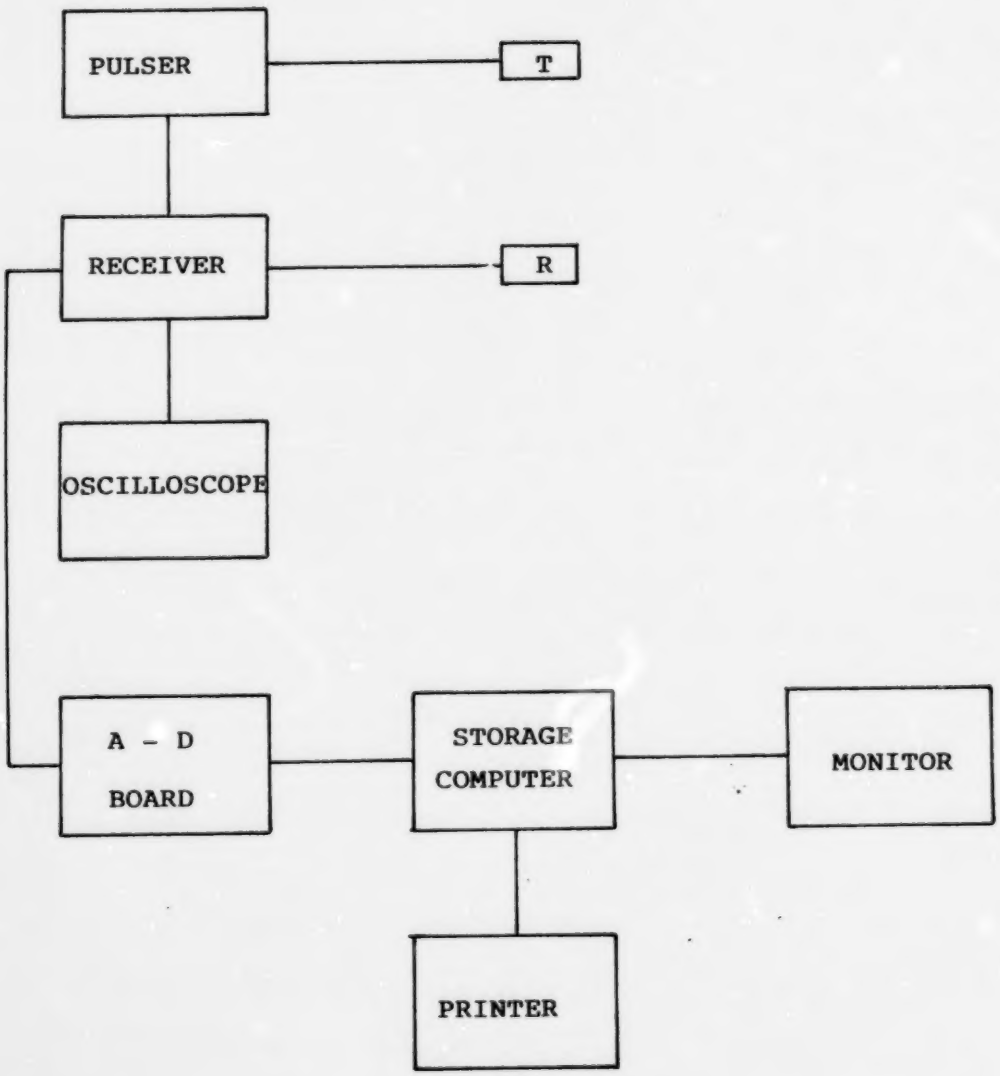

Figure 2. Block diagram of the ultrasonic system.

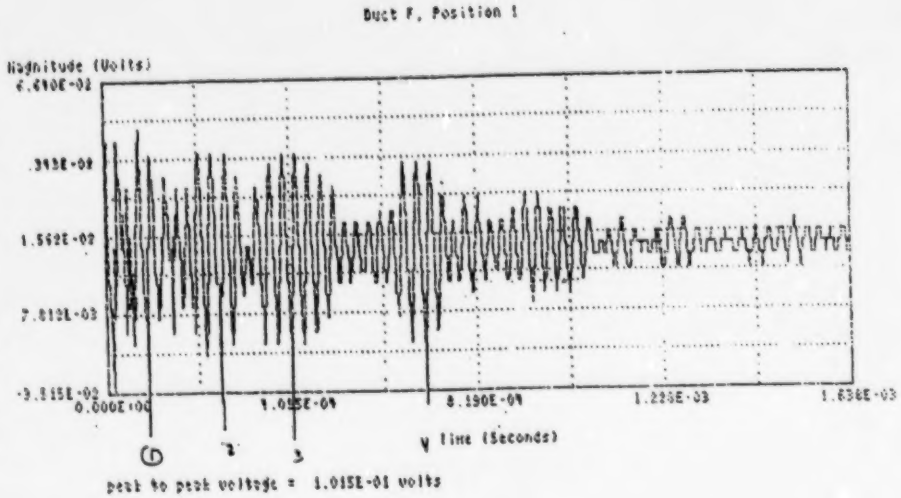

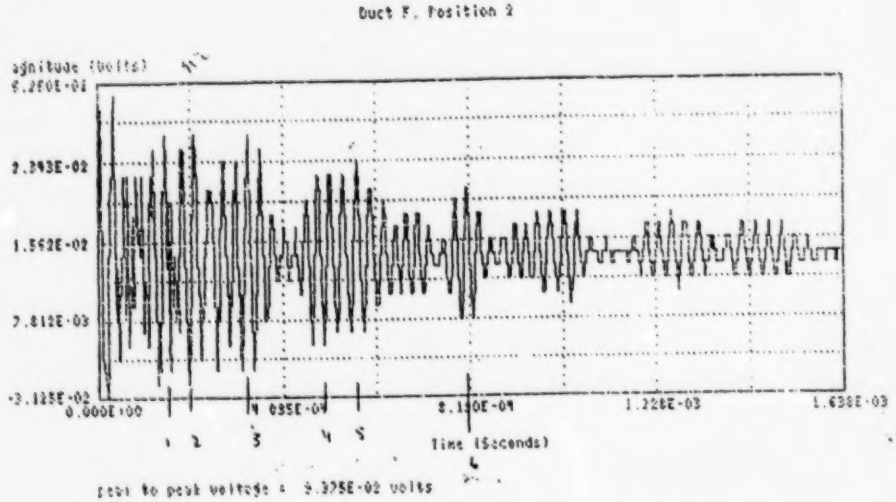

Figure 3. Typical shape of the received echo.

T and R = transmit and receive

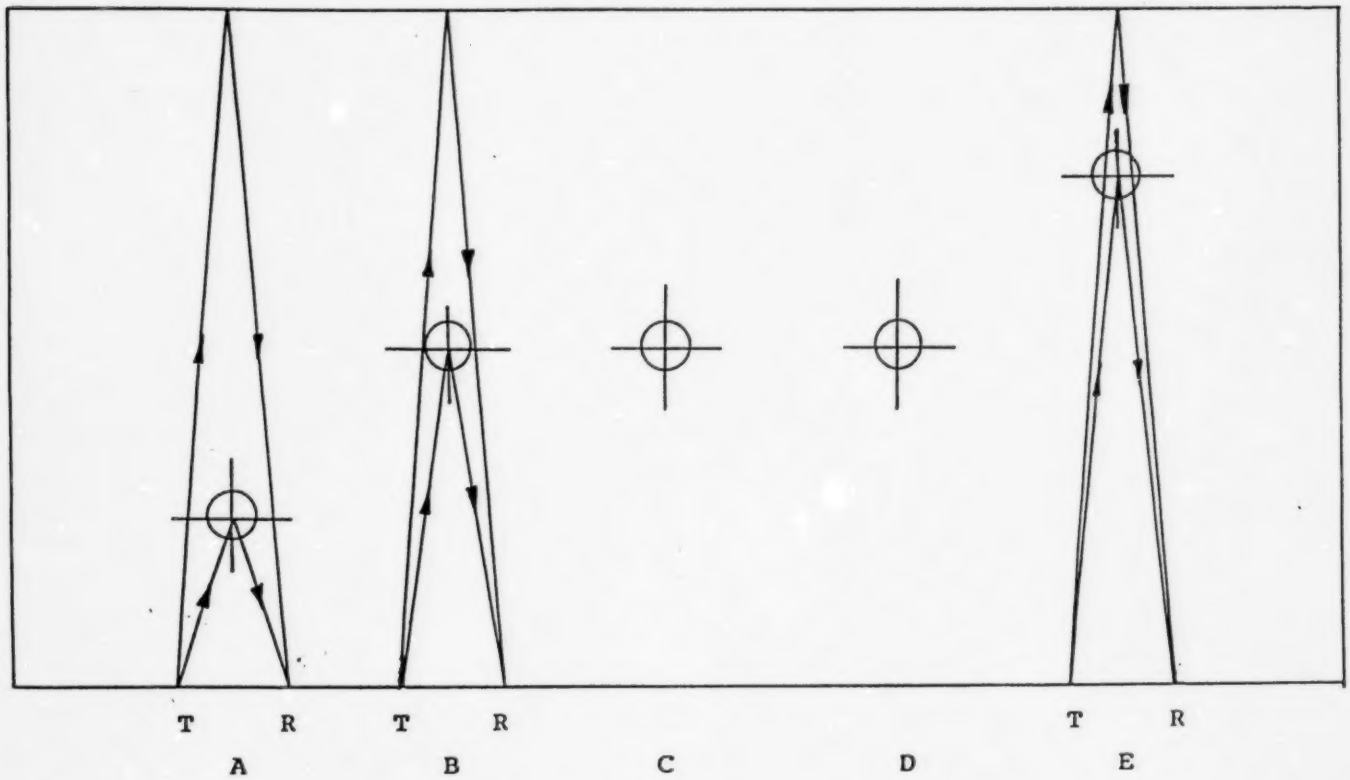

Figure 4. Interaction of the ultrasonic beam with grouting ducts in different locations.

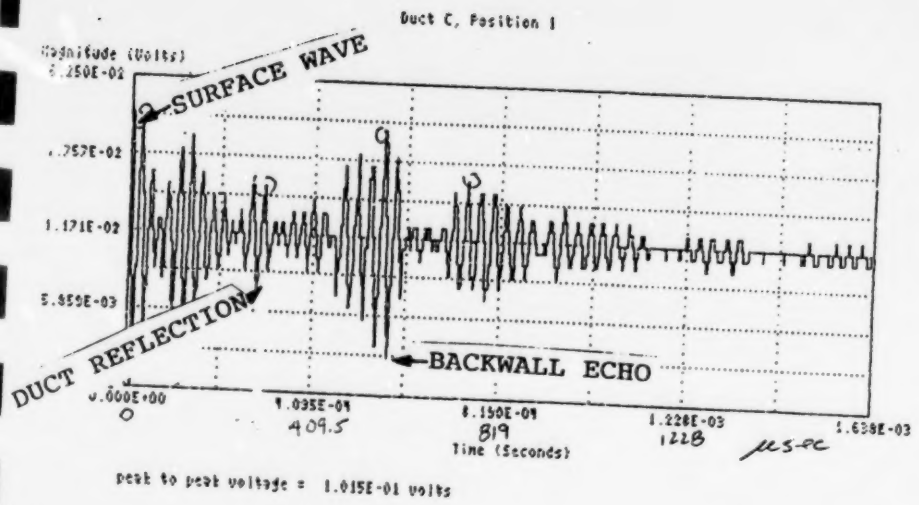

Figure 5. RF waveform of an echo showing relevant features.

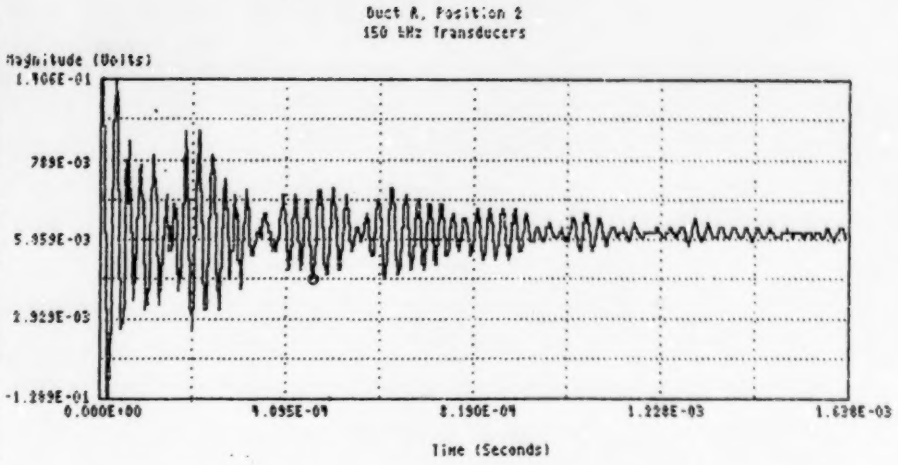

peak to peak voltage = 2.695E-01 volts

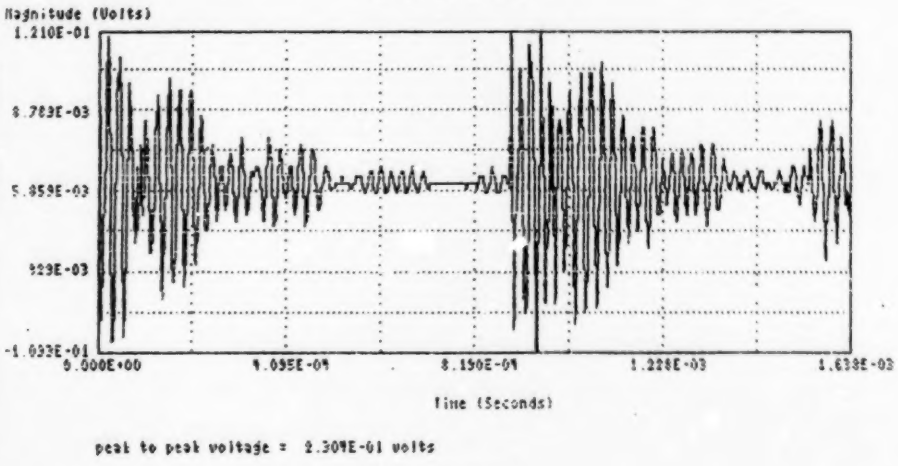

peak to peak voltage = 2.309E-01 volts

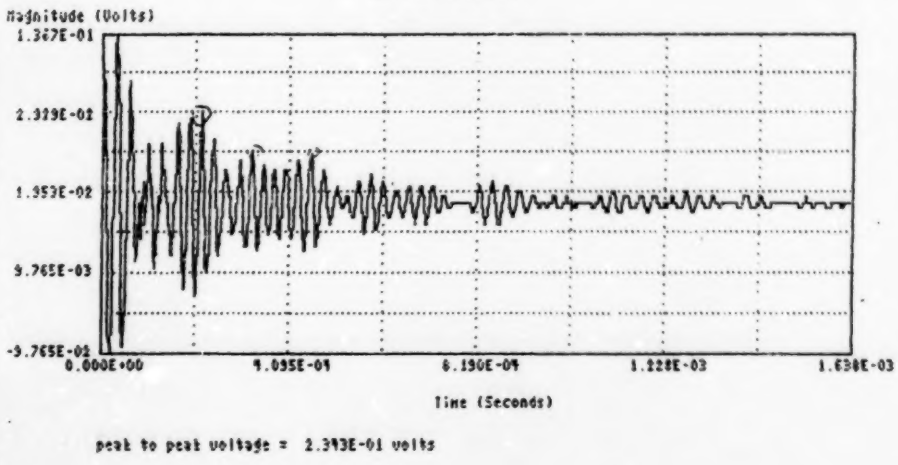

peak to peak voltage = 2.343E-01 volts

Figure 6.

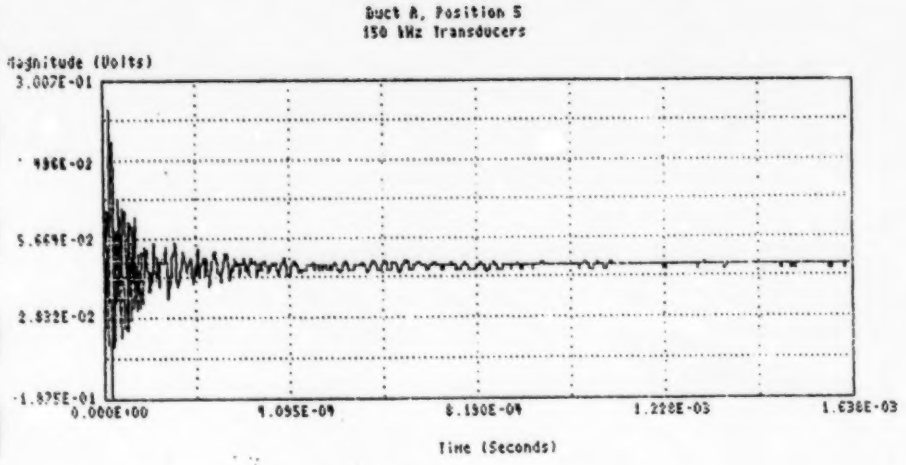

peak to peak voltage = 4.882E-01 volts

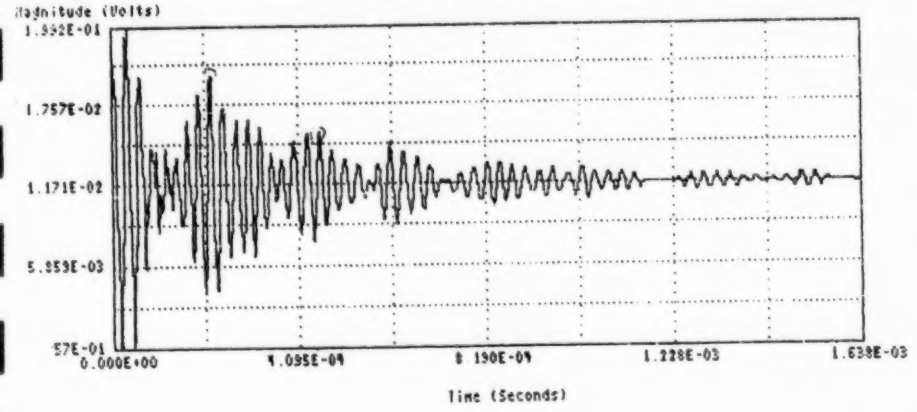

peak to peak voltage = 3.250E-01 volts

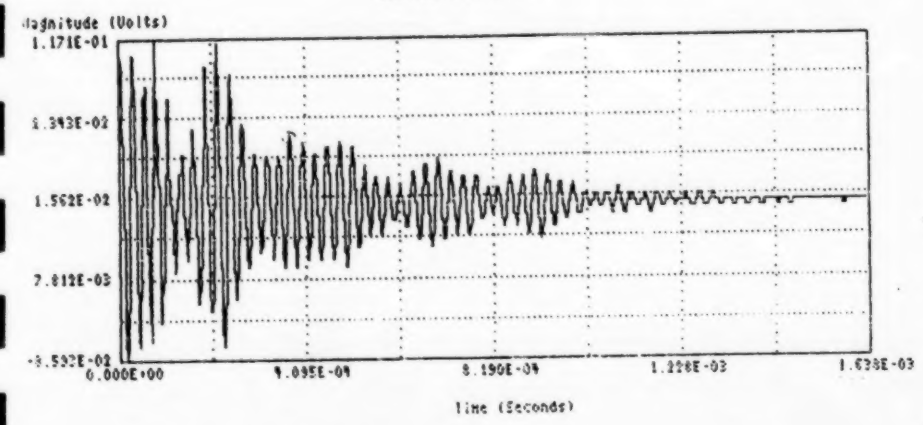

peak to peak voltage = 2.031E-01 volts

Figure 7.

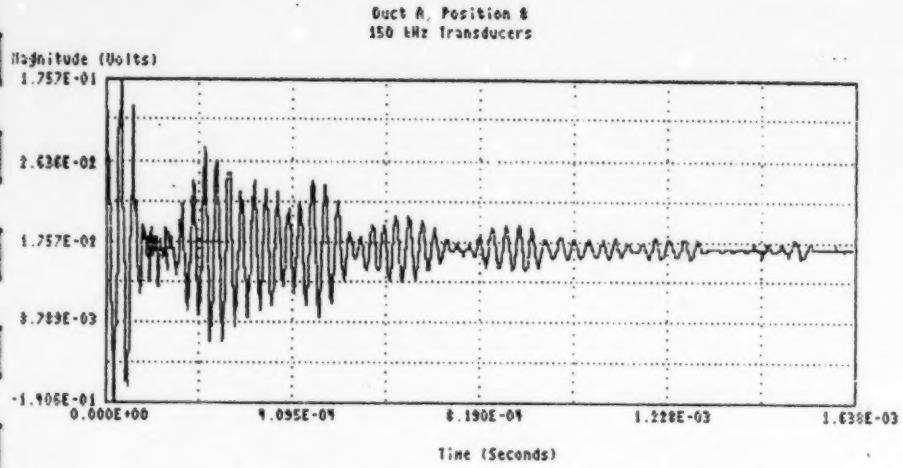
Duct A, Position 8
150 kHz Transducers
Magnitude (Volts)
1.757E-01
2.636E-02
1.757E-02
8.789E-03
-1.406E-01
0.000E+00
4.095E-04
8.190E-04
1.228E-03
1.638E-03
Time (Seconds)
peak to peak voltage = 3.1E4E-01 volts

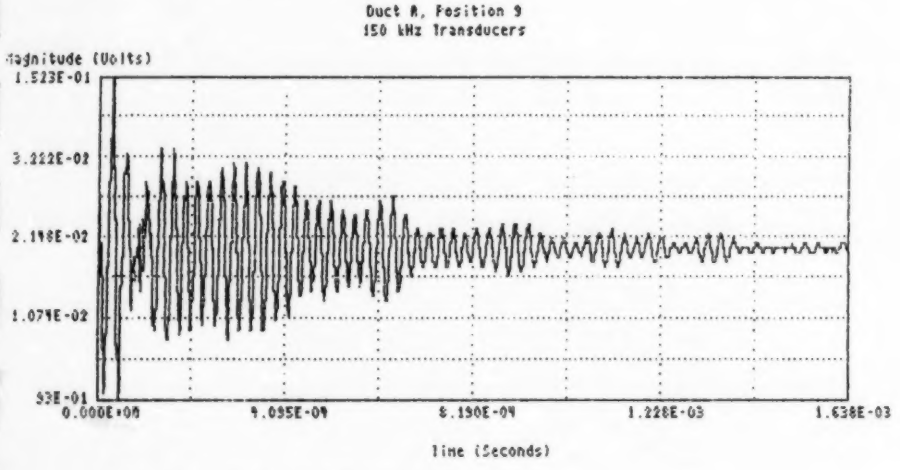
Duct A, Position 9
150 kHz Transducers
Magnitude (Volts)
1.523E-01
3.222E-02
2.198E-02
1.074E-02
93E-01
0.000E+00
4.095E-04
8.190E-04
1.228E-03
1.638E-03
Time (Seconds)
peak to peak voltage = 2.617E-01 volts

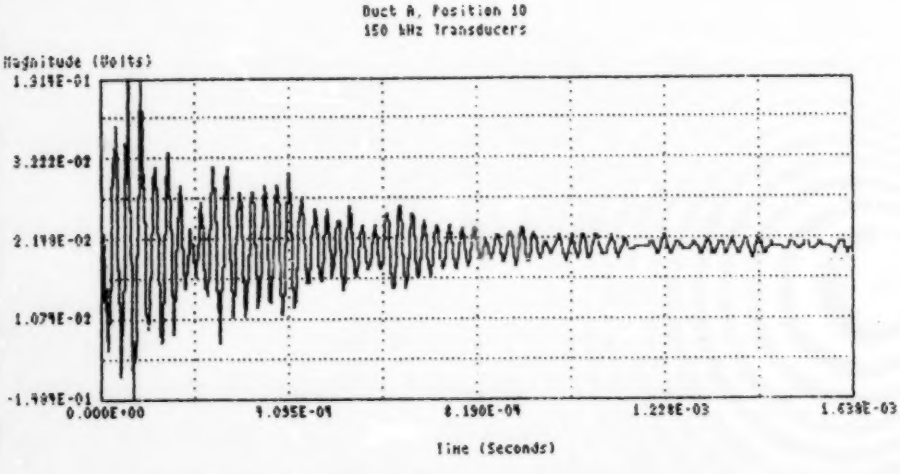
Duct A, Position 10
150 kHz Transducers
Magnitude (Volts)
1.319E-01
3.222E-02
2.198E-02
1.074E-02
-1.489E-01
0.000E+00
4.095E-04
8.190E-04
1.228E-03
1.638E-03
Time (Seconds)
peak to peak voltage = 3.399E-01 volts

Figure 8.

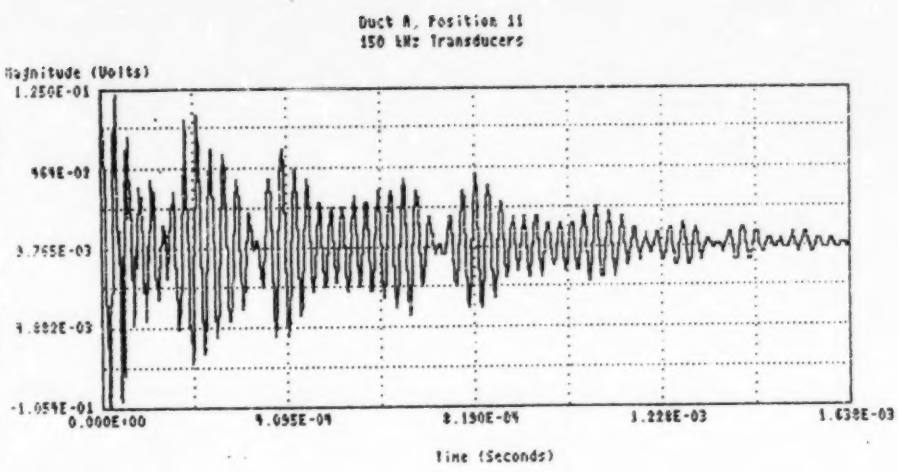

Figure 9.

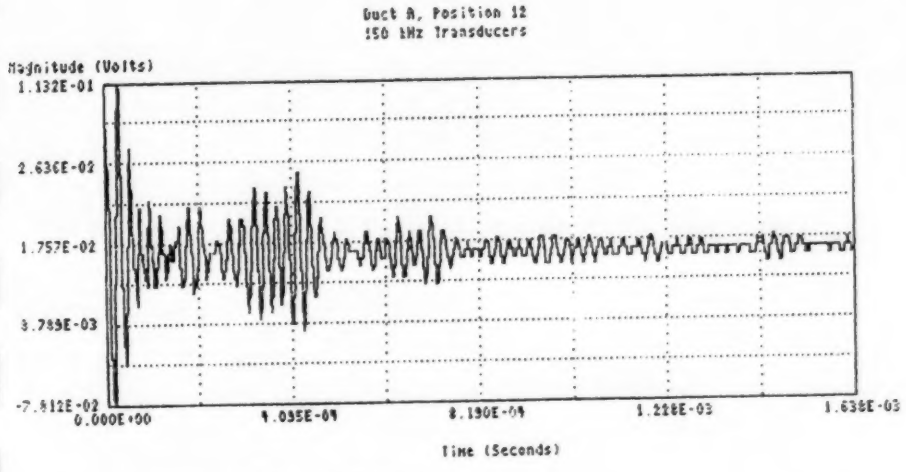

Figure 10.

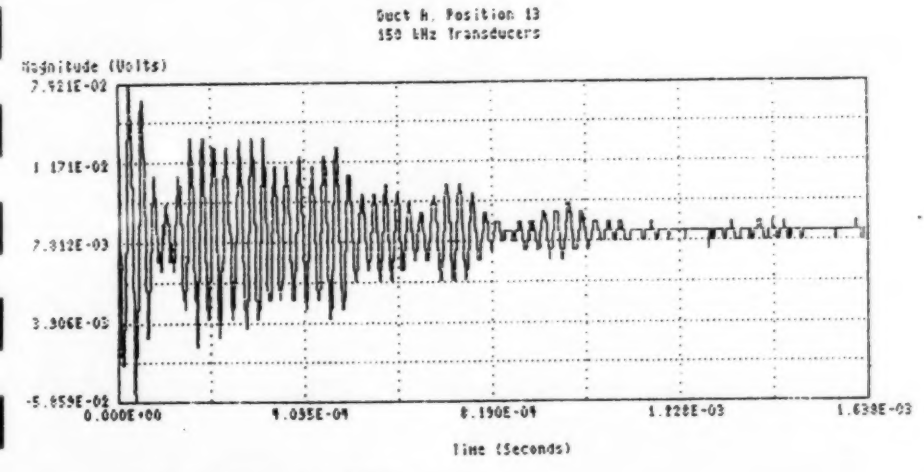

Figure 11.

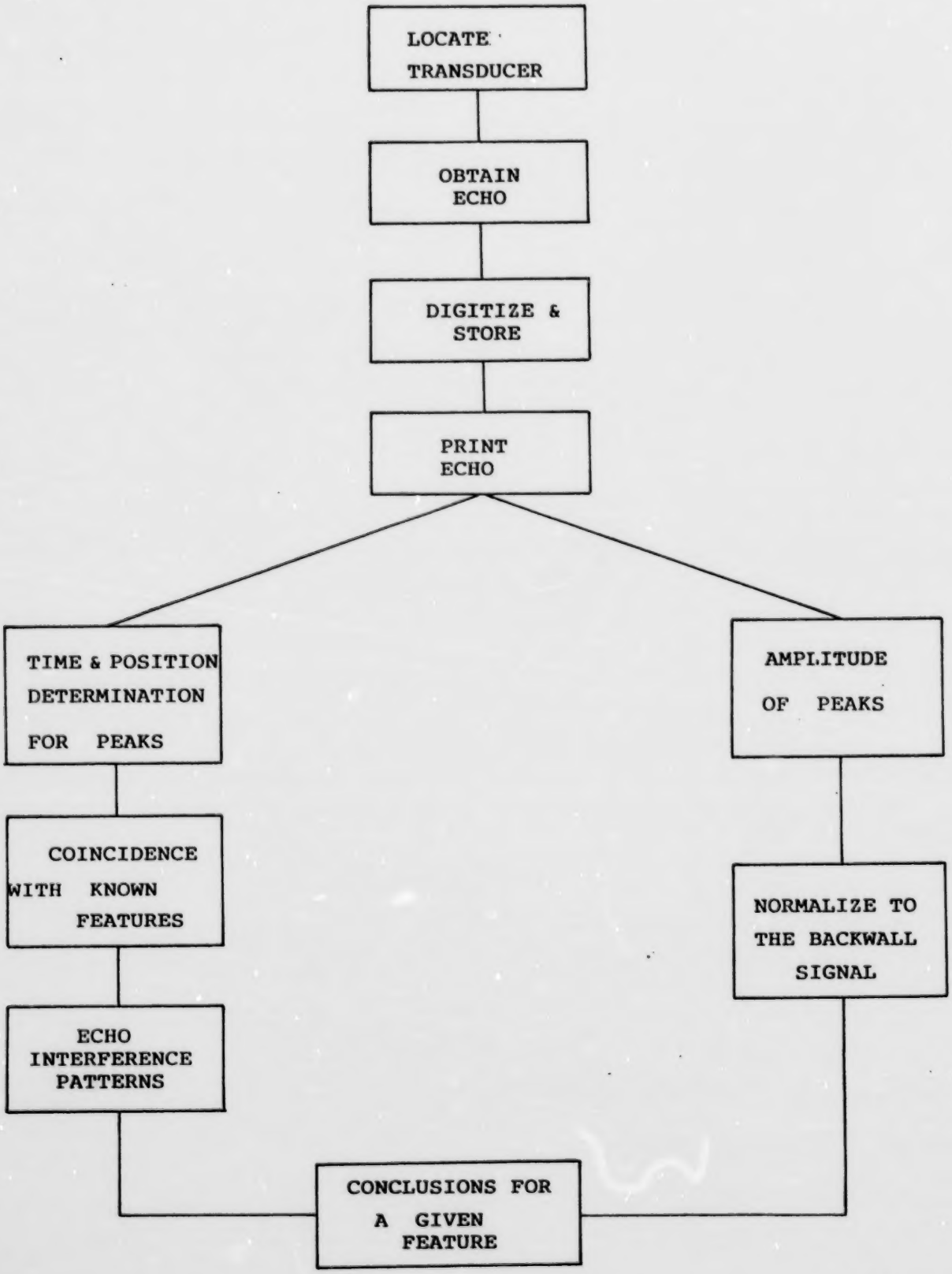

Figure 12. Signal evaluation logic

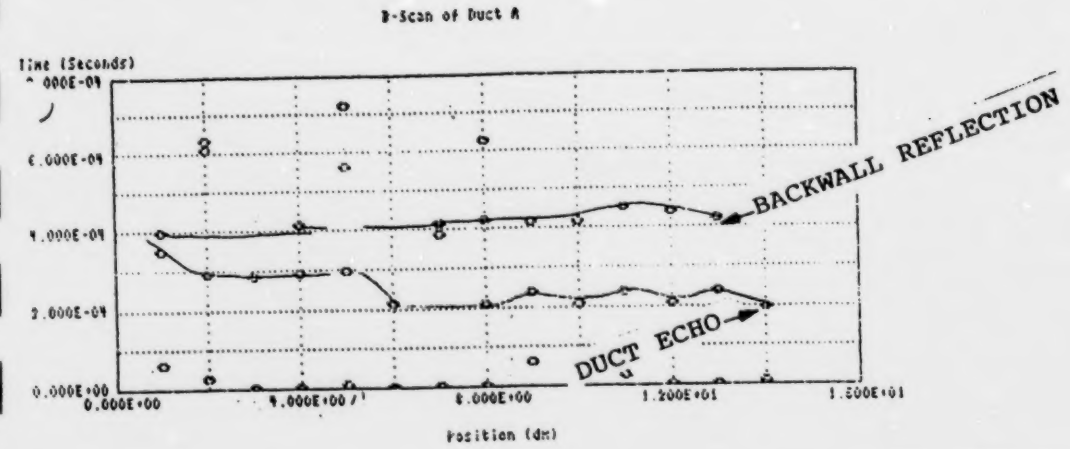

Figure 13. An example of "B-Scan" like plot based on subjective assignment of features.

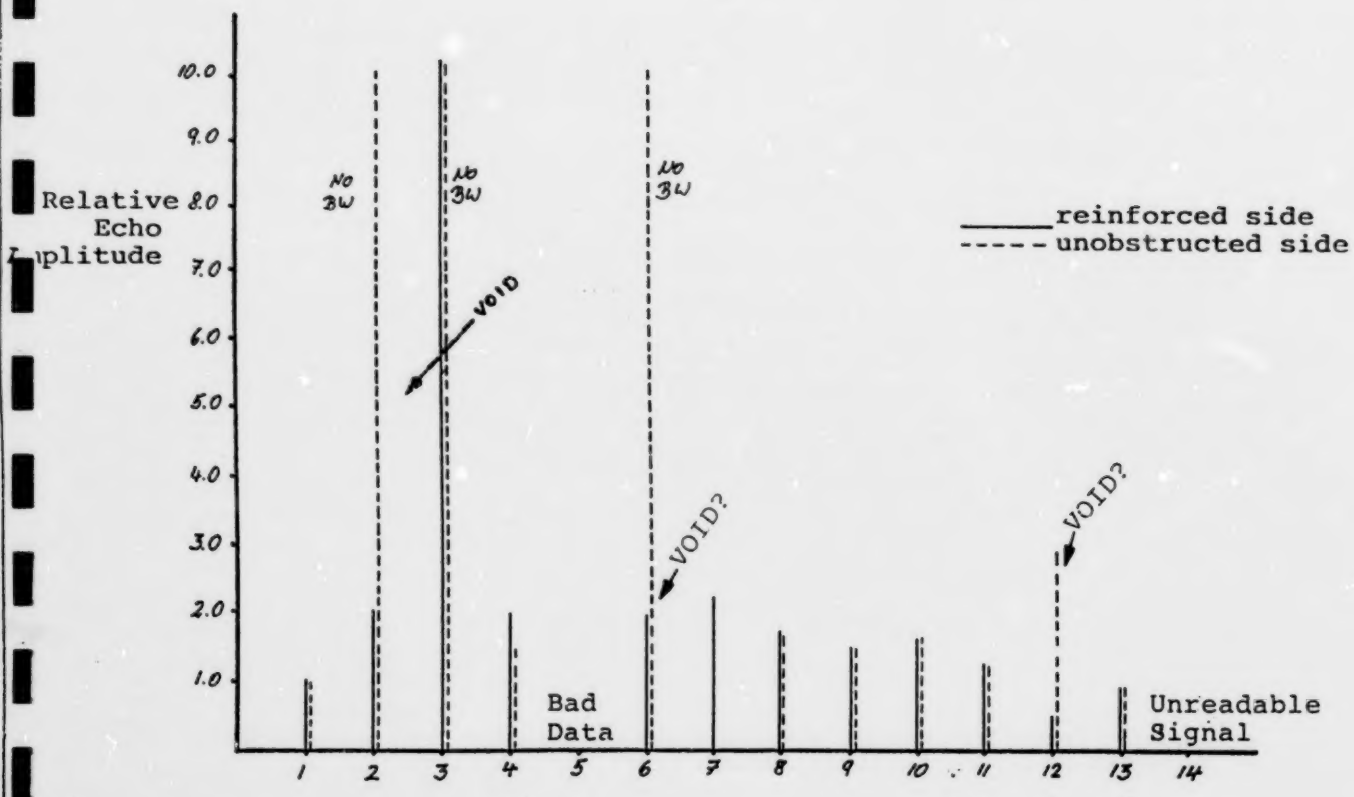

Figure 15. Duct reflection normalized to backwall reflection.

Column B

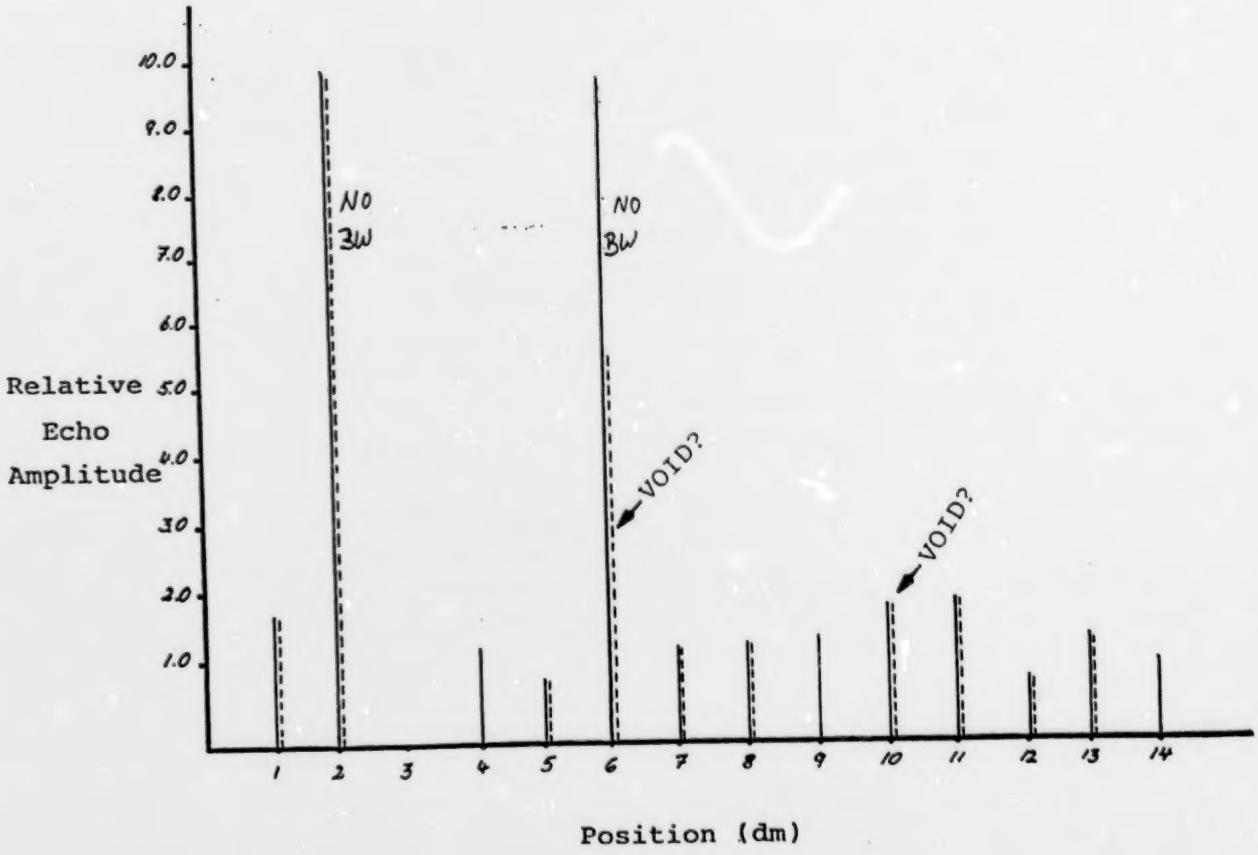
Relative Echo Amplitude
10.0
9.0
8.0
7.0
6.0
5.0
4.0
3.0
2.0
1.0
NO BW
NO BW
VOID?
VOID?
1 2 3 4 5 6 7 8 9 10 11 12 13 14
Position (dm)

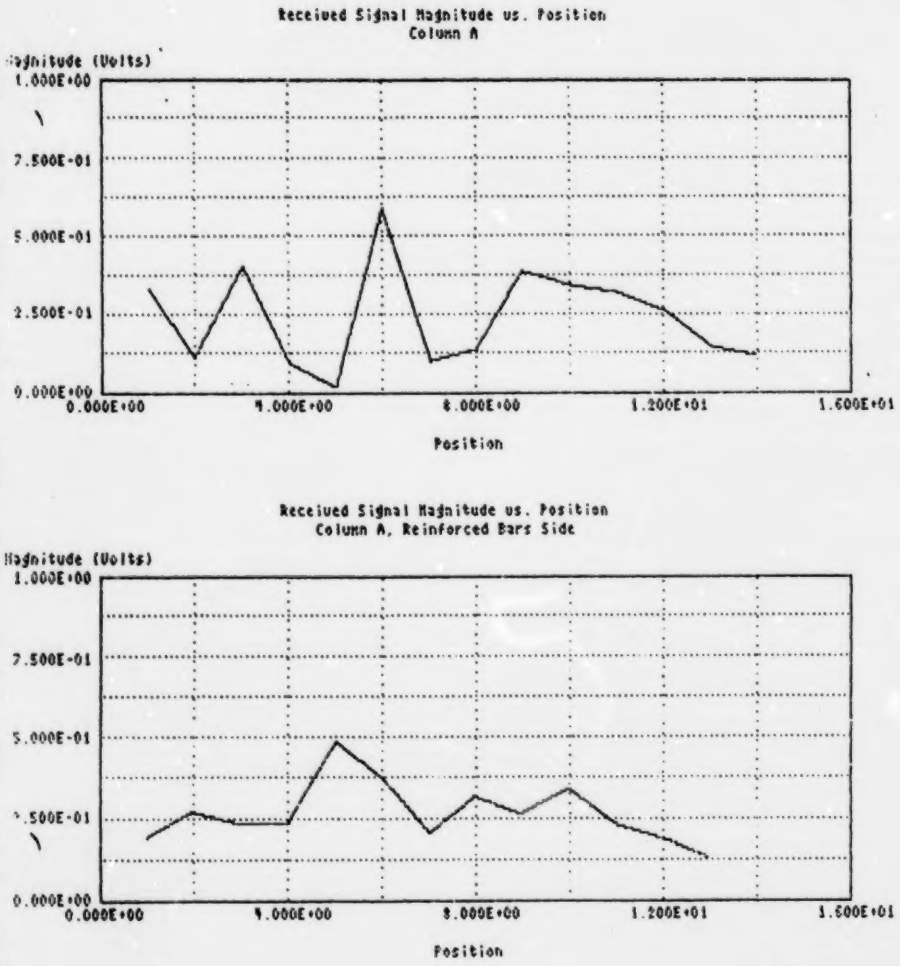

Figure 14. Duct echo amplitude as a function of position from the clean and reinforced side of the block.

Column C

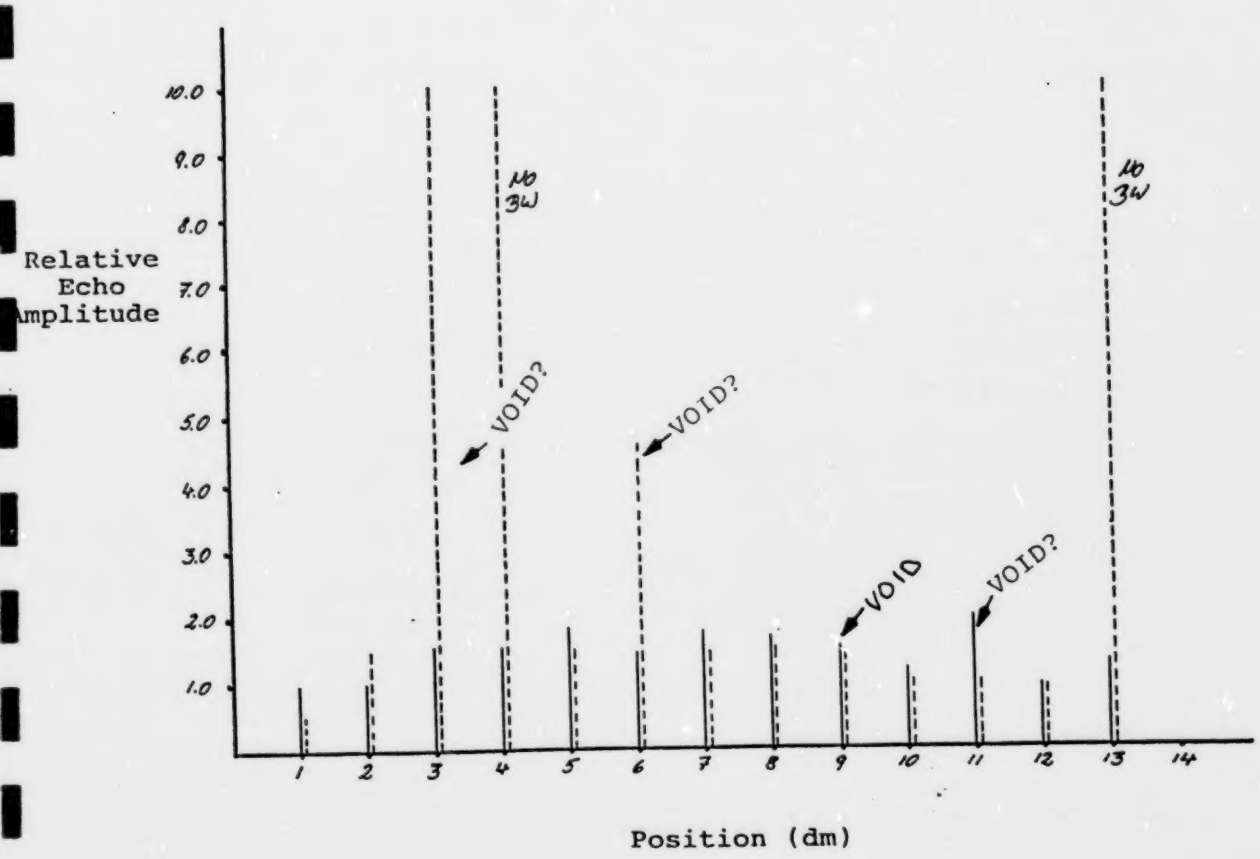
Relative Echo Amplitude
10.0
9.0
8.0
7.0
6.0
5.0
4.0
3.0
2.0
1.0
40 3W
40 3W
VOID?
VOID?
VOID
VOID?
1
2
3
4
5
6
7
8
9
10
11
12
13
14
Position (dm)

Column D

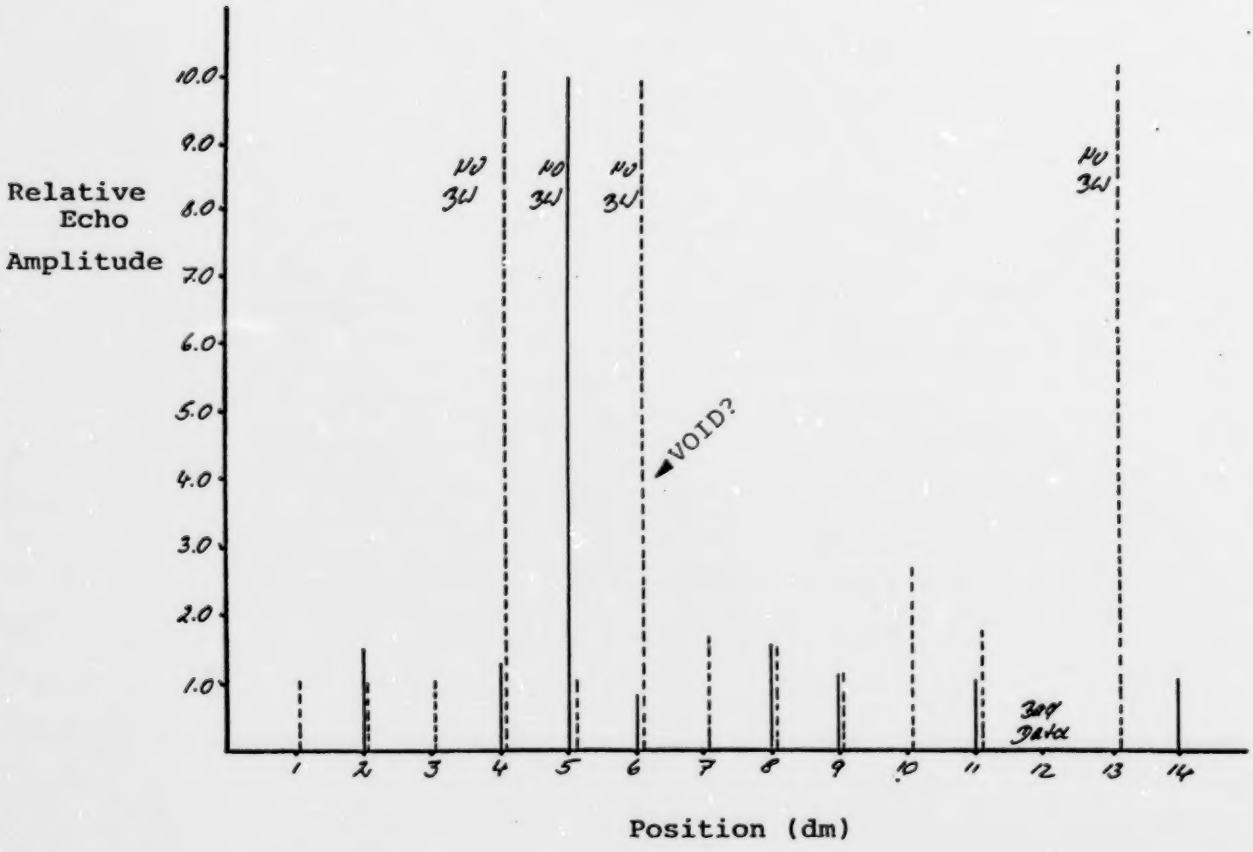
Relative Echo Amplitude
10.0
9.0
8.0
7.0
6.0
5.0
4.0
3.0
2.0
1.0
VOID?
1
2
3
4
5
6
7
8
9
10
11
12
13
14
Position (dm)

Column E

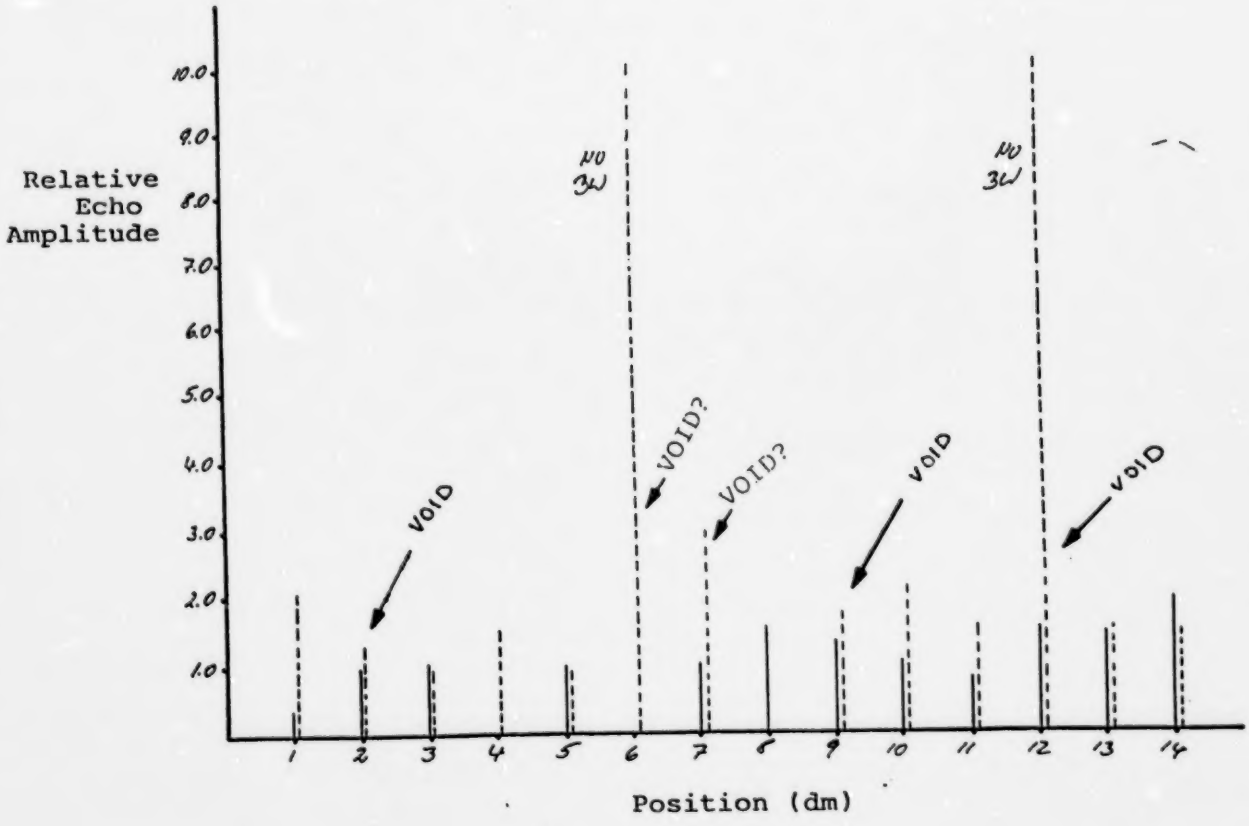
Relative Echo Amplitude
10.0
9.0
8.0
7.0
6.0
5.0
4.0
3.0
2.0
1.0
NO 3W
NO 3W
VOID
VOID?
VOID?
VOID
VOID
1
2
3
4
5
6
7
8
9
10
11
12
13
14
Position (dm)

Column F

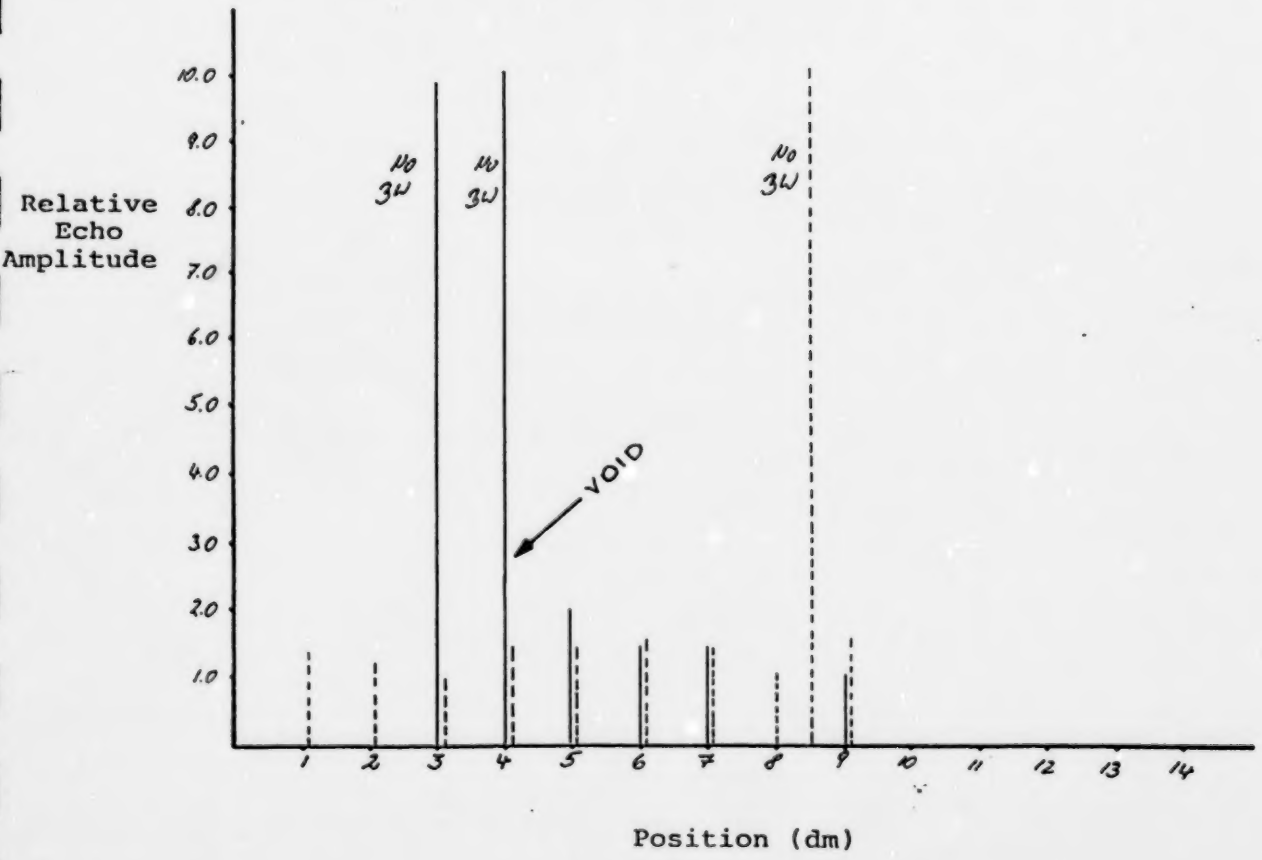
Relative Echo Amplitude
10.0
9.0
8.0
7.0
6.0
5.0
4.0
3.0
2.0
1.0
No 3W
No 3W
No 3W
VOID
1
2
3
4
5
6
7
8
9
10
11
12
13
14
Position (dm)

Column G

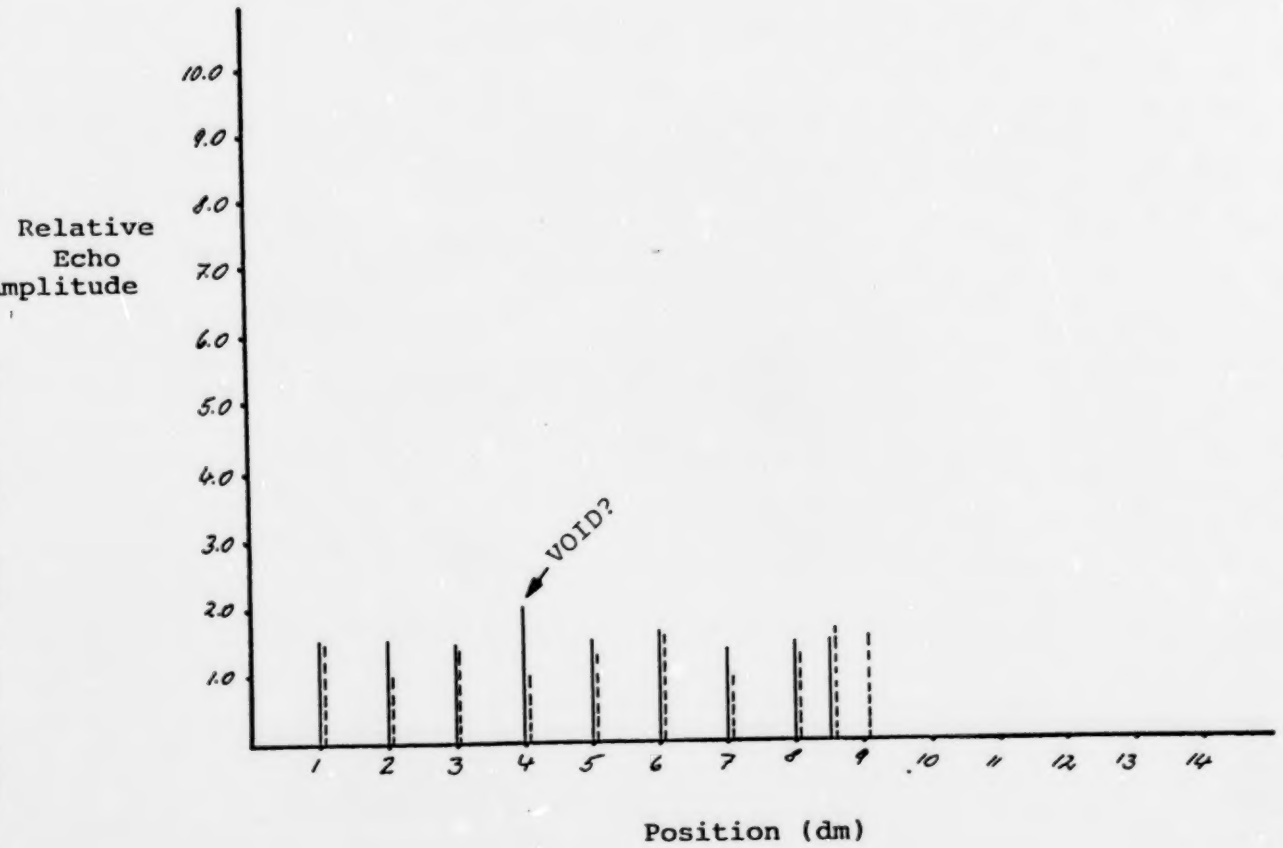
Relative Echo Amplitude
10.0
9.0
8.0
7.0
6.0
5.0
4.0
3.0
2.0
1.0
VOID?
1
2
3
4
5
6
7
8
9
10
11
12
13
14
Position (dm)

p

ADDENDUM

TSI received from Levelton and Associates the true location and type of defects embedded in the test block. Voids included artificial cavities (55mm-330mm long) and water-filled cavities in the same range. In addition, half-filled cavities with some rebar strands were also incorporated in Ducts C and D. (See the attached Figure).

After re-examining the results with the figure our results are summarized in Table I. The table lists all the defects (11 in total), their location in ducts and the positions measured from the top of the structure, type of cavity, i.e. full void, half void, air or water-filled. Additional distinguishable voids were added to illustrate the soundness of the evaluation. Table I indicates that in the original report, six out of eleven defects were positively detected, five were missed or considered marginal and two false flaws were indicated 600mm from the top of the block. These are marked with the letter "Y".

We re-examined the results taking into account the new defects. Some indications were already considered defects in the first report but by applying the same criteria afterwards, we can clearly classify them as defects (e.g. defect #1 in Col. A, defect #10 in Col. E, while more marginal, defect 8 in Col. E). The false indication around 600mm - 700mm was possibly caused by insufficient bonding during the pouring of the concrete in

layers.

In general, results were very satisfactory in Columns A - D and somewhat less satisfactory for Col. E. We noticed during our experiment that the end of the block i.e. Col. E region exhibited concrete of much poorer quality.

Estimation of size was moderately satisfactory in Col. C and Col. D. The true beam profile was not established in the concrete. Knowledge of the beam size would have aided us in the correct defect sizing.

Little attention was paid to determine the type of the cavity. We were not aware that water-filled cavities existed. Nor did we pay any attention to the rebar strands in the ducts. The method's shortcoming was the collection of data along the discreet measurements along the grid. Some of the defects were not "alligned" with our grid and edge errors were introduced.

A continous scan would have produced better results since any sudden change would have been noticed immediately. Had the system been trained for the signal response, the evaluation would have been much more successful. The results presented above show that there is room for improvement and that there is true potential in this methodology.

B.H. LEVELTON & ASSOCIATES LIMITED 8805 Osler St Vancouver, B.C V6P 4G1 ■ (604) 266-1411 ■ Telex 04-55581

PROJECT: VOIDS IN GROUTED DUCTS

SUBJECT: DESIGN OF TEST WALL
LOCATIONS OF VOIDS SHOWN AS-BUILT

PAGE: 1
DATE: 87/07/02
FILE: 184-617-11

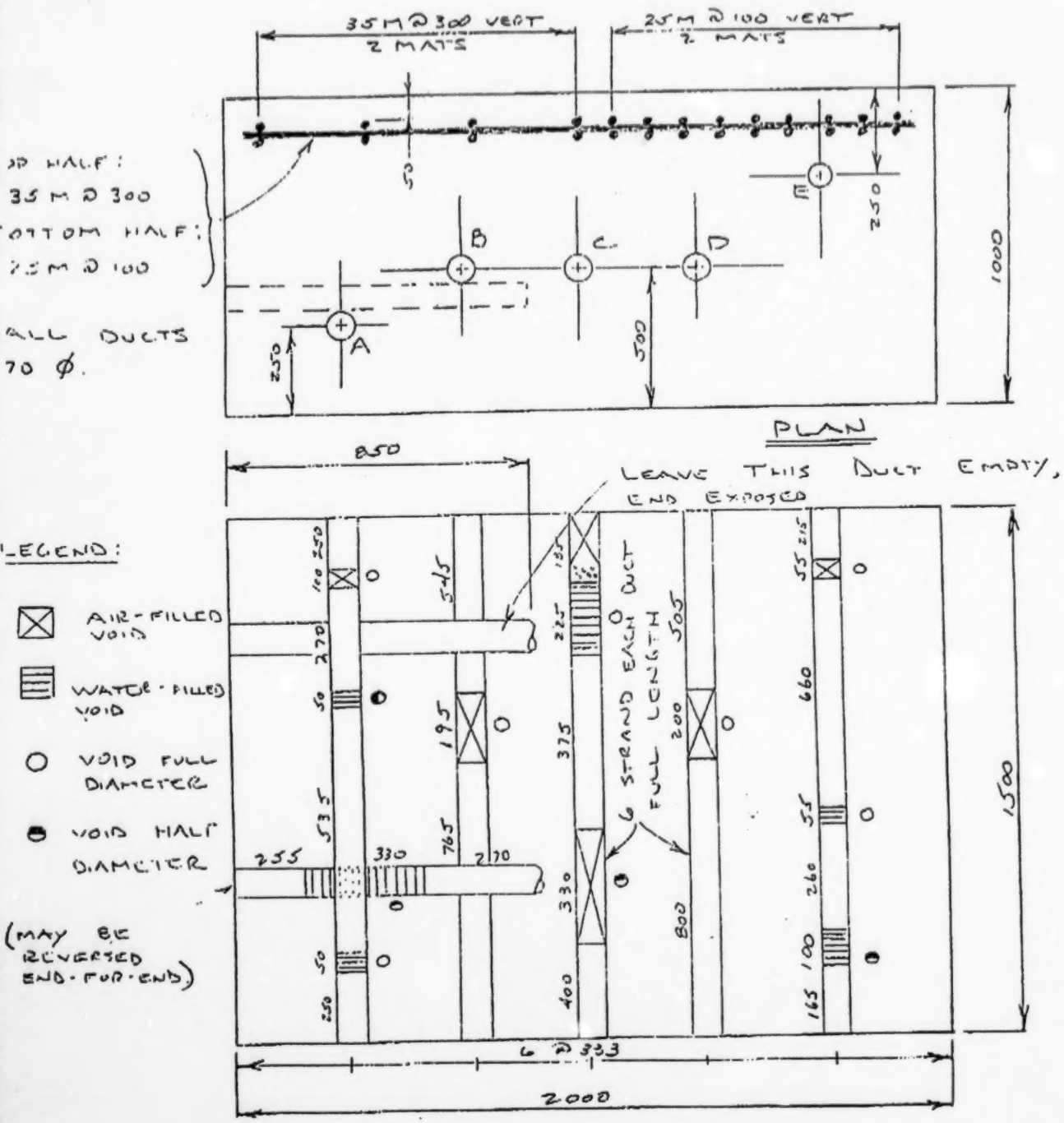

SCALE: 0.0 0.1 0.2 0.3 0.4 0.5 1.0 METRE

TABLE 1

Summary of Test Results on Mock-up Structure

Defect	Location	Size Type	Detection	Est. Size	Missed	False
1	A 255	100 OA	YY	OK	A	
2	A 620	50 OW	Y	OK		
3	A 1205	50 OA	Y	OK		
4	B 545	195 OA	Y	Poor		81200
5	C 135	225 OW	Y	OK		
6	C 785	330 OA	Y	Poor		
7	D 505	200 OA	Y	OK		
8	E 215	55 OA	YY	OK		
9	E 930	55 OW	YY	Poor		E 600, 700
10	E 1245	100 OW	YY	Poor		
11	G 255	230 OW	YY	Poor		

Original Assessment

Detected - 6
Missed - 5
False - 2

Second Assessment

Detected - 11
Missed - 0
False - 0

Full Void 0
Half Void O

Air filled A
Water filled W